AD-A085 197 SOLAR TURBINES INTERNATIONAL SAN DIEGO CA F/G 21/5
DEVELOPMENT AND EVALUATION OF PROCESSES FOR DEPOSITION OF NI/CO--ETC(U)
SEP 79 L HSU, W G STEVENS, A R STETSON F33615-76-C-5379
UNCLASSIFIED SR79-R-4571-18 AFML-TR-79-4097 NL

1 of 2

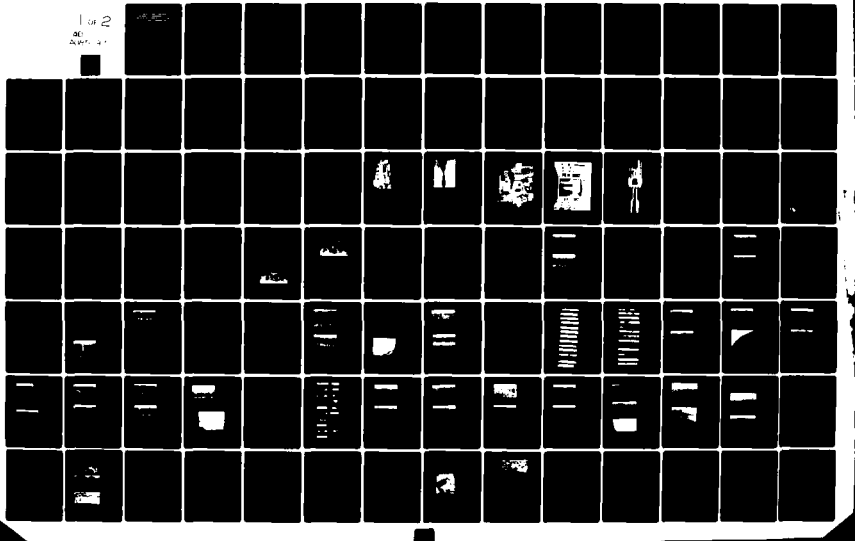

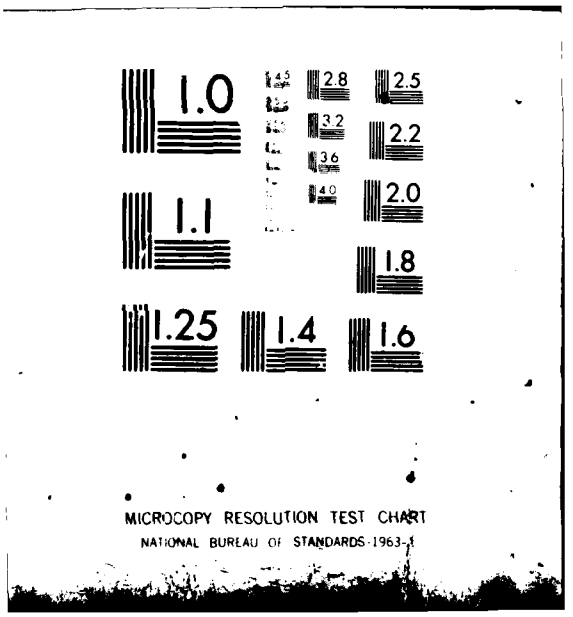
1.0
1.1
1.25
1.4
1.6
2.8
3.2
3.6
4.0
2.5
2.2
2.0
1.8
MICROCOPY RESOLUTION TEST CHART
NATIONAL BUREAU OF STANDARDS-1963-A

Development and Evaluation of Processes for Deposition of Ni/Co-Cr-AlY (MCrAlY) Coatings for Gas Turbine Components

L. Hsu
W.G. Stevens
A.R. Stetson

Solar Turbines International
P.O. Box 80966
San Diego, California 92138

September 1979

TECHNICAL REPORT AFML-TR-79-4097

Final Report for Period 1 November 1976 to 1 September 1978

Approved for public release; distribution unlimited

AIR FORCE MATERIALS LABORATORY
AIR FORCE WRIGHT AERONAUTICAL LABORATORIES
AIR FORCE SYSTEMS COMMAND
WRIGHT-PATTERSON AIR FORCE BASE, OHIO 45433

NOTICE

When Government drawings, specifications, or other data are used for any purpose other than in connection with a definitely related Government procurement operation, the United States Government thereby incurs no responsibility nor any obligation whatsoever; and the fact that the government may have formulated, furnished, or in any way supplied the said drawings, specifications, or other data, is not to be regarded by implication or otherwise as in any manner licensing the holder or any other person or corporation, or conveying any rights or permission to manufacture, use, or sell any patented invention that may in any way be related thereto.

This report has been reviewed by the Information Office (OI) and is releasable to the National Technical Information Service (NTIS). At NTIS, it will be available to the general public, including foreign nations.

This technical report has been reviewed and is approved for publication.

Norman M. Geyer

NORMAN M. GEYER
Project Engineer

FOR THE COMMANDER

Henry C Graham

HENRY C. GRAHAM
Chief
Processing and High Temperature Materials Branch
Metals and Ceramics Division

"If your address has changed, if you wish to be removed from our mailing list, or if the addressee is no longer employed by your organization please notify AFWAL/MLLM *,W-PAFB, OH 45433 to help us maintain a current mailing list".*

Copies of this report should not be returned unless return is required by security considerations, contractual obligations, or notice on a specific document.

AIR FORCE/56780/30 May 1980 — 200

UNCLASSIFIED

SECURITY CLASSIFICATION OF THIS PAGE (When Data Entered)

REPORT DOCUMENTATION PAGE

READ INSTRUCTIONS BEFORE COMPLETING FORM

1. REPORT NUMBER: AFML-TR-79-4097	2. GOVT ACCESSION NO.: AD-A085197
3. RECIPIENT'S CATALOG NUMBER:	
4. TITLE (and Subtitle): DEVELOPMENT AND EVALUATION OF PROCESSES FOR DEPOSITION OF Ni/Co-Cr-AlY (MCrAlY) COATINGS FOR GAS TURBINE COMPONENTS	5. TYPE OF REPORT & PERIOD COVERED: Final Report 1 Nov 76-1 Sep 1978
	6. PERFORMING ORG. REPORT NUMBER: SR79-R-4571-18
7. AUTHOR(s): L. Hsu, W.G. Stevens, A. R. Stetson	8. CONTRACT OR GRANT NUMBER(s): F33615-76-C-5379
9. PERFORMING ORGANIZATION NAME AND ADDRESS: Solar Turbines International, P.O. Box 80966, San Diego, California 92138	10. PROGRAM ELEMENT, PROJECT, TASK AREA & WORK UNIT NUMBERS: Project 7312, Task 731201
11. CONTROLLING OFFICE NAME AND ADDRESS: Air Force Materials Laboratory, Code FY-145, WPAFB, Ohio 45344	12. REPORT DATE: Sep 1979
	13. NUMBER OF PAGES: 158
14. MONITORING AGENCY NAME & ADDRESS (if different from Controlling Office)	15. SECURITY CLASS. (of this report): Unclassified
	15a. DECLASSIFICATION/DOWNGRADING SCHEDULE

16. DISTRIBUTION STATEMENT (of this Report)

Approved for public release; distribution unlimited.

17. DISTRIBUTION STATEMENT (of the abstract entered in Block 20, if different from Report)

18. SUPPLEMENTARY NOTES

19. KEY WORDS (Continue on reverse side if necessary and identify by block number)

Superalloy, MCrAlY coatings, turbine bucket, nozzle vane, CoNiCrAlY, CODEP B, PVD, non-line-of-sight, fluidized bed, electrophoresis, slurry spray, mechanical properties, corrosion/oxidation, controlled composition reaction sintering (CCRS)

20. ABSTRACT (Continue on reverse side if necessary and identify by block number)

The application of MCrAlY (M = Ni or Co or Ni + Co) coatings to high-temperature turbine blades and vanes is primarily provided by the electron beam, physical vapor deposition (PVD) process. Two major drawbacks of the PVD MCrAlY coating are high cost and line-of-sight (LOS) limitation. The controlled composition reaction sintered (CCRS) MCrAlY process was developed as a cost-effective, non-LOS alternative to the PVD coating process.

DD FORM 1 JAN 73 1473 EDITION OF 1 NOV 65 IS OBSOLETE

UNCLASSIFIED

SECURITY CLASSIFICATION OF THIS PAGE (When Data Entered)

326501

JOE

cont

The objectives of this program were to develop the non-LOS technique for coating complex clustered airfoil configurations and to extensively test and evaluate the mechanical, thermal shock and environmental properties of the CCRS CoNiCrAlY coating relative to commercially available PVD NiCrAlY, PVD CoCrAlY and CODEP B coatings.

The CCRS process can be either LOS or non-LOS, depending on part geometry. The former consists of slurry spraying the CoNiCrAlY powder onto the cleaned part followed by reaction sintering in a controlled activity aluminized pack. The latter utilizes an electrophoretic plus fluidized bed (E/FB) approach to deposit the CoNiCrY bisque prior to aluminization. When applied to nickel-base alloys (Rene' 125 and MA754) full densification of the CoNiCrAlY coating was achieved; however, the coating had greater porosity on cobalt-base X-40 alloy. The nominal composition of CCRS CoNiCrAlY on Rene' 125 and X-40 are Co(bal)/33-42Ni/6-10Cr/12-19Al/Y and Co(bal)/18Ni/10-20Cr/14-16Al/Y, respectively.

Testing was performed at Solar Turbines International (STI) and the Aircraft Engine Group of General Electric (GE) at Evendale, Ohio. Results are summarized as follows:

1. (STI) - The tensile properties of coated (CCRS CoNiCrAlY, PVD NiCrAlY, PVD CoCrAlY and CODEP B) Rene' 125 and X-40 were minimally and equivalently affected by coating processing.

2. (GE) - Elevated (982°C) stress-rupture life of CCRS CoNiCrAlY coated X-40 fell within the -3σ band established by GE. CCRS CoNiCrAlY and CODEP B coated Rene' 125 alloy, however, exhibited much reduced life and fell below the -3σ curve. The reason suggested for the degradation was the presence of entrapped Al_2O_3 particles near the CCRS coating surface which acted as stress risers.

3. (STI and GE) - Strain tolerance tests showed comparable ductility for PVD NiCrAlY and CCRS CoNiCrAlY coatings. CODEP B was found to be much more brittle.

4. (STI) - CCRS CoNiCrAlY coated Rene' 125 and MA754 exhibited better cyclic fatigue lives (at 20 cps and 20 cpm at 760°C) than CODEP B and PVD CoCrAlY. PVD NiCrAlY coated X-40 alloy had the longest life compared to CCRS CoNiCrAlY and CODEP B on X-40, which were equivalent in performance.

5. (GE) - CCRS CoNiCrAlY coated MA754 exhibited excellent thermal mechanical fatigue life. CCRS CoNiCrAlY and PVD CoCrAlY coated X-40 can be ranked equivalently while CODEP B/X-40 performed very poorly in thermal shock resistance.

6. (STI and GE) - In hot corrosion tests, Rene' 125 was best protected by both CODEP B and CCRS CoNiCrAlY when compared to either PVD CoCrAlY or PVD NiCrAlY. CCRS CoNiCrAlY and PVD CoCrAly coated X-40 exhibited good sulfidation resistance while CODEP B failed rapidly. Finally, GE reported that CCRS CoNiCrAlY coated MA754 was superior to PVD NiCrAlY.

7. (GE) - Dynamic oxidation (1145°C) results showed that only the dense CCRS CoNiCrAlY coating on Rene' 125 was comparable to PVD NiCrAlY in oxidation protection. CCRS CoNiCrAlY on X-40 and MA754 were inferior to PVD coatings.

The CCRS method of applying the CoNiCrAlY coating to Rene' 125 HPT buckets of the F101 engine was judged successful by both STI and GE. GE evaluation of coated buckets revealed good coating uniformity, full density and effective masking of cooling holes. The clustered TF34 vane pairs of X-40 alloy were not adequately coated with the CCRS CoNiCrAlY coating. Porosity and non-uniformity (related to cobalt-base alloy) were the main problems that need to be resolved.

FOREWORD

This report was prepared by Solar Turbines International (STI) under Air Force Contract F33615-76-C-5379. The work was performed at the Harbor Drive facilities in San Diego, California.

The contract was administered under the direction of the Air Force Materials Laboratory, Air Force Systems Command, Wright-Patterson Air Force Base, Ohio, under Project 7312, Task 731201, Title: Surface Protection, with Mr. J. Crosby as Project Engineer.

This report covers the work carried out during the period from November 1976 to September 1978. The Principal Investigators are Ms. L. Hsu and Dr. W. G. Stevens, with Mr. A. R. Stetson as Program Manager.

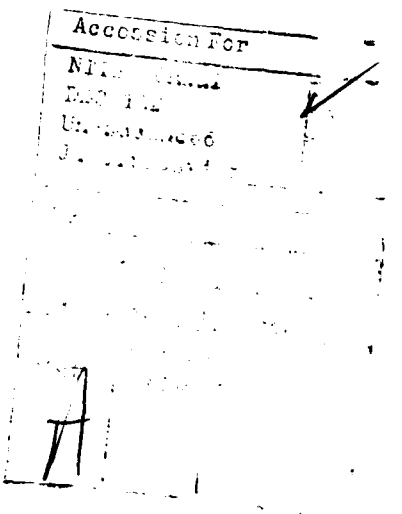

TABLE OF CONTENTS

TABLE OF CONTENTS (Cont)

LIST OF ILLUSTRATIONS

LIST OF ILLUSTRATIONS (Cont)

LIST OF ILLUSTRATIONS (Cont)

LIST OF ILLUSTRATIONS (Cont)

LIST OF ILLUSTRATION (Cont)

LIST OF ILLUSTRATIONS (Cont)

LIST OF TABLES

LIST OF TABLES (Cont)

NOMENCLATURE

CCRS	Controlled composition reaction sintering
Slurry spray	Spray gun application of metallic powders suspended in organic vehicle/binder system
Fluidized bed process (FB)	Immersion of component in bed of argon fluidized particles
Electrophoretic process	Electrophoretic deposition of organic binder onto surface of component
Electrophoretic/ fluidized bed (E/FB)	Modifier application process whereby the binder is electrophoretically deposited and the part heated above binder softening temperature followed by immersion in fluidized bed of MCrY powders. Process can be repeated as many times as necessary to achieve desired modifier thickness.
Single stage fluidized bed (SS/FB)	Immersion of heated part into argon fluidized bed of resin coated particles
Single cycle CCRS coating	CCRS coating with only one furnace cycle
Two-cycle CCRS coating	CCRS coating with two furnace cycles.

1

INTRODUCTION

1.1 BACKGROUND

Advanced aircraft turbine engines demand increasingly higher operating temperatures in blades and vanes for greater thrust and efficiency. The turbine components require coatings that significantly increase their resistance to oxidation and hot corrosion without compromising the component strength or ductility. This has placed serious constraints on permissible coating - base metal interactions and requires the use of highly compatible protective materials. Successful service experience has demonstrated that the MCrAlY coatings applied by physical vapor deposition (PVD) are effective in protecting a variety of advanced nickel- and cobalt-base superalloys, directionally-solidified alloys, and oxide dispersion-strengthened alloys over a range of critical environmental conditions, such as oxidation, hot corrosion and thermal and mechanically-induced strains. The application process, PVD, has several limitations; namely, expense and the inability to uniformly coat complex geometries and clustered turbine blade and vane airfoils. Thus, another means of applying MCrAlY coatings was sought that would retain all the desirable properties of these materials and, at the same time, have a lower application cost and the ability to uniformly coat turbine components of complex geometries and clustered turbine blade and vane airfoils.

Solar Turbines International (STI) demonstrated the feasibility of the controlled composition reaction sintering (CCRS) process for applying MCrAlY coatings in a previous program (Ref. 1). In this two-phase process the first step consists of applying the MCrY (M = Co and/or Ni) modifier to all critical surfaces of the turbine component. This modifier, in the form of a pre-alloyed powder, is applied by slurry spray and by fluidized bed deposition processes. The MCrY coated part is then reaction sintered in a controlled aluminum activity pack to density the MCrY coating through formation of beta aluminide (MAl) and to metallurgically bond the MCrAlY to the alloy surfaces.

In the previous program (Ref. 1) the need for pre-alloying the MCrY modifier for coating composition control was noted, as was the dependence of the surface finish on the particle size of the MCrY modifier. The final control of coating composition was achieved by control of the pack aluminum activity during reaction sintering to limit the amount of beta aluminide formation to lower the microhardness and increase the strain tolerance of these coatings.

Since the CCRS process uses processing steps and manipulations common to the commercially applied diffusion aluminide coatings, it potentially is a relatively inexpensive process compared to the PVD process. However, as with most other coating processes, the CCRS technique has critical processing steps which must be carefully controlled to provide satisfactory MCrAlY coatings.

1.2 OBJECTIVES

In this program the objectives were to develop the CCRS CoNiCrAlY process and to demonstrate its ability to uniformly coat advanced air-cooled turbine blades from the General Electric (GE) F101 engine and a clustered nozzle airfoil from the GE TF34 engine. Following this, a process flow sequence would be laid out which would allow cost comparisons to be made for the CCRS process relative to other methods of depositing MCrAlY coatings.

The success of process development was checked by a series of mechanical, thermal shock, and environmental tests. Part of these checks were performed by STI and the remainder by the Aircraft Engine Group of GE. Tests included strain tolerance as a function of temperature, thermal shock resistance, stress rupture, tensile, low-cycle fatigue, and dynamic rig oxidation and hot corrosion. In each test the conditions were chosen to simulate advanced aircraft turbine engine operating conditions, and both commercially applied PVD and other coatings were tested simultaneously to demonstrate the relative performance of the CCRS CoNiCrAlY coating.

Finally, a production plan was assembled for the CCRS coating of new and overhauled Air Force engine components. From this plan, estimates of the cost and time required to apply the CCRS CoNiCrAlY coating were derived and are available for comparison with the other methods of applying MCrAlY coatings to these components.

2

EXPERIMENTAL

The experimental effort in this program was divided into three major areas:

1. Development of non-line-of-sight limited CCRS coating process
2. Application of CCRS coating to test specimens and areo-engine hardware
3. Testing and evaluation of coated parts.

The following subsections provide the details of the materials and processes employed in achieving program objectives.

2.1 MATERIALS

Substrate materials used in this program included three superalloys, Rene' 125, X-40 and MA754, with the bulk of the investigation conducted on the first two alloys. The chemical analyses of the alloys supplied by the vendors are reported in Table 1. Both Rene' 125 and X-40 test pieces were cast-to-size in the standard 6.35 mm diameter test bar configuration while MA754 was available in bar stock form and was subsequently machined to size. Only the Rene' 125 specimens were heat treated after coating. The heat treatment cycle was a carbide solutioning cycle of 1117°C for 2 hours, followed by a gamma prime solutioning cycle of 1079°C for 4 hours and aging at 816°C for 16 hours (Ref. 2).

The metallic powders used to form the overlay modifiers in the MCrAlY CCRS processes were purchased from Alloy Metals, Inc. Characterization analysis of powder lots are provided in Table 2. The vehicle/binder system used in slurry spray application of the MCrY powder was a mixture of ethyl cellulose in xylene. The electrophoretic bath solution was composed of 2.5 g/l stearic acid and 10 g/l of ammonium hydroxide in deionized water. The materials used in the aluminizing packs are characterized in Table 3.

Table 1

Chemical Analysis of Cast Alloys

Alloy	Supplier	Heat Number	Chemical Analysis
Rene' 125	Misco Div. Howmet Corp.	GE 013	10Co, 8.85Cr, 6.79W, 4.70Al, 3.84Ta, 2.40 Ti, 1.88Mo, 1.53Hf, 0.10C, <0.10Mn, 0.10Si, <0.10Fe, <0.10Cb, <0.10Cu, <0.10V, 0.04Zr. 0.16B, 0.003P, 0.0014 S, Bal. Ni
X-40	Misco Div. Howmet Corp.	CB 222 (710574)	10.40Ni, 7.40W, 25.00Cr, 0.51C, 0.64Si, 0.15Fe, 0.16Zr, 0.0038S, <0.10Mn, <25 ppm Pb, <10 ppm Ag, Balance Co.
MA-754	Huntington Alloys	DT0096B	76.77Ni, 20.38Cr, 1.20Fe, $0.5Y_2O_3$, 0.39Ti, $0.36O_2$, 0.28Al, 0.08C, 0.003S.

Table 2

Powder Alloy Characterization

Powder Alloy	Lot Number	Chemical Analysis	Sizing
CoNiCrY	8864	54.90Co-25.29Cr-19.41Ni-0.51Y	98.64% <400 mesh
CoNiCrY	9653	54.70Co-24.95Cr-19.61Ni-0.64Y	98.75% <400 mesh

2.2 COATING PROCESSES

The CCRS method utilized well-established manufacturing processes such as slurry spray, pack aluminization, electrophoresis, and fluidized bed. The various stages of coating processing are:

- Precleaning
- Application of particulate modifier MCrY bisque
- Reaction sintering in a controlled activity aluminizing pack.

Table 3

Materials Used in Aluminizing Packs

Material	Supplier	Analysis	Particle Characterization
Cobalt	African Metals	0.32Ni, 0.08Fe, 0.08Ca, 0.06Si, 0.022Mn, 0.022C, 0.015S, 0.01Cr, Balance Co	94.7% <37μm
Nickel	Glidden Metals	0.005C, 99.59Ni	96.3% <44μm
Chromium (MD101)	Alcan	0.23Fe, 0.04N, 0.03Al, 0.035-0.01C, 0.01Si, 0.006P	149μm
Aluminum (201)	Alcoa	-	-
Aluminum Oxide (E1)	Norton	-	100μm, blocky
Ammonium Chloride	J.T. Baker	Analyzed Reagent 5-0660	Granular
Polyvinylchloride (PVC)	B.S. Goodrich	-	-

The precleaning and aluminizing steps are common to all components to be coated. Several methods were developed for the second step of modifier application. Depending on the complexity and gometry of the part to be coated, the modifier application process was selected for greatest compatibility. This is discussed in greater detail in the following sections.

2.2.1 Precleaning

Prior to coating processing, the coating surfaces were vapor degreased and grit blasted to remove all grease, oils and oxide scales. The grit blast also roughened the substrate surface in order to increase contact area and physical bonding between coating particles and alloy surface. An acid etch ($50\%H_3PO_4$-$50\%HNO_3$) was used for line-of-sight (LOS) limited parts such as double vane segments. Finally, the cleaned specimens were thoroughly rinsed with deionized water and acetone and oven dried at approximately 100°C.

2.2.2 MCrY Modifier Application

Conventionally, the MCrY modifier was slurry sprayed on cleaned substrate surfaces and air dried to form a bisque. However, this method is a LOS limited process and could be used only with simple test specimens and blades. The advantage of this process is that the alloy particles gather sufficient momentum between the gun nozzle and the part to produce a dense arrangement in the bisque and thus produce denser coatings. Slurry spray application of program specimens (single airfoil turbine components and test specimens) were accomplished as described in Table 4.

Table 4

Slurry Spray Process Steps

1.	Prepare a slurry of specific gravity 2.0 to 2.5 of sized MCrY powder in ethyl cellulose and xylene.
2.	Mask areas of turbine part or test specimen to remain uncoated with a strippable latex or pressure-sensitive tape.
3.	Record weight of part.
4.	Attach fixture for circulating air or other gas through the internal passages of the cooled turbine blade.
5.	With the air or other gas flowing through the part, spray coat the critical gas path surfaces with the MCrY slurry until the pre-determined deposition has been obtained. On highly curved concave surfaces, care must be taken to minimize over-spraying which will lead to excessively thick bisques that will not be fully aluminized.
6.	Remove air or gas flow fixture.
7.	Weigh part to determine MCrY deposition.
8.	If coating defects or excessive deposition are encountered, this part may be stripped in ultrasonically agitated xylene and re-coated.

Alternate, non-LOS-limited processes for modifier application were sought for multiple vane segments.

Initially, process development was concerned with the single-stage fluidized bed concept. This is shown in Figure 1 and consisted of first resin coating the MCrY metal particles followed by argon gas fluidizing (cold) of coated particles. A wide range of resins (and plasticized resins) were experimented with, all of which had softening temperatures below 250°C. Details of the process steps are provided in Table 5. This process was found to produce uniform part coverage. The thermal conductivity of the coated particle was

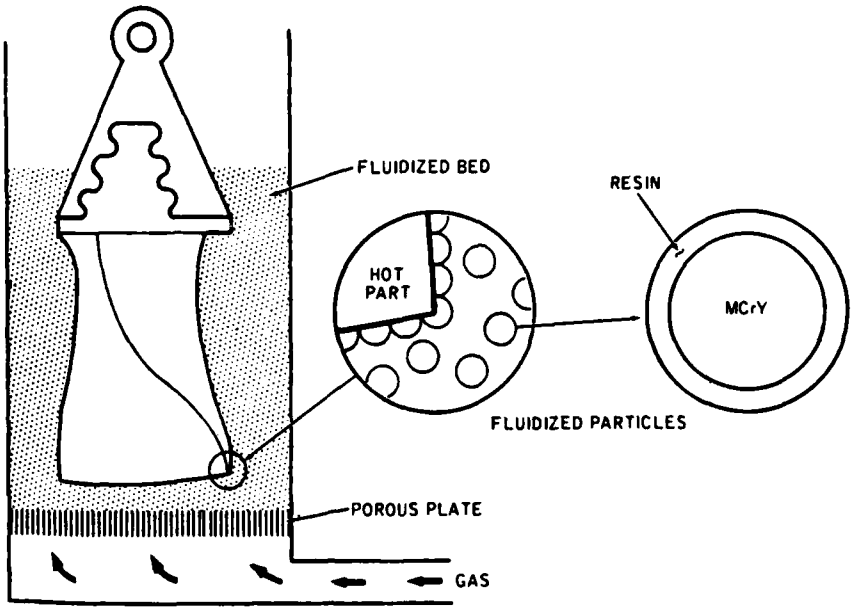

Figure 1. Single-Cycle Fluidized Bed Application of the MCrY Modifier

comparable to that of the heated part and upon contact heat was efficiently transmitted and bonding occurred readily. However, a major drawback was that very porous coatings were formed. The bisque could not be densified by the volume expansion of beta-MAl formed during pack aluminization. Porous coating may be a consequence of two factors - too high a resin content or lack of directional driving force to help compact the 'sticky' modifier particles. Since neither one of these factors can be readily corrected, the single-stage fluidized bed process (SSFB) was dropped in favor of a more favorable modifier application process, a dual-stage process described below.

Electrophoretic/fluidized bed (E/FB) deposition of MCrY powders was developed in this program as a non-LOS alternative. Instead of pre-coating the metal particles, the bonding resin was applied to the substrate surface by electrophoresis, followed by immersion of the sticky part into a fluidized bed of metal powder. This technique is called the 'tacky' surface approach (Ref. 4) and is described in Table 6.

The amount of resin applied was carefully controlled in order to prevent an excessively thick layer from building up since it was important to use the minimum amount of resin for bonding. In theory, electrophoresis of electrically non-conductive materials such as resin is a self-limiting process. Under the imposed voltage difference across the electrode terminals, the initial layers of resin particles migrating to the specimen has an insulating effect which lowers the rate of change transfer. Eventually, a state is reached where little deposition occurs when the part is fully insulted/coated with resin. The fluidized bed step allowed the metal particles to be trapped in the 'tacky' resin layer. Multiple cycles in the electrophoretic bath followed by fluidized bed immersion resulted in buildup of the modifier to the desired thickness.

Table 5

Fluidized Bed Process Steps

1.	Select resin to be used for coating, e.g., polymethyl methacrylate, polyvinyl butynal, polyvinyl alcohol and appropriate amount of plasticizer.
2.	Prepare a slurry of sized MCrY powder resin (and plasticizer, if necessary) in a solvent.
3.	Spray dry above slurry to coat the MCrY powder with the resin (and plasticizer).
4.	Place the coated powder in the fluidized bed setup.
5.	Adjust fluidizing gas flow to cause the bed to fluidize (see Ref. 3).
6.	Mask the turbine part surface where coating is not wanted with strippable latex or resin masks and provide for air or gas flow through the cooling passages while part is immersed in the fluidized bed.
7.	Weigh part.
8.	Heat the masked turbine part in an air circulating oven or by radiation to a temperature above the softening point of the plasticized resin on the MCrY powder, i.e., 150°C for polyvinyl butynal, 180°C for polymethyl methacrylate, 200°C for polyvinyl alcohol.
9.	With air or gas flowing through the internal passages of the turbine part, immerse the part in the fluidized bed of resin coated MCrY powder.
10.	The fixture for immersing the turbine part must be oriented to prevent stagnation of the fluid bed when the part is immersed. Otherwise, excessive MCrY will be deposited in the stagnant areas.
11.	Reheat the MCrY coated part after withdrawal from the fluidized bed to enhance the bonding of the resin coated particles.
12.	Weighing of the part before and after coating can be used to determine the amount of MCrY pickup to control the coating thickness.
13.	Remove the air or gas flow fixture for circulating these gases through the internal cooling passages.

Table 6

Electrophoretic/Fluid Bed Process Steps

1.	Prepare an electrophoretic bath of 6gm of stearic acid per liter of deionized water and adjust pH (at 52° to 57°C) to 8 - 9 with addition of up to 10cc of concentrated ammonium hydroxide.
2.	Record weight of part.
3.	Mask the areas to remain uncoated with a strippable coating or electroplating masking tape.
4.	Attach fixture for circulating air or another gas through the internal cooling passages of cooled turbine components.
5.	Insert a removable cathode between the concave and convex surfaces of adjacent airfoils to improve the uniformity of resin deposition.
6.	Connect the masked turbine part to the positive side of a constant current dc power supply with a compliance of 50 volts. The current should be adjusted to supply 1.5 to 2.0 mA per cm^2 of turbine part surface area.
7.	Connect the negative side of this power supply to the removeable cathode and other cathodes surrounding the part in the electrophoretic bath.
8.	Immerse the turbine part in the electrophoretic bath maintained at 52° to 57°C.
9.	Electrophoretically coat the part by passing current for 30 seconds to 1 minute.
10.	Remove part from electrophoretic bath and turn on air or gas flow to the internal passages.
11.	Rinse excess resin from part with stream of water; pressure not to exceed 138 kPa (20 psig).
12.	Place sized MCrY powder in a fluidized bed with a diffuser whose pressure drop is greater than the pressure drop of the MCrY powder.
13.	Adjust the argon fluidizing gas flow until the MCrY powder is fluidized and gently boiling.
14.	Heat the resin coated part in an air circulating oven at 150° to 175°C to soften the resin film. The part should appear wet when the resin has softened.
15.	Immerse the heated part in the fuidized bed of MCrY powder for 5 to 30 seconds.
16.	While part is immersed, turn on air or gas flow to internal cooling passages to keep these clear of MCrY powder.
17.	Without stopping air or gas flow to internal passages, remove part from fluid bed and shake top gently to remove excess MCrY powder.
18.	Reheat part to 150° to 175°C to improve bond between resin and the MCrY powder.
19.	Weigh part to determine amount of MCrY deposit.
20.	Repeat steps 7 through 11 and 15 to 19 until desired MCrY coating thickness has been deposited. A 3 mil coating requires two to three repetitions and a 5 mil coating requires five to seven repetitions.
21.	Remove removable cathodes and internal cooling passage gas flow mixture.
22.	Weigh part to verify MCrY deposition.

2.2.3 Reaction Sintering

While virtually any source of aluminum vapor could be used to form the MAl and hence the CCRS MCrAlY coating, it is known from considerable previous work on diffusion aluminide coatings (Ref. 5) that 25-30 weight percent aluminum beta NiAl coatings have high DBTTs, between 650° and 850°C. Thermal cycling producing severe thermal strains can produce cracks which propagate into the substrate. One advantage of the PVD MCrAlY coating was the ability to produce lower aluminum coatings in the gamma-beta field, which had correspondingly lower DBTT. In the CCRS process, these needed low aluminum levels are obtained by careful control of the aluminum activity in the reaction sintering pack. By restricting the weight ratio of aluminum to cobalt in the aluminizing pack to between one-fourth and two-fifths limits, the aluminum content is lowered, the time for coating formation increases, thus a balance must be struck between the time required for coating and the degree of coating ductility.

Regardless of the MCrY bisque application process, the coated parts were all reaction sintered (aluminized) as described in Table 7. Initially, only one furnace cycle was used; however, heat treat and test results indicated non-uniform pickup. A second shorter furnace cycle was therefore introduced which appeared to alleviate the problem. This will be referred to as the two-cycle CCRS coating. Unless otherwise noted, all references to the CCRS CoNiCrAlY coating imply the two-cycle process.

Weight change data for all CCRS CoNiCrAlY coated test specimens are reported in Appendix A. It should be noted that the amount of aluminum pickup in the bisque during reaction sintering varied depending on the substrate alloy. This is shown in Figure 2. The CoNiCrY bisque on nickel-base alloys, Rene' 125 and MA754, picked up 15 and 11 mg/cm^2 aluminum, respectively, while the coated X-40 alloy had an aluminum weight gain of about 8 mg/cm^2. This difference, therefore, would contribute to the increased porosity found in CCRS coated X-40 specimens.

2.2.4 Masking

Masking of the turbine parts is required in both the modifier application step and reaction sintering steps. In the modifier application steps, a strippable latex resin, Turco 5696 or Organoceram, was applied to the surfaces of the turbine vane segment not to receive the MCrAlY coating. Large planar areas of the components were masked with electroplating pressure-sensitive tape. After modifier application, the maskants were removed for component weighing.

Upon conference with GE personnel, it was decided that only the firtree sections of the F101 HPT buckets need to be masked during pack aluminization. The TF34 vanes were to be fully aluminized. The root mask consisted of ethyl cellulose xylene slurry of approximately 100 mesh Al_2O_3, which was applied in multiple coats to a thickness of 2 to 3 mm. Then a slurry of approximately -325 mesh of NiO with clay and water was applied over the air dried Al_2O_3

Table 7

Formation of Low Activity Reaction Sintering Packs

Materials

Cobalt	<40μm
Chromium	<44μm
Aluminum	<44μm
Al_2O_3	105μm Norton E-1
Polyvinyl chloride	B.F. Goodrich Geon 124F-1
Argon	

Apparatus

Inconel 600 Retort	TIG Welder
Vacuum Pump	Ball Mill Drive

Procedure

1. Weigh out the appropriate amounts of the pack constituents; for example: 14.4%Co, 5%Cr, 5.6%Al, balance Al_2O_3 ≤0.25 w/o PVC.

2. Blend by tumbling for 1/2 to 1 hour.

3. Place blended mixture in retort and seal by welding.

4. Evacuate the retort and its contents to less than 27 pascals then backfill with argon to 1.0 KPa.

5. Repeat step 4 two times, leaving the retort and its contents under a positive pressure of argon.

6. Place the purged retort and its contents in a gas or electric fired furnace at 1134°C for 16 hours with outlet tube vented through an oil or mercury trap.

7. After cooling retort to ambient temperature, remove content of retort pack and store in a sealable container and take a sample for acid soluble metal analysis. This step prepares the pack for use.

8. Add another amount, <0.25 w/o, of PVC to the prepared pack and place it and the MCrY coated parts in the retort and seal by TIG welding.

9. Using steps 4 and 5, evacuate and cycle purge the retort and its contents, leaving the contents under a slight positive pressure of argon.

10. Place purged retort and contents in a gas or electric fired furnace at 1135°C for 16 hours for formation of the MCrAlY coating.

11. Upon cooldown, the retort is cut open and the parts removed. Another portion of the PVC (<0.125 w/o) is added and mixed in with the powder pack. The parts are replaced in the pack and the retort is welded.

12. Repeat steps 4 and 5.

13. Repeat step 6 except for the firing time which is reduced to 4 hours for this second cycle.

14. Repeat step 7. The coated parts are now ready for use.

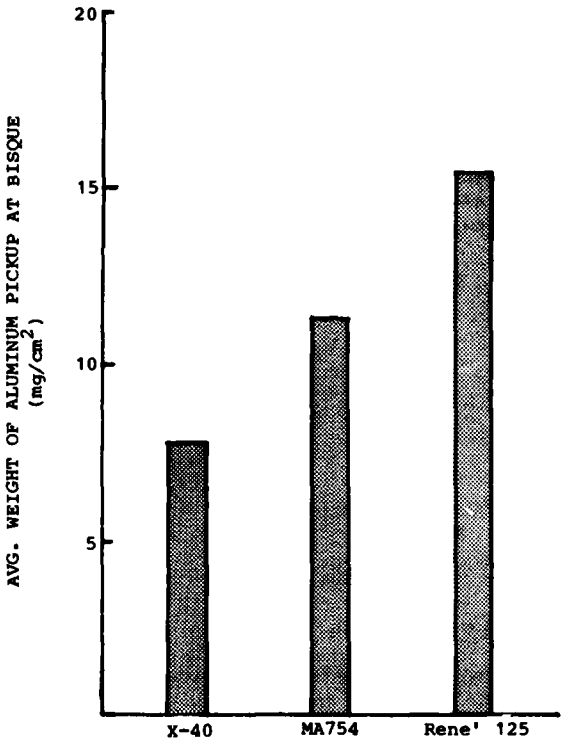

Figure 2. Aluminum Diffusion Into CoNiCrY Bisque on Three Alloys

layer. After air drying these composite coatings for 16 to 24 hours, the part was ready for reaction sintering. Mask removal was accomplished by pressure washing after the reaction sintering step. Care was taken in the application of the NiO layer to ensure that it did not touch any metallic surface. Otherwise, during reaction sintering, the nickel and nickel-aluminide produced as a result of the reaction:

$$2Al \text{ (from pack)} + 3NiO \rightarrow Al_2O_3 + 2NiAl + Ni$$

would sinter to the surface and could only be removed by grinding or remachining.

2.3 TESTING

The second phase of this program was to test and evaluate the CCRS coating. At the same time, comparisons to commercially available coatings currently in service on aircraft engines were made to assess its relative performance. Testing scope of program coatings included mechanical properties and environmental (hot corrosion/oxidation) resistance. The Aircraft Engine Group at GE in Evendale, Ohio was contracted to perform as testing subcontractor and Table 8 summarizes the type of testing to be performed at STI and GE. The final report prepared by GE on their test results is included as Appendix B.

Table 8

Test Schedule

STI	GE
Strain tolerance Hot corrosion Cycle fatigue Tensile	Strain tolerance Hot corrosion Tensile Creep Oxidation Thermal fatigue

2.3.1 Tensile Testing

At STI, testing was performed using an Instron model TT-D screw type testing machine. The strain rate used was 0.005 mm/mm/min. up to 0.2% strain offset and 0.05 mm/mm/min. to the point of failure. Load-strain curves were recorded autographically from an extensometer attached to each specimen. Elevated-temperature tests were performed by equilibrating the specimens in a regulated Satec furnace (±25°C) prior to straining. Specimen configuration is shown in Figure 3. Specimens were tested in the as-coated condition and heat-treated condition and also after oxidation exposure for 500 hours at 899°C (1650°F) for Rene' 125 alloy and 982°C (1800°F) for X-40 alloy.

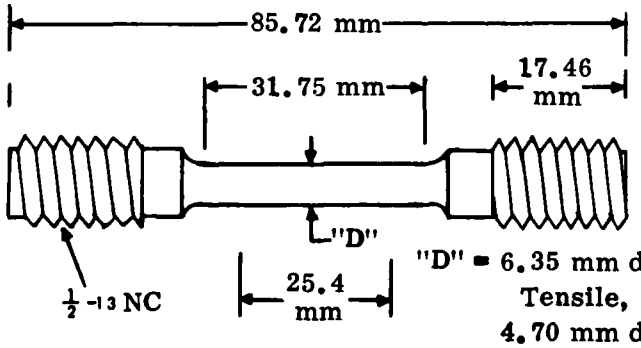

Figure 3. Test Specimen for Strain Tolerance, Low-Cycle Fatigue and Stress-Rupture Tests

A total of 38 test specimens (18 each of Rene' 125 and X-40) were tested, and a flow chart is shown in Figure 4.

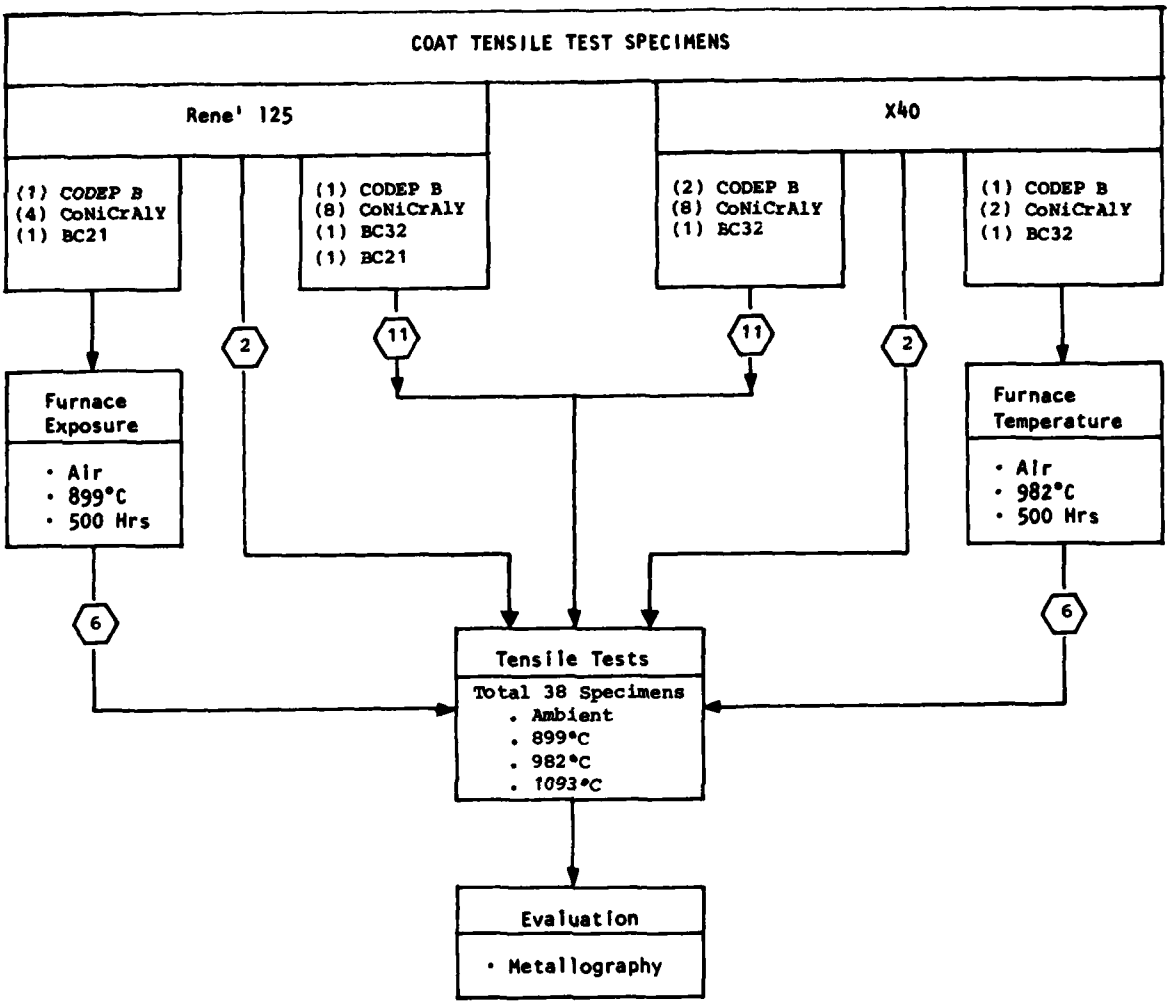

Figure 4. Flow Chart for Tensile Tests

2.3.2 Strain Tolerance/Ductile-Brittle Transition Temperature Testing

One of the important considerations in this program was the ductility or strain accommodation of the coating. Cracks which appear in the coating due to substrate strain can lead to stress concentration points and subsequent failure of the substrate. In order to evaluate the ductile-brittle nature of the program coatings, strain tolerance tests were performed on coated Rene' 125 alloy as described below.

The specimen configuration is shown in Figure 3. Prior to testing, each specimen was penetrant examined (Zyglo penetrant) for any surface cracks or defects.

The specimens were loaded onto the testing machine and brought to temperature. A series of temperatures were selected between ambient and 760°C (1400°F), and at each temperature the specimen was incrementally strained until coating cracks appeared. The strain rate was kept at 0.005 mm/mm/min., and the strain increments were varied according to the strain tolerance of each coating. After each increment, the test secimens were cooled, unloaded, and dye penetrant examined for cracks. The process was continued until a detectable crack(s) was found.

Two lots of CCRS CoNiCrAlY coated Rene' 125 specimens were strained at five temperatures; ambient; 427°C (800°F); 538°C (1000°F); 649°C (1200°F); and 760°C (1400°F). Post-testing evaluation was done by metallographic inspection of failed specimens. CODEP B and PVD NiCrAlY (BC-32) coated Rene' 125 specimens were also subjected to the same test at selected temperatures of 427°C (800°F) and 538°C (1000°F). The effects of long-term high-temperature exposure on the coated alloys were evaluated by subjecting one specimen of each coating to 100 hours at 982°C (1800°F). Following exposure, these specimens were strained as described above at 427°C (800°F).

2.3.3 Fatigue Testing

Elevated-temperature fatigue testing was performed at Peabody Testing Services of Magnaflux in Los Angeles, California. A flow chart of the test is shown in Figure 5.

A Tatnall-Krouse axial fatigue machine, model DDS-5000, was used for all tests. This machine is a combination mechanical/hydraulic machine which applies the alternating load by means of a variable eccentric cam, and automatically maintains the mean load hydraulically. Figure 6 shows the machine with furnace and pull rods installed.

A strain gage load cell in line with the test specimen was used to read actual load on the specimen. An Ellis Associates model BA-13 bridge/amplifier read the fatigue loads dynamically during the test.

Figure 7 shows the pull rod assembly with a specimen installed. Two chromel-alumel thermocouples were wired to the 1/4-inch diameter immediately adjacent to the specimen reduced section. Both thermocouples were read with a Leeds & Northrop model 8686 potentiometer. Differences in temperature between top and bottom were adjusted by raising or lowering the 3-inch core Marshall single zone furnace until both thermocouples read 760 $\pm$6°C (1400 $\pm$10°F). A 15-minute soak time at temperature was used before the specimen was loaded.

For the tests at 20 cycles/second the standard direct current variable speed drive motor was used. Prior to application of a load, the machine speed was checked and/or adjusted using a General Radio "Strobotac". The maximum error in testing speed was approximatly $\pm$2 percent of the nominal 20 cycles/second.

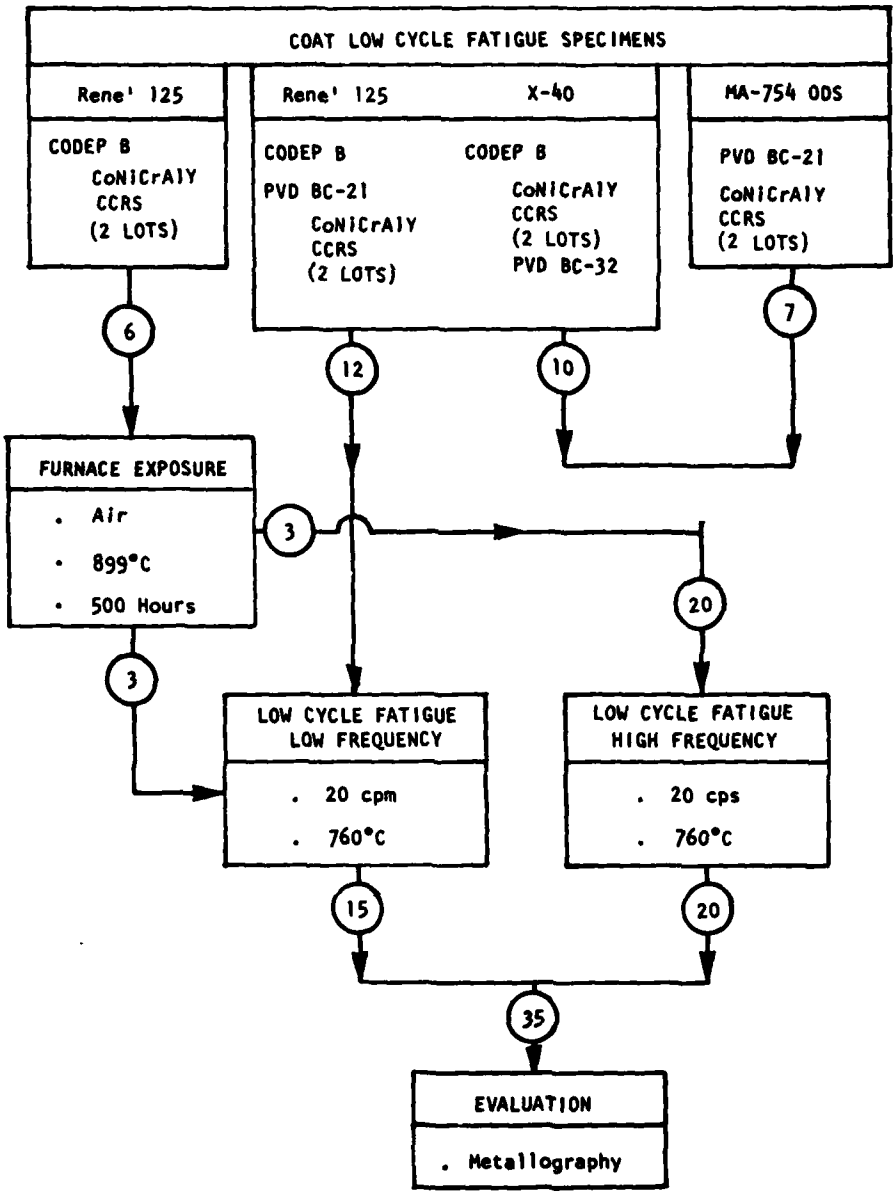

Figure 5. Flow Chart of Low Cycle Fatigue Tests

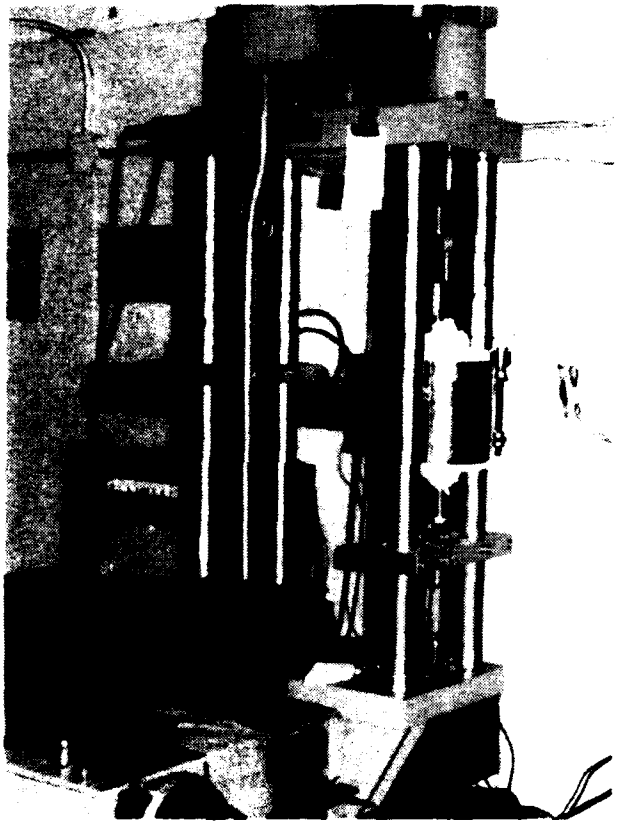

Figure 6.

Axial Fatigue Machine With Furnace and Pull Rods Installed

The low speed tests at 20 cycles/minute used a constant speed three-phase worm gear drive motor, which provided a constant testing speed of 19.6 cycles/minute measured over a time span of 20 minutes. The speed variation was less than $\pm$1 percent and provides a sinusoidal load wave form. All tests were run at an R ratio of 0.2 (min. strain/min. stress). The test loads were calculated using the uncoated diameters of each specimen.

2.3.4 Hot Corrosion Rig Tests

Field service of coated turbine hardware in a salt-containing environment is the ultimate test of the hot corrosion resistance of the turbine materials such as coatings and/or alloys. The gas turbine environmental simulator (burner rig) used in this program at STI is similar in design features to those of STI's gas turbine combustors. Introduction of sea salt into the rig test environment is used to accelerate hot corrosion to permit comparisons to be made for the coating/alloy systems' hot corrosion resistance. Figures 8 and 9 show the burner rig used in this program. The liquid fuel used throughout the test was JP-5 (MIL-J-5624F). The maximum specified sulfur content of JP-5 aviation turbine fuel is 0.40 percent by weight. From past work (Ref. 6)

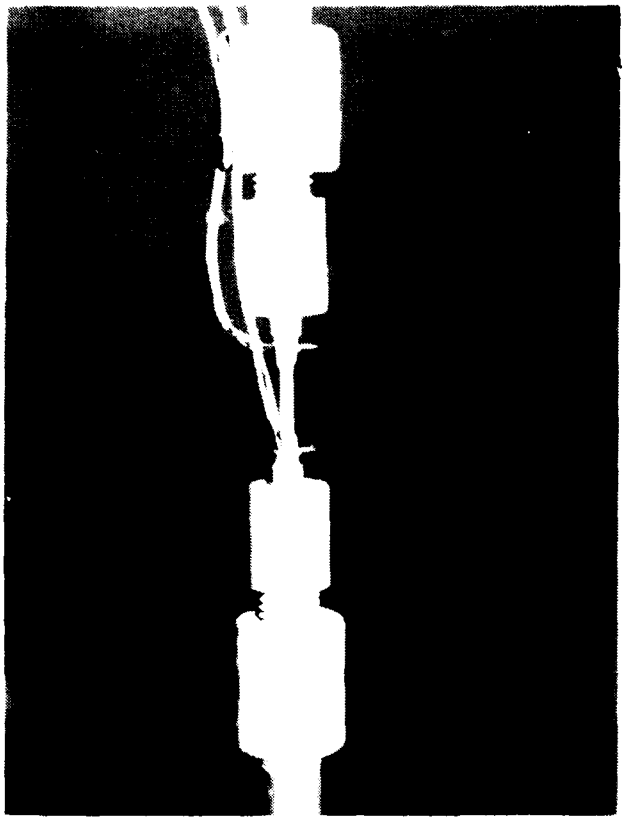

Figure 7.

Pull Rod Assembly With Specimen Installed

it has been shown that the average sulfur level in the fuel tanks is consistently less than specification limits. Sampling of JP-5 fuel used in the program showed sulfur was present at 0.09 weight percent.

A straight-through, can-type combustor is used for long-term, trouble-free operation. From Figure 8, it can be seen that the combustor is mounted vertically and the hot gas stream is exhausted up the insulated stack. The specimens are mounted in a specimen holder (Fig. 10) attached to an electric motor and rotated perpendicular to the hot gas stream at a rate of 1725 rpm. The rotation assures that each of the 14 specimens experience the same test contact at all times between the chromel-alumel thermocoules and a potentiometer-type strip chart recorder and the three-mode temperature controls. Any deviation between the temperature set point and the specimen temperature is sensed in the temperature recorder-controller, which continuously activates an electric-to-pneumatic converter, thereby controlling a pneumatic operated fuel flow control valve. Fuel flow is changed automatically as required to maintain the set temperature.

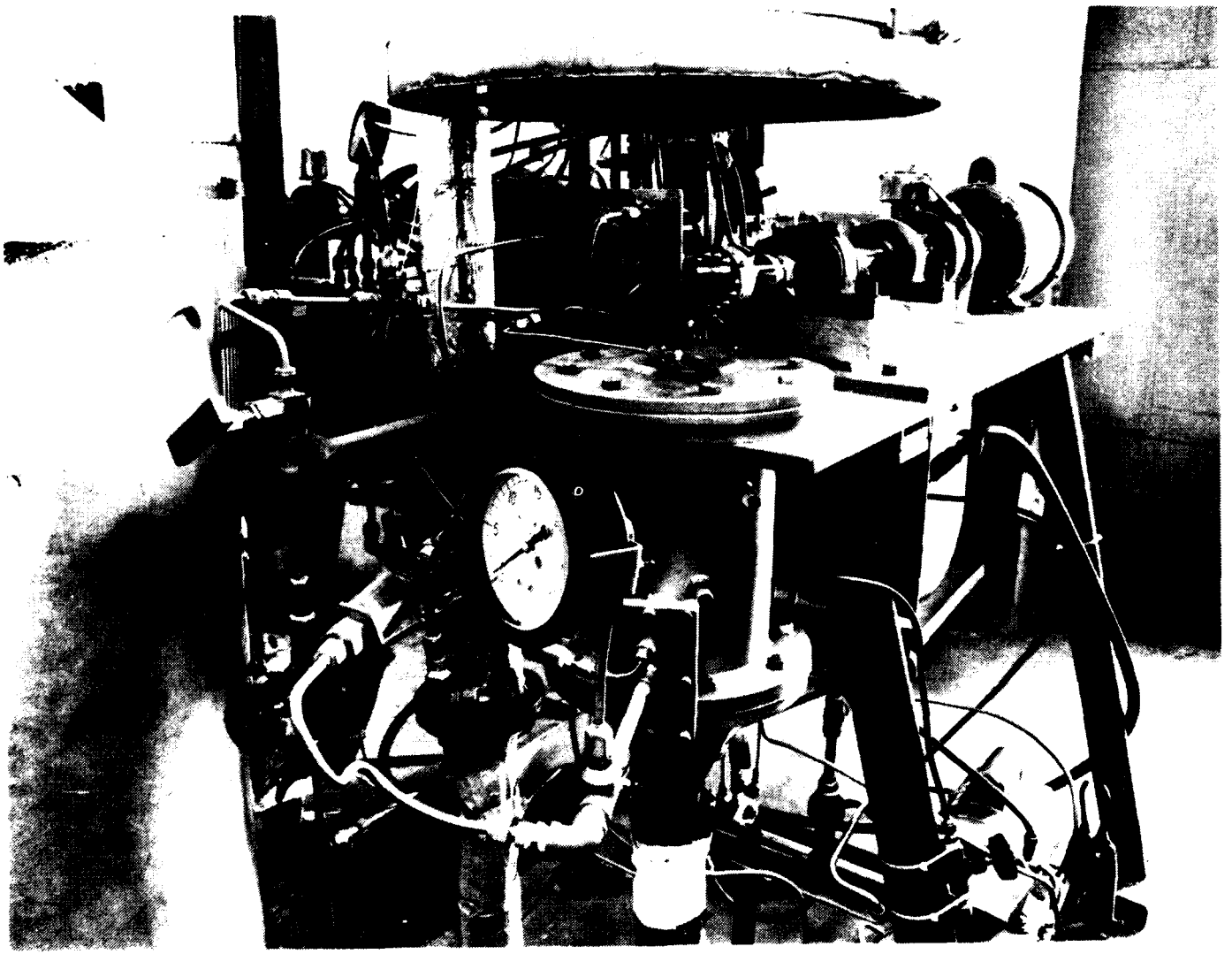

Figure 8. Environmental Simulator Rig

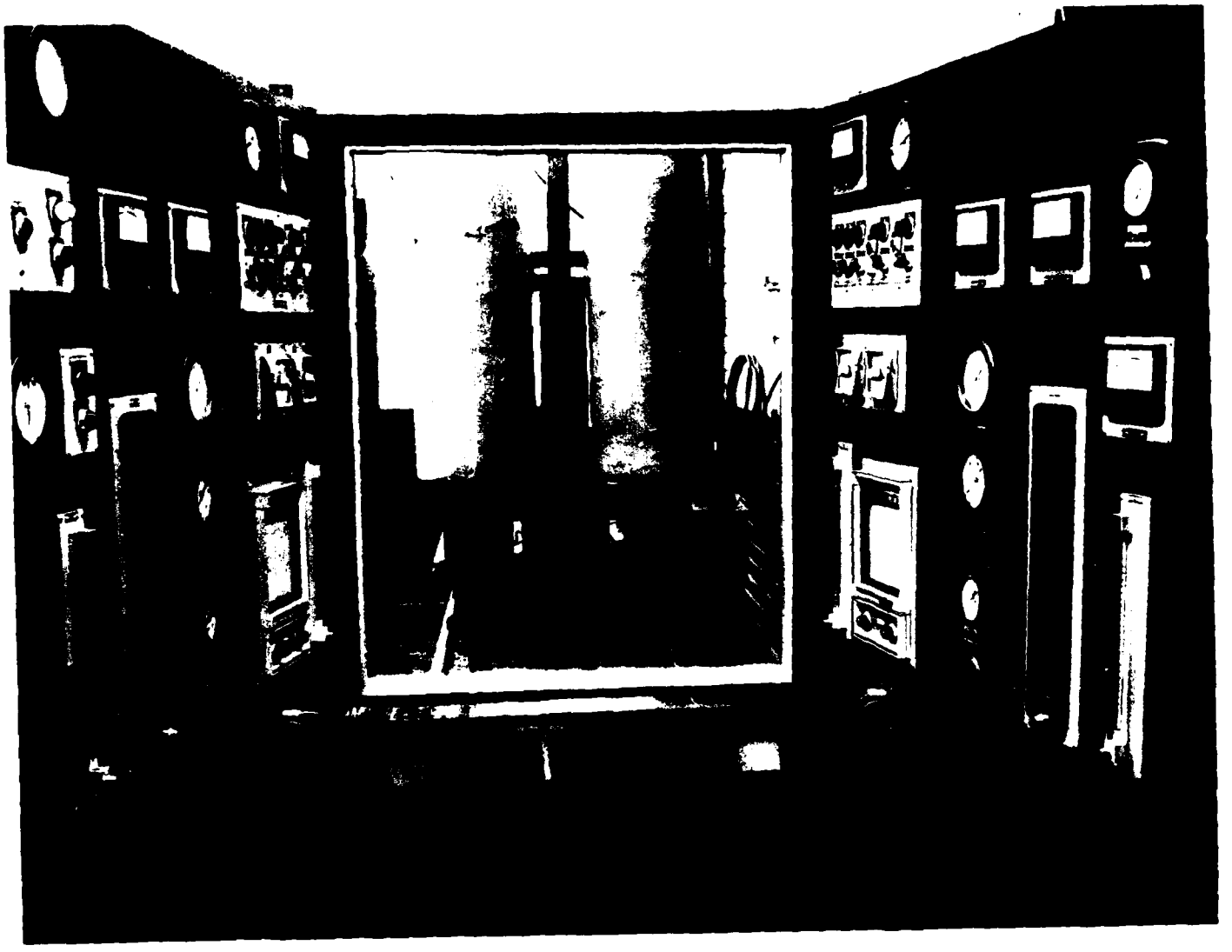

Figure 9. Control Console for Gas Turbine Environmental Simulators

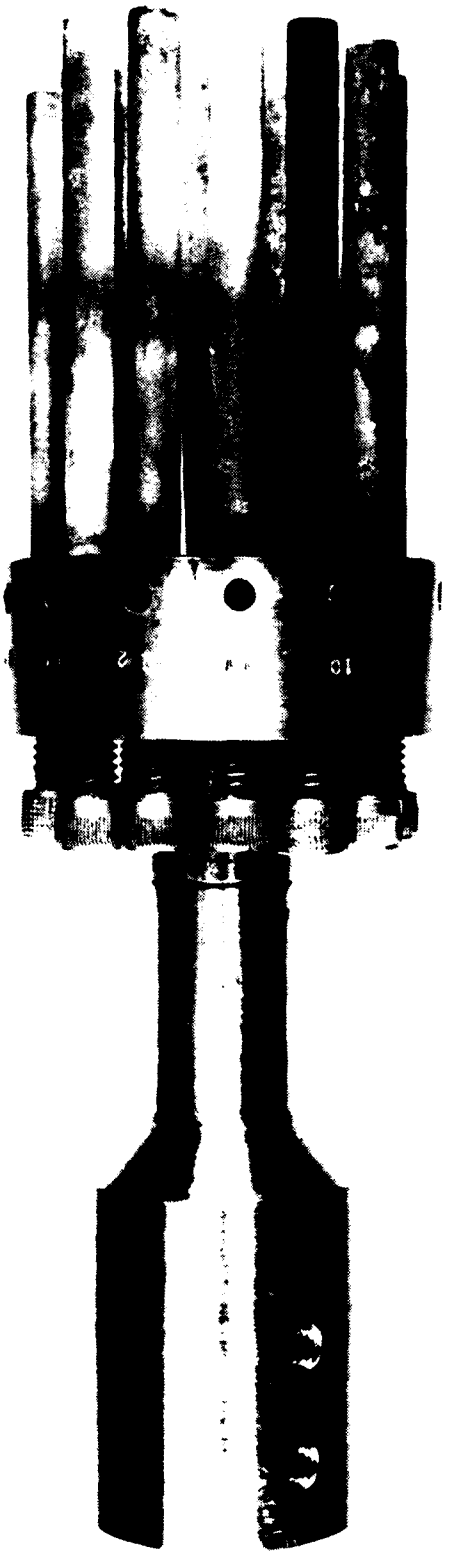

Figure 10. Specimen Holder for Burner Rig Test

Sea water salts were added to the system in two ways. In the first set of hot corrosion tests, the specimens were dipped in an aqueous salt solution (Federal Test Method Standard No. 151, Method 812) of composition as given in Table 9, such that the surfaces receive a salt film of approximately 1 to 2 mg/cm_2. This was repeated at 24- to 48-hour intervals after washing off residual salt deposits. A schematic of the rig setup is shown in Figure 11.

Table 9

Synthetic Sea Water
(F.T.M. Std. No. 151, Method 812)

Salt	Concentration (mg/l)
Potassium Chloride	50
Potassium Bromide	200
Magnesium Chloride	1550
Calcium Chloride (hexahydrate)	240
Sodium Chloride	5040
Sodium Sulfate	770

A different method was used in the second rig test. Instead of dip coating test specimens in sea water solution, the salt solution was introduced into the fuel line and sprayed into the combustor along with the liquid fuel. This allows the salt solution droplets to form dry salt particles in the combustor and impact on the specimens as molten splats, maintaining a corrosive environment throughout the test. The synthetic sea water solution was carefully diluted and pumped into the fuel line so as to obtain sea salt concentration of 4 ppm in the air. A drawing of the setup used is shown in Figure 12. The salt solution was introduced by means of a 3.2 mm (1/8 in.) tube welded within the 6.4 mm (1/4 in.) fuel line and opposing the direction of fuel flow. A little further downstream from the point of entry, both salt solution and fuel are homogenized or mixed in a filter containing eight overlapping pieces of 144 micron wire screen. Figure 13 shows some typical impacted salt particles collected on a metal slide at the approximate location of nearest approach of specimens to the exhaust nozzle.

Rig parameters for both tests are reported in Table 10 and Figure 14 shows the typical specimen temperature profile obtained during testing.

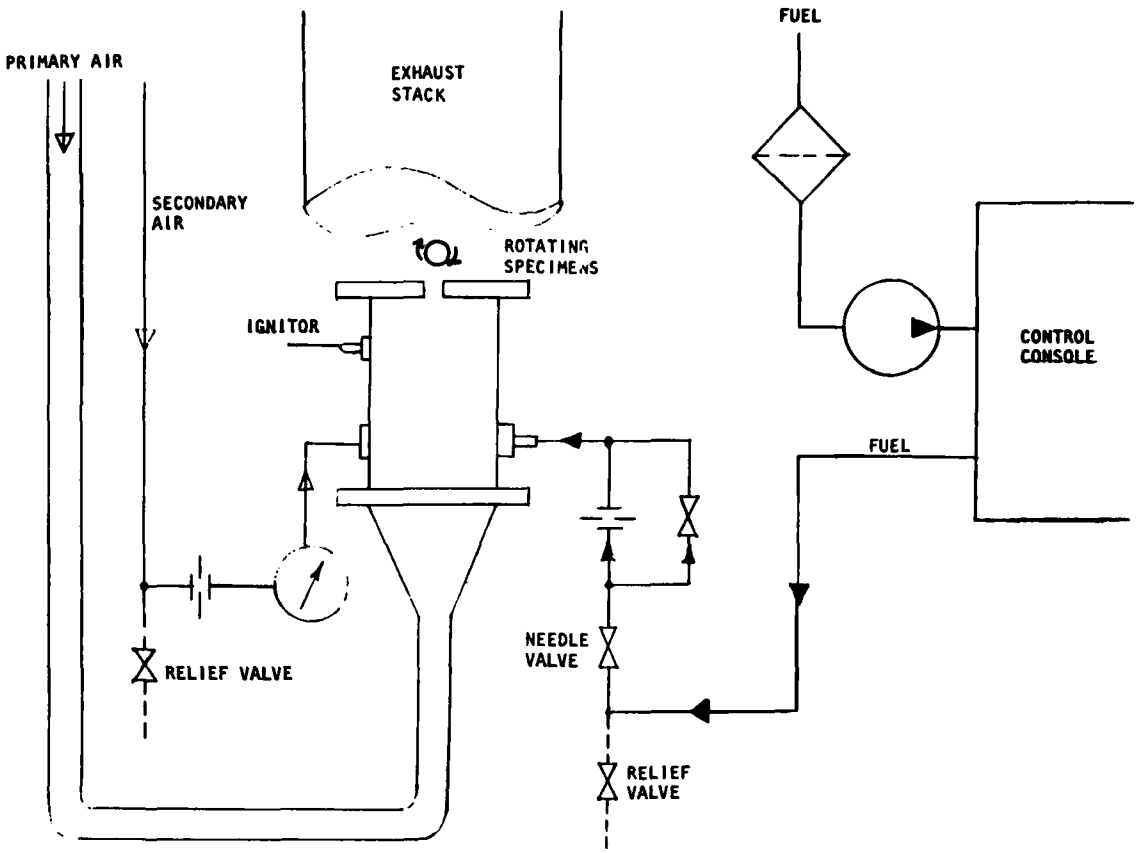

Figure 11. Schematic of Hot Corrosion Rig Burning Uncontaminated Fuel

Determination of Rig Operating Conditions

In order to determine the characteristics of the burner rig test, the key elements of flow, pressure and temperature must be carefully regulated. The major items used to ensure reproducible rig operation are:

- Fuel flow and pressure regulators
- Combustor pressure regulator
- Airflow on five Δp manometers
- Airflow reducing regulator controls
- Temperature controller and recorders

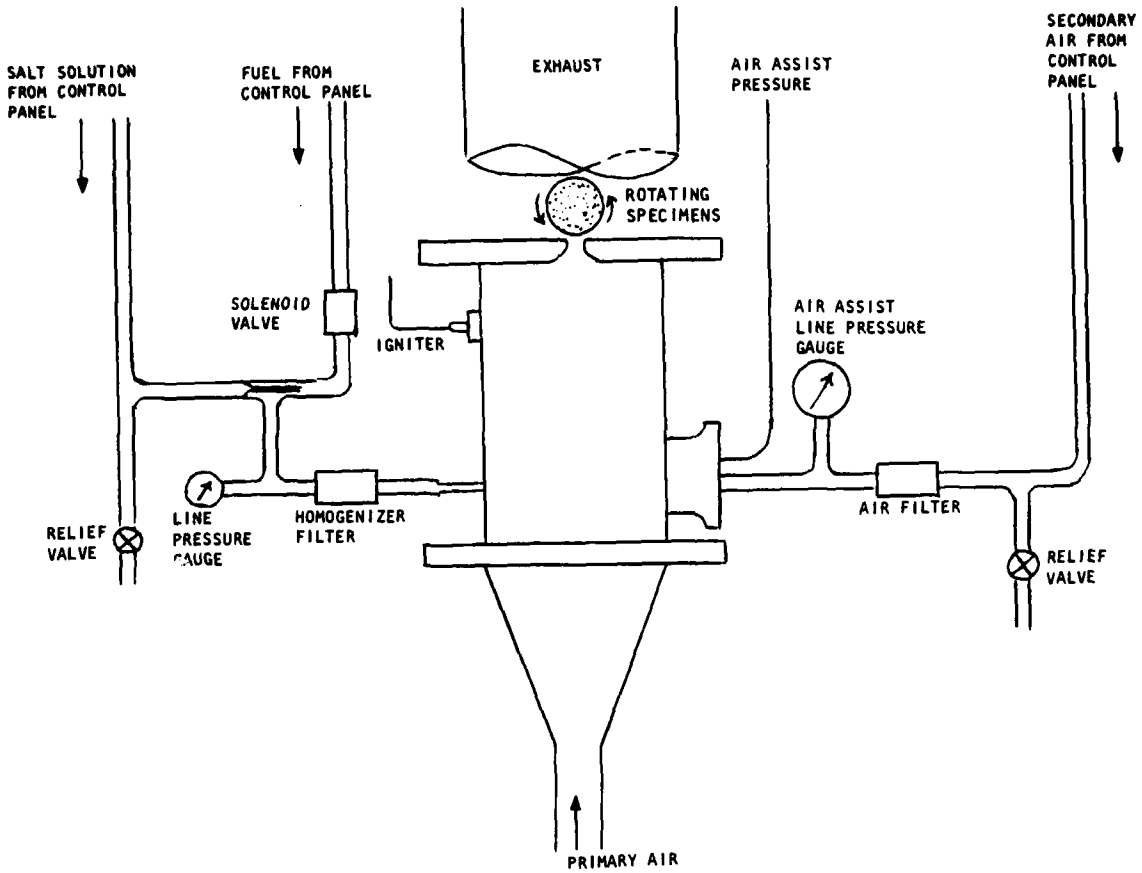

Figure 12. Schematic of Hot Corrosion Rig Burning Salt-Contaminated Fuel

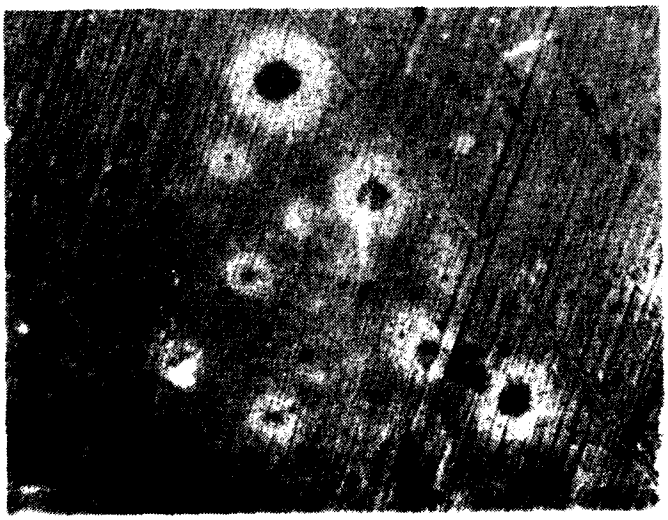

Figure 13.

Salt Particles from Fuel-Salt Solution Mixture

Magnification: 200X

Table 10

Parameters for Hot Corrosion Burner Rig Tests

Parameters	Test No. 1	Test No. 2
Specimen temperature	871°C	871°C
Flame temperature	1110°C	1110°C
Gas velocity	604 m/sec	604 m/sec
Salt	1-2 mg/cm^2	4 ppm in air
Fuel	JP-5	JP-5
Cycle	1 cycle/hour	1 cycle/hour
Combustor pressure	23.2 psia	23.2 psia
Preheat air temperature	160°C	150-325°C
Air assist pressure	29-32 psia	29-32 psia
Duration of test	238 hours	173 hours
Air flow	345 Kg/hr	345 Kg/hr
Fuel flow	9.8 Kg/hr	9.8 Kg/hr
Air/fuel ratio	35.2	35.2

Flow

Fuel flow was measured by means of a Brooks type 1560 (250 mm) Rotormeter Direct-Reading Flow Meter, with a maximum capacity of 20 kg/hr (44 lbs/hr) of JP-5 fuel. Calibration was performed prior to testing, and the fuel flow required to attain temperature and velocity requirements was found to be 9.8 kg/hr (21.6 lb/hr).

The air flow was determined by calculating the incoming air across a 304 stainless steel orifice plate (radius tap) with a 1-inch diameter orifice and a 1.5-inch pipe diameter. The equation for compressible fluid flow through an orifice is:

$$W_a = Y\, C_d M A \sqrt{2g\rho_a\,(P_1-P_2)}$$

where W_a = air flow rate

Y = expansion factor of stainless steel plate

C_d = coefficient of discharge

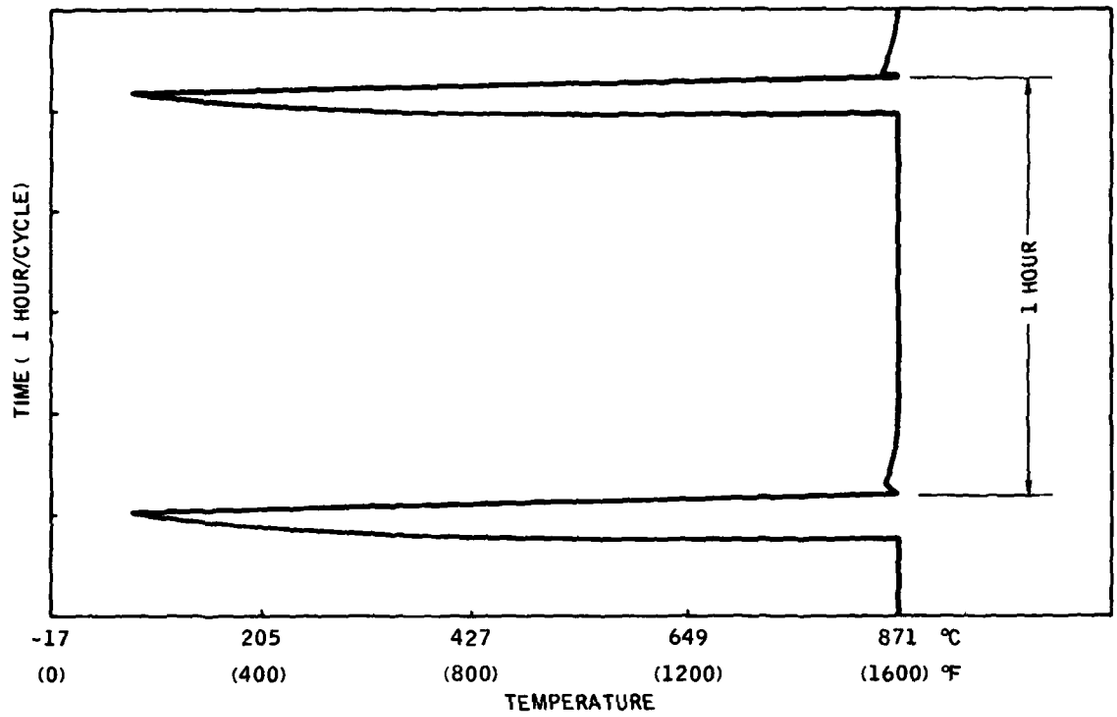

Figure 14. Temperature Profile of Rig Specimens

M = velocity of approach factor

A = area of orifice

g = gravitational constant

ρ_a = air density

P_1 = upstream air pressure

P_2 = downstream air pressure.

A computer program was set up to perform the above calculations over a range of pressure values across the orifice plate and at several inlet air temperature readings. The calculated air flow from the operating conditions used in the rig tests was determined to be 345 Kg/hr (760 lbs/hr). The air-to-fuel ratio value was 35.2.

Temperature

The gas stream temperature was determined in two ways. Initially, a platinum-rhodium thermocouple was placed in the hot gas stream one inch above the nozzle plate and the temperature was read directly, indicating 1110°C (2030°F). A second method was to calculate the gas temperature (assuming complete combustion) based on the fuel-to-air ratio, together with the incoming air temperature. (The incoming shop air going through a heat exchanger in the exhaust stack was preheated before entering the combustor.) For JP-5, the ideal temperature rise for 71°C (160°F) incoming air with a W_f/W_a ratio of 0.284 was found to be 1039°C (1870°F). Combining this with the temperature of the inlet air gives a total flame temperature of 1110°C (2030°F), in excellent agreement with the measured temperature.

Pressure

Since the specimens are located one inch downstream of the combustor nozzle, the static pressure (P_S) may be safely assumed to be very nearly equal to atmospheric pressure. The total pressure of the gas stream (P_R) is the combustor pressure, which was set at 8.5 psig or 23.2 psia. The pressure ratio P_T/P_S was calculated to be 1.5782.

Velocity

From standard gas charts, the function of $V/\sqrt{T}$ can be related to the pressure ratio, P_T/P_S, at given vaues of gamma (ratio of specific heats). Figure 15 shows the chart used to calculate air velocity for gamma = 1.31.

For $P_T/P_S = 5.5782$

$V/\sqrt{T} = 39.7$

Air velocity $= 39.7\sqrt{2490°R} = 1981$ ft/sec $= 604$ in./sec.

Mach number $= 0.87$.

Burner rig tests (oxidation and hot corrosion) performed at GE used low-velocity, high-flow combustors. The oxidation test had a gas temperature of 1149°C with natural gas combustion, and thermal cycles from the test to ambient occurred six times an hour. Both hot corrosion and oxidation specimens were rotated at 5 rpm. The hot corrosion rig was fueled with JP-5.

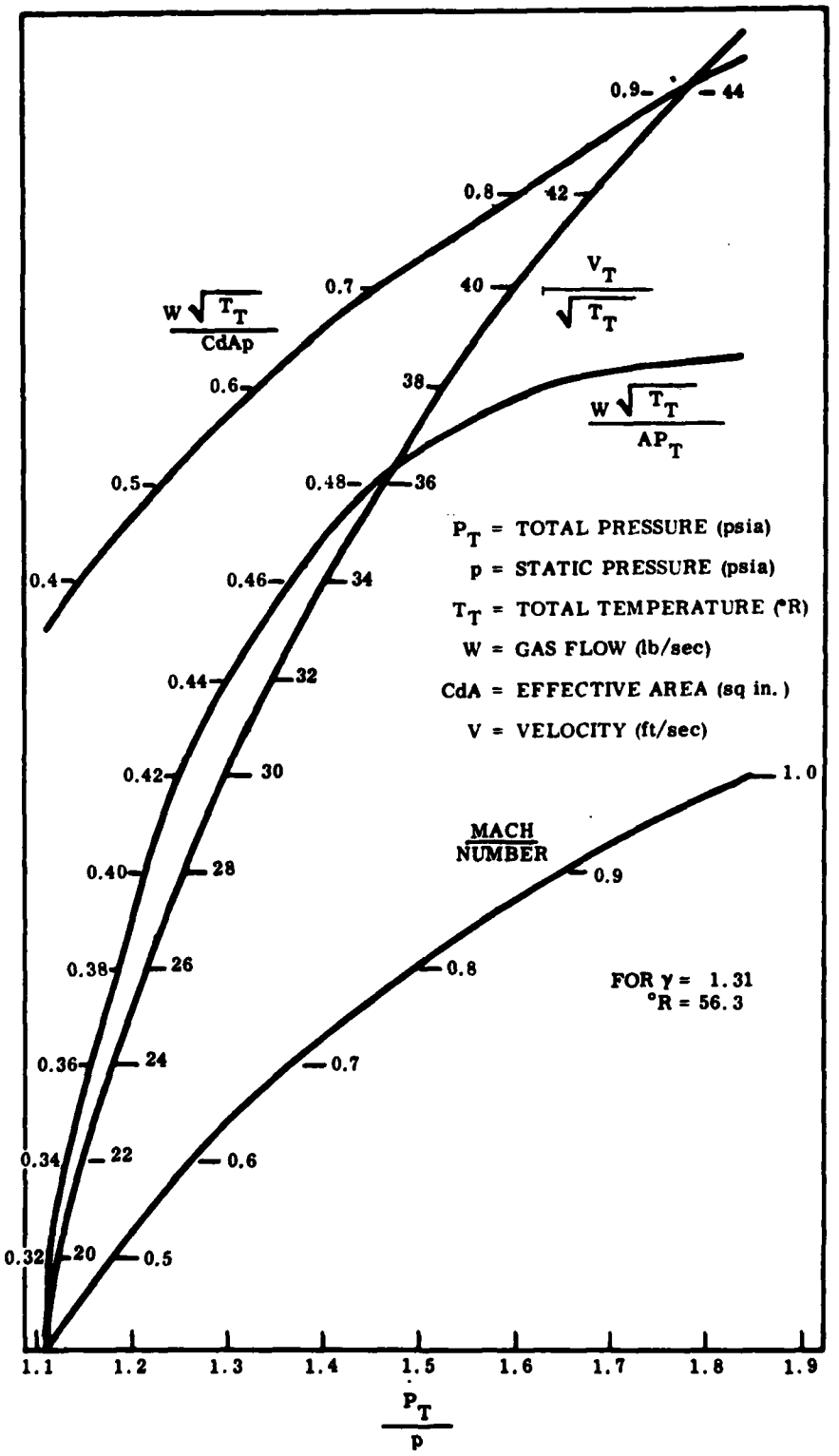

Figure 15. Erosion Rig Gas Chart; For Calculation of Hot Gas Stream Velocity

2.4 METHODS OF EVALUATION

2.4.1 Qualitative and Semi-Quantitative Analyses

Metallography was employed routinely throughout the program to examine microstructure and metallurgical bonding of the coatings to the substrate. Other methods of semi-quantitative analyses utilized include X-ray fluorescence, electron microprobe and scanning electron microscopy (energy dispersive X-ray detection) analyses. In general, standards used were ASTM specified except in cases where the substrate provided a convenient and reliable matrix of known composition.

2.4.2 Cooling Passage Airflow Measurements

One of the considerations in evaluating the coating and coating process is being able to maintain the cooling airflow through the internal passages of the TF34 vane pairs and F101 buckets. The air-cooling passages have to retain their flow characteristics after coating application in order to maintain the designed metal substrate temperature. To check the cold mass flow, the parts were flow checked on a cold flow bench before and after coating to demonstrate the degree of flow constriction induced as a result of the CCRS process. Two fixtures were devised and fabricated for each engine component to alloy controlled flow of shop air through each part to monitor total mass flow. The fixtures are shown in Figures 16 and 17.

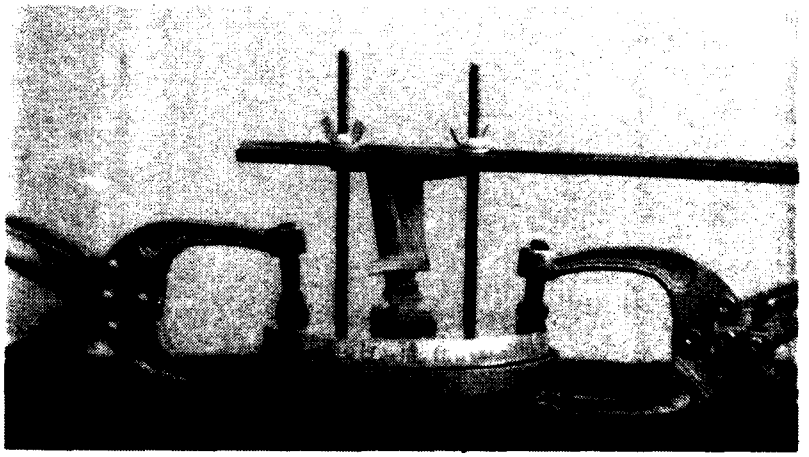

Figure 16. Cold Flow Check of F101 Bucket

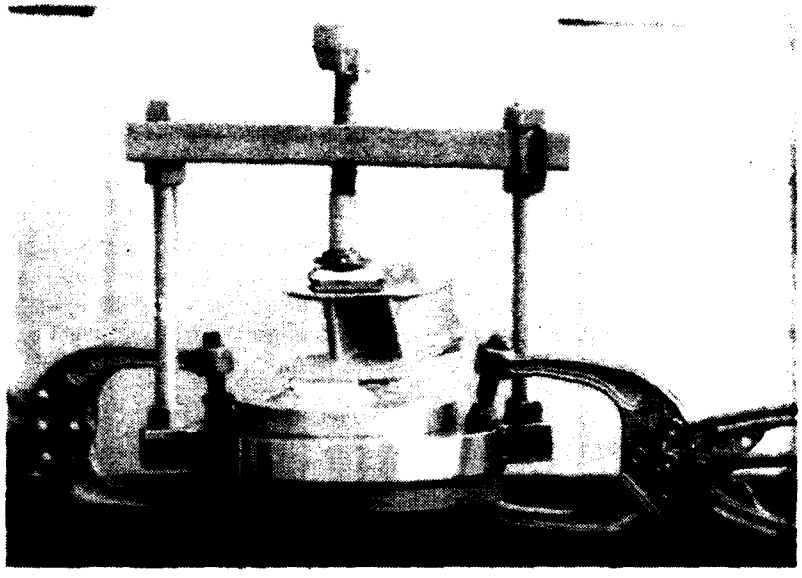

Figure 17. Cold Flow Check of TF34 Vane Pair

3

RESULTS AND DISCUSSION

3.1 TENSILE TESTS

A total of 38 test specimens were tensile tested at Solar under the conditions described in Section 2.3.1. These were divided into two groups, nickel-base Rene' 125 and cobalt-base X-40, and the coatings included the CCRS CoNiCrAlY, CODEP B, PVD CoCrAlY (BC21) and NiCrAlY (BC32). Each alloy was tested in the as-received form and also after heat treatment. The cobalt-base alloy, X-40, was tested in the as-received and coating heat treated conditions.

3.1.1 Tensile Test Data of Coated Rene' 125 Alloy

Table 11 shows that both as-received and heat-treated Rene' 125 had approximately equivalent tensile and yield strengths (0.2% offset) at 899°C, providing baseline data for comparison with coated specimens. The heat-treated specimen exhibited greater elongation and area reduction relative to the as-received specimen. Two lots of CCRS processed CoNiCrAlY coatings were tested at four temperatures, and 899°C was selected as the temperature for comparison with the other coating systems, CODEP B, PVD CoCrAlY (BC21) and NiCrAlY (BC32).

The test results in Table 11 show very good agreement at all test temperatures between the two lots of CCRS processed CoNiCrAlY specimens. The average tensile strength values of the two lots are plotted in Figure 18 as represented by the line drawn through the solid circles. The gradient of the graph shows about 260 MPa loss in strength for each 100°C rise in temperature.

The tensile strength data reported in Table 11 for the various coatings at 899°C are plotted in Figure 18. It appears that all six data points lie within a bond of 70 MPa (or 10 ksi) at 899°C. This would seem to indicate that coating processing followed by the recommended heat treatment did not grossly affect the tensile strength of Rene' 125.

Specimen elongation remained in the 1 to 10 percent range at all temperatures with one exception. Single-cycle CCRS, Lot 9653, coated specimen No. R20 was elongated to 10.9 percent at 899°C. At ambient temperature, specimen No. R56 (Lot 8864, CoNiCrAlY coated) exhibited unusually high elongation relative to its counterpart, No. R96.

Table 11

Tensile Strength of Rene' 125 Alloy

Coating	Specimen Number	Test Temperature (°C)	Test Temperature (°F)	Tensile Strength (mPa)	Tensile Strength (ksi)	Yield Strength 0.2% Offset (mPa)	Yield Strength 0.2% Offset (ksi)	R.A. (%)	Elong. (%)
None (As-Rec'd)	R57	899	1650	764	110.9	586	85.0	2.4	1.5
None (H.T. Only)(1)	R91	899	1650	744	108.0	610	88.5	5.3	3.7
CCRS	R96	25	77	1036	150.3	905	131.4	-	3.9
CoNiCrAlY	R20(2)	899	1650	725	105.2	649	94.2	9.7	10.9
Lot 9653	R76	982	1800	503	73.0	369	53.6	-	3.5
	R55	1093	2000	234	34.0	187	27.2	-	7.7
	R74(3)	899	1650	674	97.8	462	67.0	6.4	9.1
	R94(3)	982	1800	458	66.5	338	49.1	-	3.7
CCRS	R56	25	77	1087	157.7	916	133.1	-	7.0
CoNiCrAlY	R49(2)	899	1650	760	110.3	635	92.1	4.7	5.4
Lot 8864	R60	982	1800	513	74.5	393	57.1	-	4.7
	R61	1093	2000	262	38.0	185	26.9	-	6.4
	R53(3)	899	1650	644	93.6	478	69.4	3.2	5.0
	R50(3)	982	1800	492	71.4	327	47.5	3.2	9.0
Codep B	R83	899	1650	789	114.5	610	88.7	9.0	6.9
	R82(3)	899	1650	703	102.1	500	72.5	8.1	8.2
PVD CoCrAlY (BC-21)	R85	899	1650	779	113.0	596	86.5	8.2	6.8
	R84(3)	899	1650	710	103.0	499	72.4	9.1	9.7
PVD NiCrAlY (BC-32)	R86	899	1650	785	113.9	610	88.7	7.4	6.5

Notes

(1) 1177°C/2 hours, 1079°C/4 hours, 816°C/16 hours.

(2) Single-cycle CCRS CoNiCrAlY coating.

(3) Pre-oxidized at 899°C (1650°F) for 500 hours.

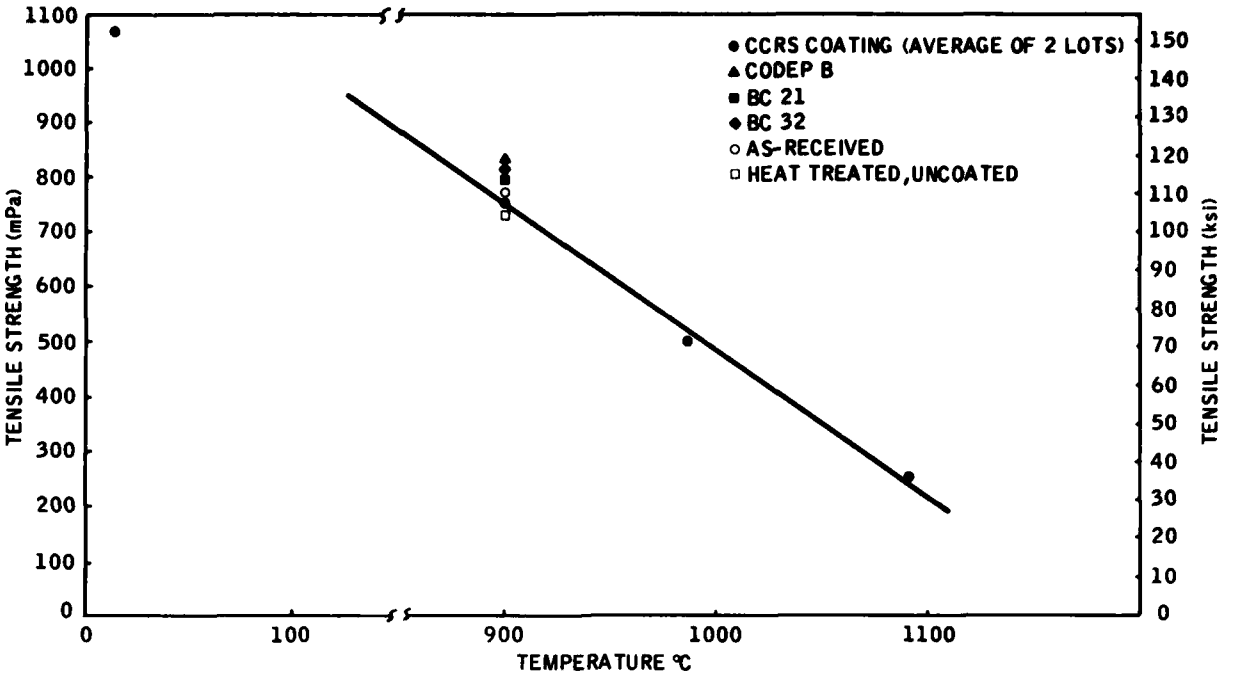

Figure 18. Tensile Strength of Coated Rene' 125 Alloy

Another aspect of this evaluation was to note the effect of long-term, high-temperature exposure on coated alloy. The exposure process was 500 hours in air at 899°C and 982°C. Results show that, generally, all pre-oxidized coated specimens exhibited 10 percent reduction in tensile strength with the exception of CCRS Lot 8864 processed specimen No. R53, which registered a loss of 15 percent at 899°C. The observed degradation of tensile strength may be due to over-aging or the result of interfacial diffusion. Figure 19 shows two CCRS coatings after rupture in the pre-oxidized and unexposed conditions. Note the increased porosity in the pre-oxidized coating and the less distinct demarcation at the coating/substrate interface. Aluminum depletion in the pre-oxidized coating had resulted in breakdown of the beta matrix to discrete pockets of beta in a low aluminum matrix.

3.1.2 Tensile Test Data of Coated X-40 Alloy

X-40 test results are reported in Table 12. Specimen No. X34 (uncoated) was exposed to the CCRS heat cycles and the test results show a small gain in strength at the expense of a drop in ductility. Both as-received and heat-treated specimen tensile properties appeared to fall a little short of the values found in the literature. However, elongation was significantly higher.

The two lots of CCRS processed CoNiCrAlY coated specimens were tested at 25, 899, 982 and 1093°C and the results again showed excellent reproducibility with a maximum difference in strength being not more than 33 MPa or 4.8 ksi. The average ultimate tensile strengths of these two lots are plotted in Figure 20 and the straight line obtained in the elevated-temperature region represents a negative gradient of ≈85 MPa/100°C or 12 ksi/180°F.

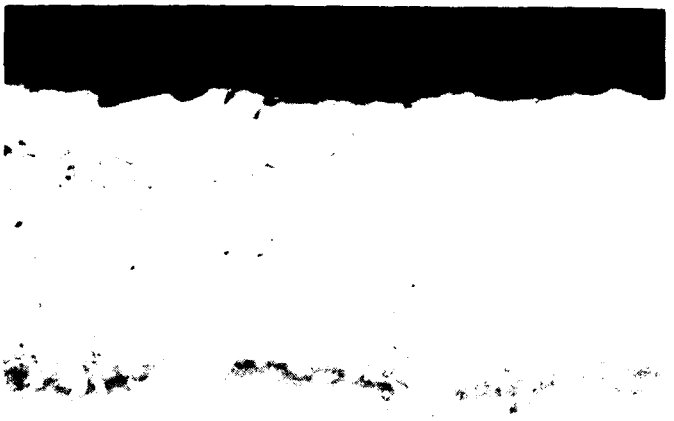

Specimen No. R60

No Pre-oxidation

Coating: CCRS CoNiCrAlY

Etchant: 2% Chromic
Electrolytic

Magnification: 250X

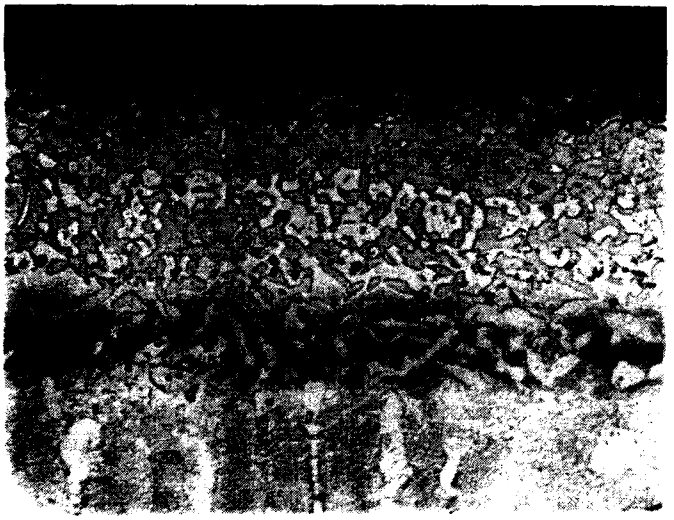

Specimen No. R50

Pre-oxidation

Coating: CCRS CoNiCrAlY

Etchant: 2% Chromic
Electrolytic

Magnification: 250X

Figure 19. Microstructures of Rene' 125 Tensile Specimens With and Without 500 Hours Pre-oxidation at 899°C in Air

Table 12

Tensile Test Data of X-40 Alloy

Coating	Specimen Number	Temperature (°C)	Temperature (°F)	Tensile Strength (MPa)	Tensile Strength (ksi)	Yield Strength (0.2% Offset) (MPa)	Yield Strength (0.2% Offset) (ksi)	R.A. (%)	Elong. (%)
None (As-rec'd)	X17	982	1800	176	25.6	123	17.8	55.9	58.0
None(1) (H.T. only)	X34	982	1800	187	27.2	130	18.9	40.5	44.3
None	See Ref.	982	1800	200	29.0	-	-	-	31.0
CCRS CoNiCrAlY Lot 9653	X26	25	77	712	103.4	484	70.3	0.3	2.5
	X28(2)	899	1650	269	39.1	174	25.2	39.3	35.4
	X40	982	1800	198	28.8	127	18.5	43.4	34.0
	X22	1093	2000	112	16.2	78	11.3	83.2	-
	X38(3)	899	1650	302	43.8	208	30.2	34.2	38.3
	X24(3)	982	1800	206	29.9	138	20.1	43.4	34.8
CCRS CoNiCrAlY Lot 8864	X25	25	77	737	107.0	477	69.3	0.3	2.5
	X39	899	1650	290	42.1	207	30.0	39.3	41.6
	X27(2)	982	1800	198	28.7	120	17.4	47.2	50.3
	X21	1093	2000	108	15.7	81	11.8	86.8	58.5
	X37(3)	899	1650	285	41.4	187	27.2	35.4	35.6
	X23(3)	982	1800	207	30.0	133	19.3	40.2	31.7
CODEP B	X30	899	1650	278	40.3	179	26.0	38.2	40.0
	X14	982	1800	222	32.2	147	21.4	59.0	34.0
	X13(3)	982	1800	222	32.2	138	20.1	42.1	37.6
PVD NiCrAlY (BC-32)	X16	982	1800	198	18.7	133	19.3	63.2	43.4
	X15(3)	982	1800	214	31.0	136	29.8	51.0	43.8

(1) Simulated coating cycle of 1179°C/16 hours in argon atmosphere.
(2) Single-cycle CCRSCoNiCrAlY coating.
(3) Pre-oxidized at 982°C for 500 hours.
Ref. Nickel Base Alloys, International Nickel Company, 1964 edition.

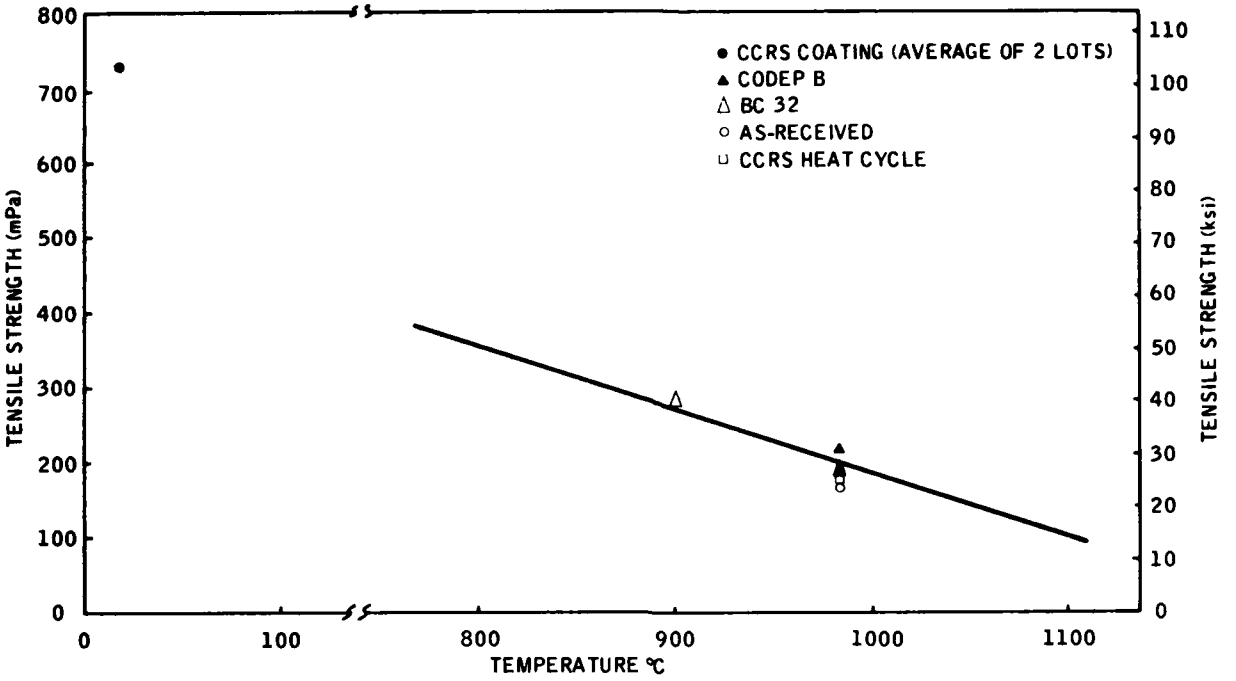

Figure 20. Tensile Strength of Coated X-40 Specimens

Two other coating systems were also tensile tested at 982°C, CODEP B and PVD NiCrAlY. Specimen No. X14, coated with CODEP B, exhibited 11 percent greater tensile strength than either the CCRS or PVD coated specimens. The yield strengths of these coated specimens ranged from 120 MPa (CCRS) to 147 MPA (CODEP B), the total range being not more than 27 MPa or 4 ksi. At 899°C, data for the CCRS processed specimens and the CODEP B specimens appeared to be equivalent. In general, the reduction in area and percent elongation at elevated temperature were high, i.e., >34 percent. There also appeared to be a trend toward greater reduction in area and elongation values with increase in temperature. At 1093°C, maxima of 83 and 86 percent reduction in area were observed for the CCRS processed specimens.

A pre-oxidation exposure (500 hours in air at 982°C) was imposed on several coated test specimens prior to testing. The 899°C tensile strength of pre-oxidized CCRS processed specimens (Nos. X37 and X38) differed minimally from unexposed specimens. At 982°C, a small increase in ultimate tensile strength was noted for the CCRS specimen and also for the pre-oxidized CODEP B and PVD NiCrAlY specimens. The 899 and 982°C yield strengths of CCRS specimens appeared to have suffered from the 500-hour pre-oxidation while those of the CODEP B and PVD specimens were unaffected.

Figure 21 shows the microstructure of pre-oxidized and unexposed tensile specimens near the fracture surface. Note the formation of a discrete secondary phase in the coating matrix of the pre-oxidized specimen as beta NiAl deteriorated to gamma and gamma prime. Furthermore, interdiffusion across the interface resulted in merging the coating layer with the substrate.

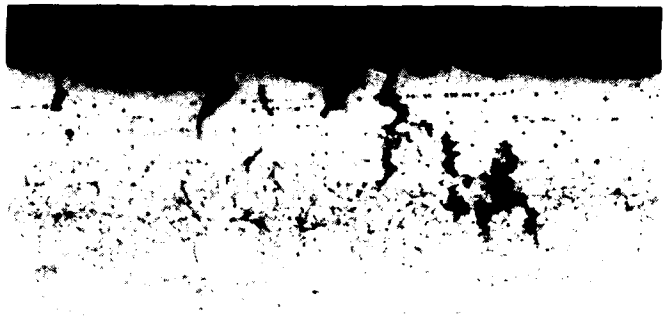

Specimen No. X40

No Pre-oxidation

Coating: CCRS CoNiCrAlY

Etchant: 2% Chomic

Magnification: 250X

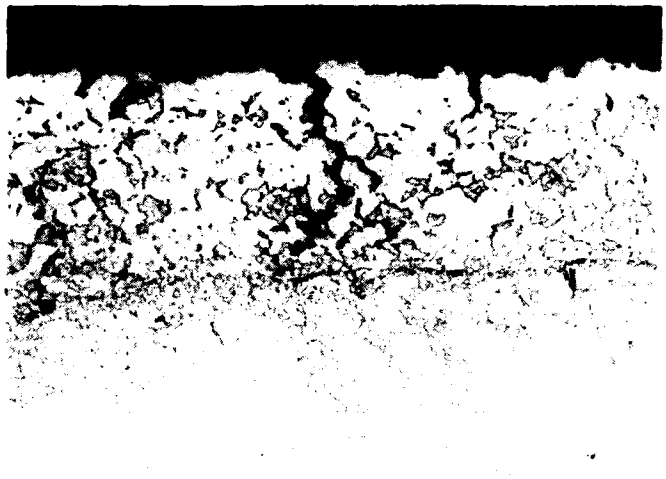

Specimen No. X24

Pre-oxidation

Coating: CCRS CoNiCrAlY

Etchant: 2% Chromic

Magnification: 250X

Figure 21. Microstructures of X-40 Specimens After Tensile Testing With and Without 500-Hour Pre-oxidation at 987°C in Air

3.1.3 Summary Of Test Results

The tensile properties of Rene' 125 and X-40 alloys are not grossly affected by coating processing. The difference between coated and uncoated specimens were small and would probably be contained with the minimum 3σ band.

Of the four coatings evaluated, little difference was noted in tensile behavior other than the usual scatter typically found in such tests. Therefore, it can be concluded that tensile equivalency was established for CCRS (two lots), CODEP B, PVD NiCrAlY and CoCrAlY coatings.

3.2 STRAIN TOLERANCE/DBTT

One of the important characteristics of the coating processes and effects on substrate bulk properties is the ductility of the finished coating. Cracks which appear in the coating due to substrate strain can lead to stress concentration points and subsequent cracking and failure of the substrate itself. The strain values which are experienced in a typical gas turbine airfoil range between 0.15 and 0.35 percent.

Both STI and GE conducted strain tolerance tests on the CCRS CoNiCrAlY coating and results will be discussed together. Table 13 summarizes STI's data obtained from testing 20 coated Rene' 125 specimens. (Strain tolerance testing of coated X-40 alloy was not a part of the program.) Two powder lots of the CCRS coating were used. Some of the CCRS coatings reported in Table 13 are the single-cycle CCRS coating (see Sec. 2.1), the predecessor of the two-cycle CCRS process. Because of the unusual ductility of this single-cycle coating, it has been incuded here for discussion.

The data reported in Table 13 are plotted in Figure 22. The broken curve represents GE data. Note that Lot 8864 was processed mostly with the single-cycle CCRS method while Lot 9653 underwent the two-cycle process. There appears to be a significant ductility difference between the two coatings, which is clearly evident in Figure 22. The single-cycle coating exhibited excellent strain tolerance as shown by the upper curve in the band. The room-temperature, strain-to-cracking values were 0.5 percent, which is significantly higher than the two-cycle coating, PVD NiCrAlY or CODEP B coatings. The two-cycle CCRS coating data points form the lower curve of the envelope.

The broken line representing GE's results appears to fall below STI's two-cycle ductility curve. Generally, the DBTT is obtained by the intersection of the linear portions of the strain-to-cracking versus temperature plot. Based on their data, GE reported a DBTT in the range 677 to 732°C (1250 to 1350°F). STI's data extrapolates to about 650°C for the two-cycle coating. In the case of the single-cycle coating, there appears to be no sharp transition between ductile and brittle behavior which is indicative of the highly ductile nature of this material.

Table 13

Strain Tolerance Test Results (Rene' 125 Alloy)

Coating	Specimen Number	Temperature (°C)	Temperature (°F)	Strain-to-Cracking (%)
CCRS CoNiCrAlY Lot 8864	R46	25	77	0.7(1)
	R47	427	800	2.3(1)
	R88	427	800(2)	[8.7](1)
	R62	482	900	0.9
	R48	538	1000	2.9(1)
	R89	649	1200	[8.8](1)
	R90	760	1400	[6.5](1)
CCRS CoNiCrAlY Lot 9653	R63	25	77	0.4
	R77	427	800	2.78(1)
	R58	427	800(2)	[5.4](1)
	R95	482	900	0.4
	R64	538	1000	0.5
	R75	649	1200	0.5
	R93	760	1400	[>1.0](3)
PVD NiCrAlY (BC-32)	R42	427	800	0.3
	R41	427	800(2)	2.0
	R45	538	1000	0.6
Codep B	R29	427	800	0.1
	R28	427	800(2)	0.2
	R30	538	1000	0.5

Notes

(1) CCRS single-cycle process. See explanation in Sec. 2.1. All other CCRS coatings were reaction sintered in two furnace cycles.

(2) These specimens were furnace oxidized in air at 982°C (1800°F) for 100 hours.

(3) Furnace malfunctioned and temperature dropped to 315°C (600°F) and specimen failed at 2.3 percent strain.

[ ] Specimen substrate failed.

Figures 23 and 24 show the microstructure of two CCRS coatings. Note that the single-cycle coating appears to be multi-phased throughout while the two-cycle coating has a single-phase beta layer near the coating surface. The additional second heat cycle in the latter may have caused further diffusion of aluminum into the coating, resulting in a more brittle matrix phase at the surface.

At 538°C, both PVD NiCrAlY and CODEP B coatings fall within the envelope of the CCRS curves. However, at the lower temperature of 427°C, neither coating was as ductile as the CCRS coatings. The CODEP B coating, in particular, was extremely brittle, having cracked at 0.1 percent strain.

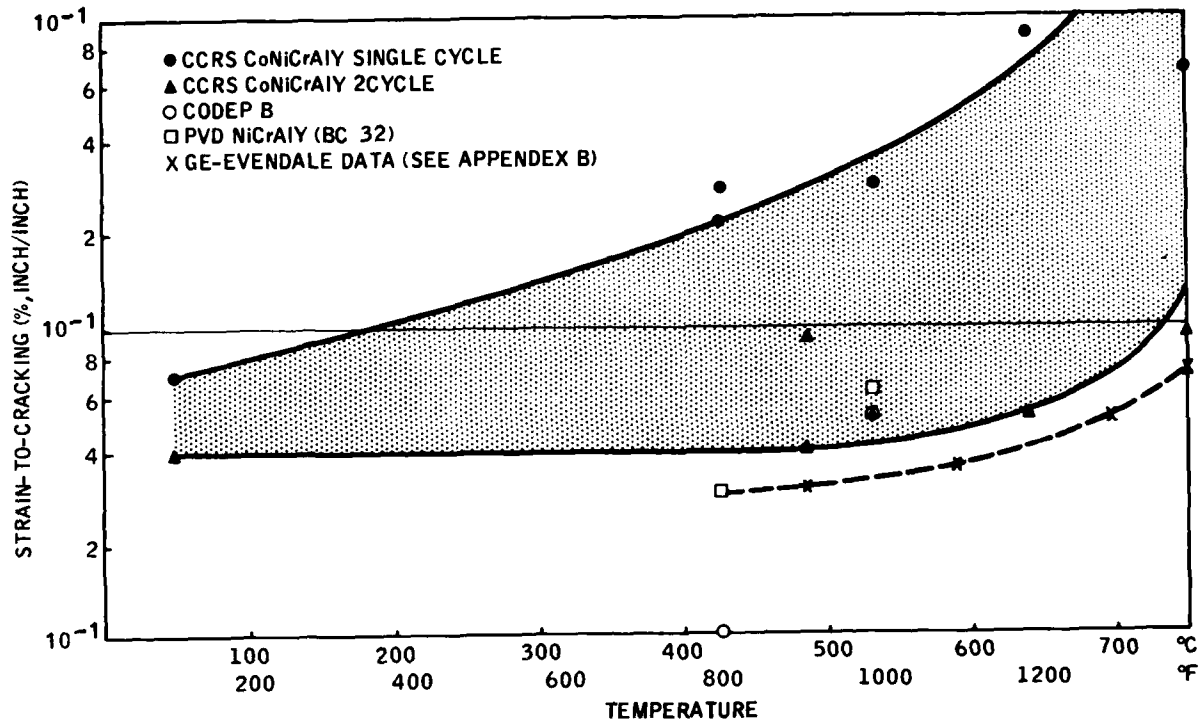

Figure 22. Strain-to-Cracking Versus Temperature Curves for Coated Rene' 125 Alloy

Figure 23.

Failed Strain Tolerance Specimens With Single-Cycle CCRS CoNiCrAlY Coating on Rene' 125

Specimen No. R77

Magnification: 250X

Figure 24.

Failed Strain Tolerance Specimen With Two-Cycle CCRS CoNiCrAlY Coating on Rene' 125

Specimen No. R95

Magnification: 250X

Four coated specimens were pre-oxidized at 982°C for 100 hours and strained at 427°C until cracks were initiated. The results in Table 13 show that coating ductiity was enhanced in all cases. Pre-oxidized CODEP B was twice as ductile as unaged CODEP B coating. The strain tolerance of the PVD NiCrAlY coating was raised from 0.3 to 2.0 percent, a ten-fold increase. The single-cycle CCRS coating also experienced notable increases in ductility as a result of the pre-oxidation, viz., 2.3 to 8.7 percent and 2.78 to 5.4 percent. Note that the latter values are actually strain values for the substrate itself since the specimen failed at these strain levels.

The conclusions that may be drawn from this set of tests are summarized below:

1. Based on STI's data, the two-cycle CCRS CoNiCrAlY coating was, at the very least, equivalent in ductility to PVD NiCrAlY (BC32) and superior to CODEP B.

2. The CODEP B coating had the poorest overall strain tolerance of the coatings tested.

3. Pre-oxidation at 982°C significantly improved the ductility of the CCRS and BC32 coatings strained at 427°C.

4. The single-cycle CCRS CoNiCrAlY coating exhibited the highest ductility.

5. All coatings tested, with the exception of CODEP B, appeared to be sufficiently ductile at strain values which are expected in a typical gas turbine airfoil.

6. The DBTT of the two-cycle CCRS CoNiCrAlY coating was about 650°C according to STI's results. GE reported values in the 677 to 732°C range.

3.3 CYCLIC FATIGUE RESULTS

The application of a protective coating to the surface of hot section components such as vanes and blades may have beneficial or deleterious effects on performance under cyclic loading. This is usually a consequence of differences in elastic modulus and yield strength of the coating and substrate alloy. In general, the fatigue properties of the applied coatings are poorer than in the underlying substrate, and the strain cycling experienced during engine service causes cracks to initiate in the coating, providing a direct path to oxidation attack.

Cyclic fatigue tests at 760°C (1400°F) were conducted on Rene' 125, X-40 and MA754 alloys coated with three types of coatings, simple aluminide (CODEP B), PVD (NiCrAlY and CoCrAlY), and CCRS (CoNiCrAlY) coatings. The objective was to compare the effects of these coatings on the substrate alloy in the thermomechanical strain cycling situation that is typically found in service. The 760°C fatigue life of coated test specimens and the test conditions are summarized in Table 14.

The first group of Rene' 125 specimens was subjected to tension-tension type cycles at a rate of 20 cycles per minute at temperature. This low frequency was selected as representative of the cyclic stresses present during engine transients. The fatigue life data show considerable variation even within the same coating lot. The best performance obtained was with specimen No. R11, coated with the CCRS Lot 8864 CoNiCrAlY, which survived over 30,000 cycles before the substrate failed. Figure 25 shows the microstructure of this coated specimen. Note the absence of surface or subsurface cracks in the coating. In general, the two lots of CCRS coated specimens had a minimum life of 2200 cycles, as compared to those specimens coated with CODEP B and CoCrAlY, all of which failed at less than 2000 cycles. Of the three test pieces which were oxidized for 500 hours at 899°C prior to testing, no noticeable loss was observed. Specimen No. R1, CODEP B coated and aged, failed upon loading while No. R7 lasted 3600 cycles, which is well within the wide scatter band of data points for the Lot 8864 specimens. Another coated (Lot 9653) and oxidized specimen, No. R9, appears to have been slightly affected adversely by the 500-hour soak.

The second group of Rene' 125 specimens were all exposed for 500 hours in an oxidizing environment at 899°C. However, the cycle frequency used in comparing fatigue life was higher, 20 cycles per second. A single specimen of each coating was available, and the results indicate that the CODEP B coated specimen was the most short-lived of the three. Both lots of CCRS processed specimens had fatigue lives more than one order of magnitude greater than the CODEP B specimen. A typical example of the CCRS CoNiCrAlY coating microstructure after testing is shown in Figure 26. Note the formation of a secondary phase in the grain boundaries and the wide interface band. The fine equiax grain structure of the coating is in general a unique feature not seen in any other overlay or diffusion formed coating.

Table 14

Cyclic Fatigue Test Results at 760°C (R=0.2)

Coating	Specimen Number	Maximum Stress (ksi)	Minimum Stress (ksi)	Cycles to Failure
Rene' 125 Alloy	(Frequency = 20 cpm)			
CODEP B	R1(1)	127	27	0(2)
	R3	136	27	500
	R4	136	27	200
PVD CoCrAlY (BC-21)	R5	137	27	900
	R6	136	27	1,700
CCRS CoNiCrAlY Lot 8864	R7(1)	136	27	3,600
	R11	136	27	32,900
	R12	136	27	2,300
	R21	136	27	2,200
	R25	136	27	7,300
CCRS CoNiCrAlYY Lot 9653	R9(1)	136	27	1,900
	R13	136	27	2,800
	R14	136	27	5,800
	R17	136	27	3,800
	R18	136	27	2,700
Rene' 125 Alloy	(Frequency = 20 cps)			
CODEP B	R2(1)	125	25	100
CCRS CoNiCrAlY Lot 8864	R8(1)	125	25	5,100
CCRS CoNiCrAlY Lot 9653	R10(1)	125	25	3,300
X-40 Alloy	(Frequency = 20 cps)			
CODEP B	X1	76	15	4,100
	X2	76	15	4,500
PVD NiCrAlkY (BC-32)	X3	76	15	7,900
	X4	76	15	27,111
CCRS CoNiCrAlY Lot 8864	X5	76	15	1,100
	X9	76	15	4,600
	X10	76	15	3,100
CCRS CoNiCrAlY Lot 9653	X7	76	15	700
	X11	76	15	4,000
	X12	77	15	5,600
MA754	(Frequency = 20 cps)			
PVD CoCrAlY (BC-21)	A1	60	12	3,200
CCRS CoNiCrAlY Lot 8864	A2	60	12	3,200
	A3	60	12	4,200
	A4	60	12	5,900
CCRS CoNiCrAlY Lot 9653	A5	60	12	7,600
	A6	60	12	14,500
	A7	60	12	9,100

(1) Pre-oxidized at 899°C for 500 hours.
(2) Failed on loading.

Specimen No. R11

Coating: CCRS CoNiCrAlY, Lot 8864

Magnification: 250X

Etchant: 2% Chromic

Figure 25. Microstructure of CCRS CoNiCrAlY Coated Rene' 125 Fatigue Specimen After 3.29×10^4 Cycles at 20 Cycles/Minute (R = 0.2) at 760°C

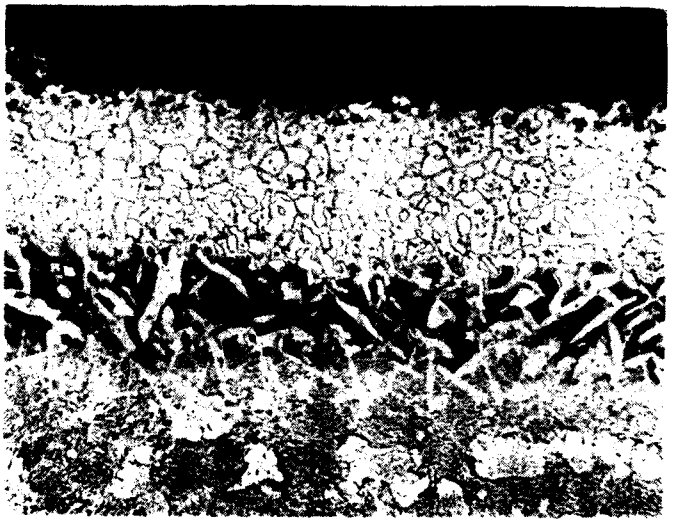

Specimen No. R8

Coating: CCRS CoNiCrAlY, Lot 8864

Magnification: 250X

Etchant: 2% Chromic

Aged: 500 Hours at 899°C in Air

Figure 26. Microstructure of Pre-Oxidized CCRS CoNiCrAlY Coated Rene' 125 Fatigue Specimens After 5.1×10^3 Cycles at 20 Cycles/Second (R - 0.2) at 760°C

All coated X-40 specimens were tested at a frequency of 20 cycles per second, Table 14. Once again, reproducibility was poor with one of the specimens, No. X14, exhibiting a fatigue life an order of magnitude greater than the others. Specimens coated with PVD NiCrAlY (BC32) appeared to have longer fatigue lives than either the CODEP B or the CCRS coated cobalt-base specimens. The latter two coated specimens performed equivalently. Figures 27 and 28 show the microstructure of a PVD NiCrAlY coated specimen and a CCRS CoNiCrAlY coated specimen, respectively. In the case of the former, no coating cracks were observed and coating structure appeared to be entirely intact with a single row of small voids forming in mid-zone. The coating surface was unaffected, as was the interface. Figure 28 shows the presence of numerous voids and cracks in the CCRS CoNiCrAlY matrix after fatigue testing.

Another nickel-base alloy was selected for fatigue testing, MA754. Seven coated specimens were cycle fatigued at 760°C at a frequency of 20 cycles per second. The results, Table 14, indicate that the CCRS CoNiCrAlY coated specimens performed equal or better than the PVD CoCrAlY coated specimen. There appeared to be a performance difference between Lot 9653 and Lot 8864 with a factor of two favoring Lot 9653. This disparity between the two CCRS coating lots is the only indication of any measurable difference of the two batches in the results obtained by STI.

A typical example of the CCRS coating on MA754 after fatigue testing is shown in Figure 29. Note the fine grained layer near the interface and the absence of any cracks.

Specimen No. X4

Coating: PVD NiCrAlY (BC32)

Magnification: 250X

Etchant: 2% Chromic

Figure 27. Microstructure of PVD NiCrAlY Coated Fatigue Specimen After 2.7×10^4 Cycles at 20 Cycles/Second (R = 0.2) at 760°C

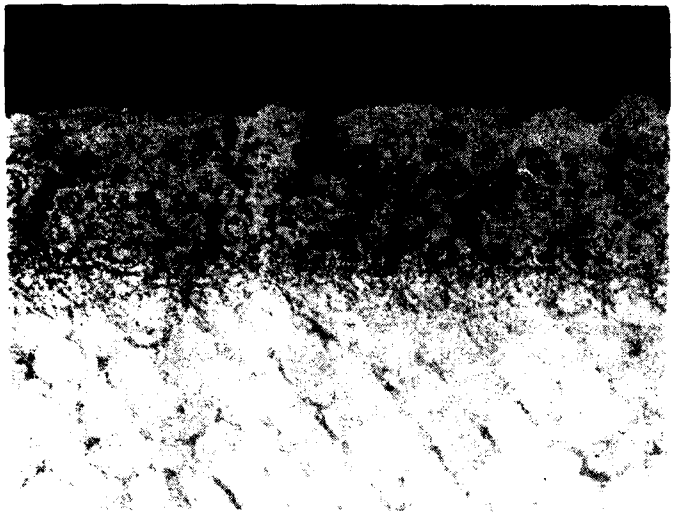

Specimen No. X12

Coating: CCRS CoNiCrAlY, Lot 9653

Magnification: 250X

Etchant: 2% Chromic

Figure 28. Microstructure of CCRS CoNiCrAlY Coated Fatigue Specimen After 5.6×10^3 Cycles at 20 Cycles/Second (R - 0.2) at 760°C

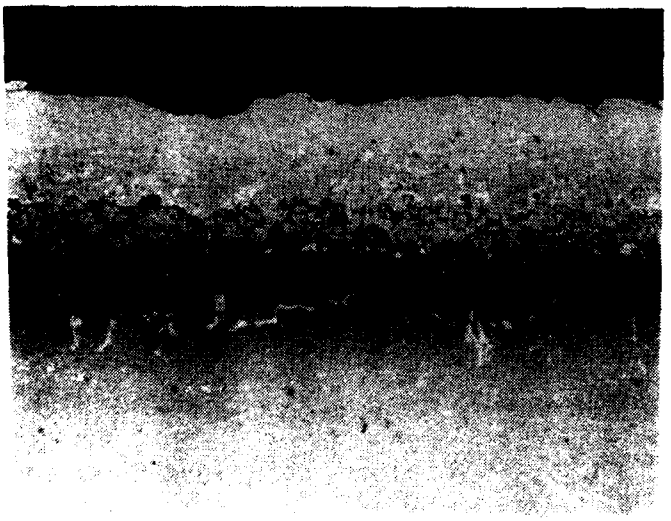

Specimen No. A6

Coating: CCRS CoNiCrAlY, Lot 9653

Magnification: 250X

Etchant: 2% Chromic

Figure 29. Microstructure of CCRS CoNiCrAlY Coated MA754 Fatigue Specimen After 1.45×10^4 Cycles at 20 Cycles/Second (R = 0.2) at 760°C

In conclusion, CCRS CoNiCrAlY coated nickel-base alloys (Rene' 125 and MA754) appeared to have the better fatigue life, with cycle stresses of 20 cycles per second at 760°C, than CODEP B and PVD CoCrAlY. This is also true in the case of CCRS coated Rene' 125 alloy at the lower frequency of 20 cycles per second. However, the same coatings when applied to the cobalt-base alloy, X-40, were ranked differently. The PVD NiCrAlY coated specimens exhibited the best life while the CODEP B and CCRS CoNiCrAlY coated specimens were equivalent in performance.

3.4 HOT CORROSION TESTS

Burner rig hot corrosion testing of various coating/substrate combinations were performed at STI and GE. STI combustor rigs were operated at high velocity (0.85 Mach number) using JP-5 fuel with a specimen temperature of 870°C (1600°F). Introduction of salt has been described in Section 2.3.4. The GE test used low-velocity burners which were also fueled with JP-5, and specimen temperature was 927°C (1700°F) with 5 ppm salt in the gas stream.

3.4.1 Rene' 125

Surface appearance of coated Rene' 125 after 25 and 239 hours of testing at STI are shown in Figures 30 and 31. At 25 hours, PVD NiCrAlY showed some coating distress while the others were essentially unaffected. At the end of 239 hours, areas of pitting attack were observed on NiCrAlY coated specimen No. S14. Subsequent metallography revealed that the CODEP B coating exhibited good resistance against the hot corrosion environment, as can be seen in Figures 32 and 33. (The "cooler zone" microstructure was located approximately 2.5 cm away from the center of the hot zone.) However, note that while the CODEP B coating is virtually 100 percent protective severe cracking was found as a result of the thermal cycling. In Figure 33B, cracking at 45-degree angles appeared to be aggravating coating spallation and allowed corrodents to penetrate to the interface.

Figure 34 shows the microstructure of PVD CoCrAlY after 174 hours of testing. Coating continuity was good with no cracking or spallation. However, the coating itself showed internal oxidation and porosity. The PVD NiCrAlY coating exhibited poor corrosion resistance. Figures 35 and 36 show microstructures of PVD NiCrAlY coated Rene' 125. In the hot zone the coating was initially 100 percent penetrated with widespread voiding and internal oxide formation. Note that in Figure 36B corrosion attack was concentrated in the leaders which are the weakest structural feature in PVD coatings. These leaders provide a direct path for gaseous corrodents to the interface and substrate.

CCRS CoNiCrAlY coating applied to Rene' 125 performed best in hot corrosion testing. Typical microstructures are shown in Figure 37. Kirkendall voids are noted in the coating as aluminum is depleted and beta-NiAl is converted to low aluminum phases (gamma solid solution). Specimen No. S4 was found to be locally degraded, as shown in Figure 38, with a maximum penetration of approximately 50 percent.

GE's test results for coated Rene' 125 showed excellent performance of CCRS CoNiCrAlY relative to CODEP B and PVD NiCrAlY. After 478 hours at 972°C, the CCRS coating still retained full protectivity, Figure 39, with retention of the two-phase compositions of beta and gamma phases. The CODEP B coating after the same exposure was reported by GE to be 70 percent consumed, and PVD NiCrAlY failed totally at 190 hours.

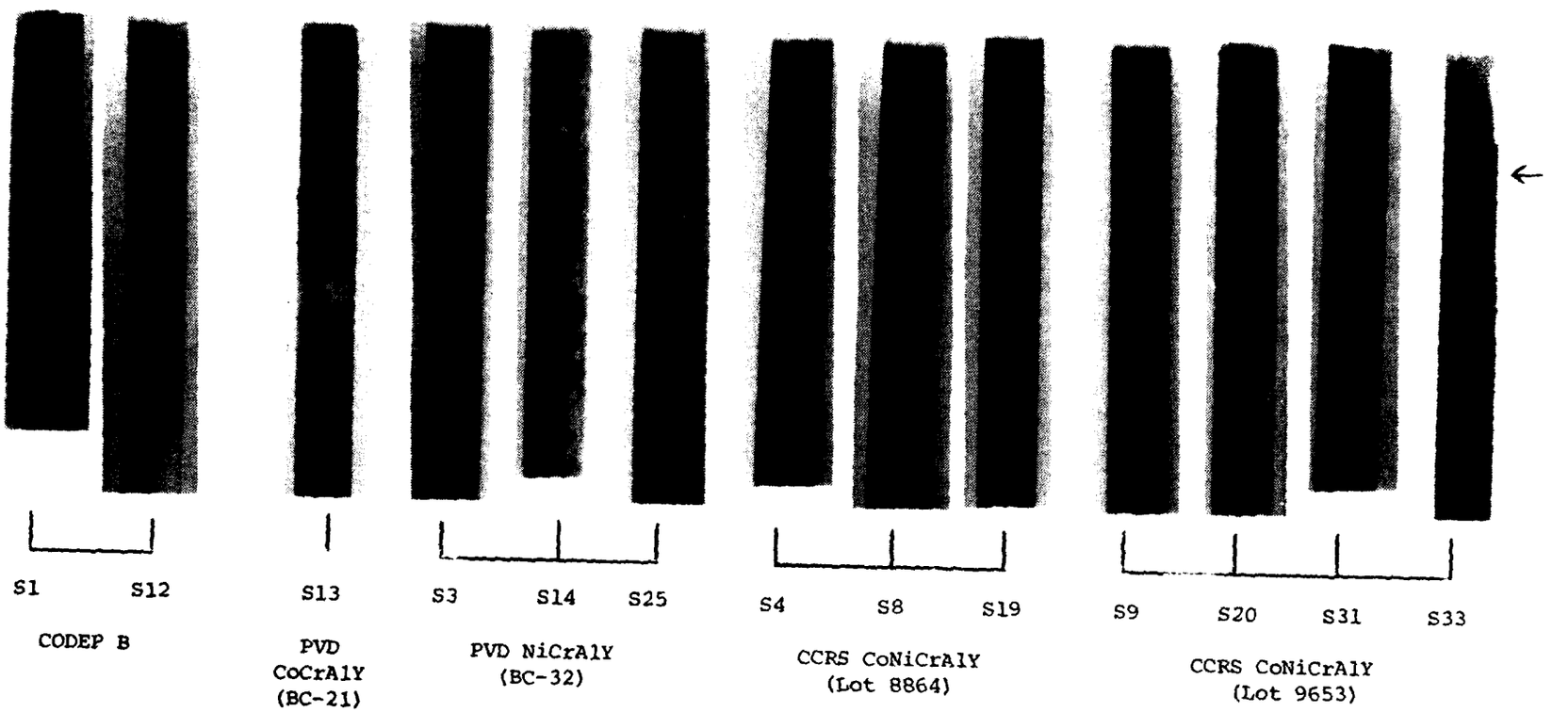

Figure 30. Macro Appearance of Coated Rene' 125 Specimens After 25 Hours of Hot Corrosion Testing at 871°C (Arrow Indicates Test Area)

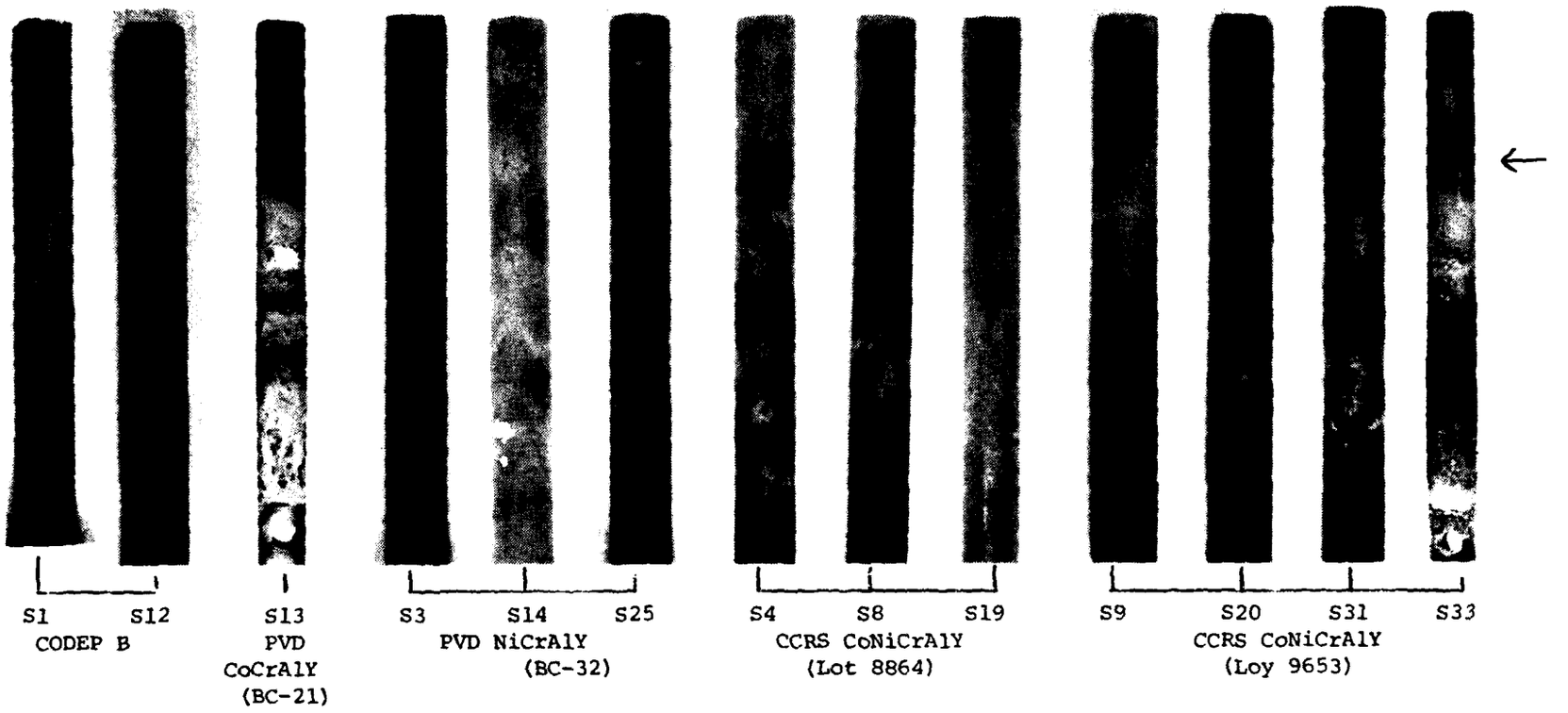

Figure 31. Macro Appearance of Coated Rene' 125 Specimens After 239 Hours of Hot Corrosion Burner Rig Testing at 871°C (Arrow Indicates Test Area)

A. Specimen No. S1

Hot Zone

Magnification: 250X

Etchant: 2% Chromic

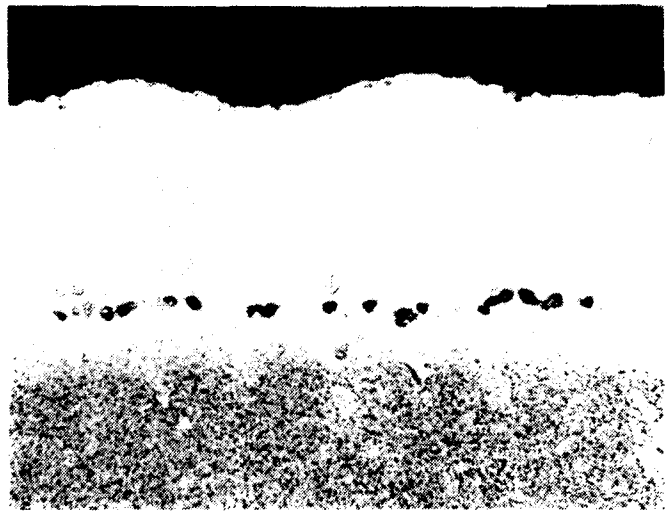

B. Specimen No. S1

Cooler Zone

Magnification: 250X

Etchant: 2% Chromic

Figure 32. Microstructures of CODEP B Coated Rene' 125 Specimen After 239 Hours of Hot Corrosion Rig Test

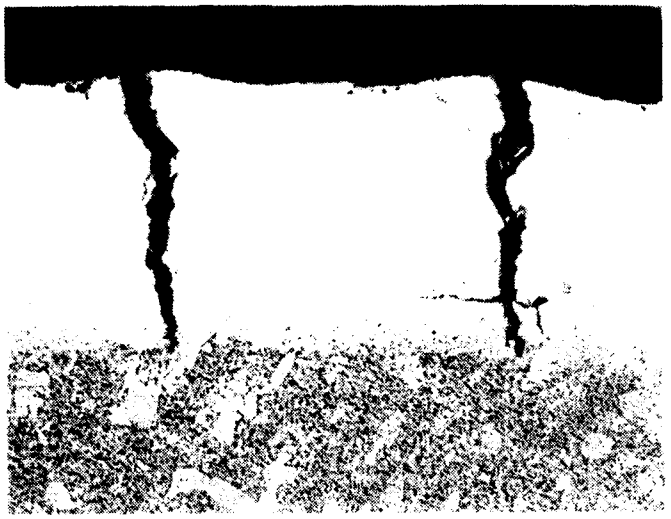

A. Specimen No. S12

Hot Zone

Magnification: 250X

Etchant: 2% Chromic

B. Specimen No. S12

Cooler Zone

Magnification: 250X

Etchant: 2% Chromic

Figure 33. Microstructures of CODEP B Coated Rene' 125 Specimen After 239 Hours in Hot Corrosion Rig Test

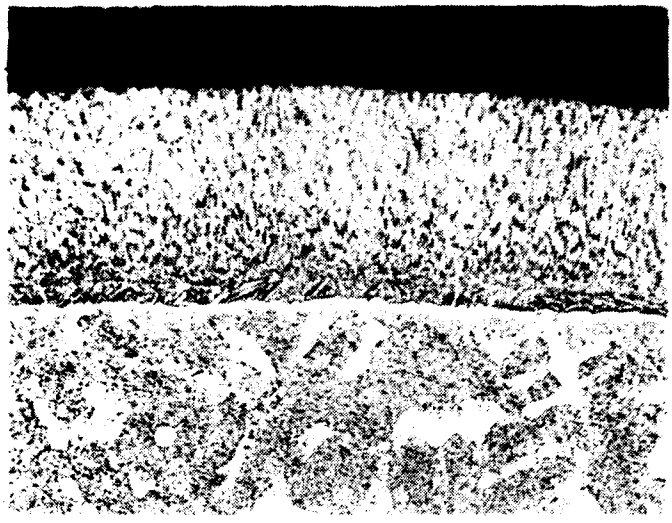

A. Specimen No. S13

Hot Zone

Magnification: 250X

Etchant: 2% Chromic Acid

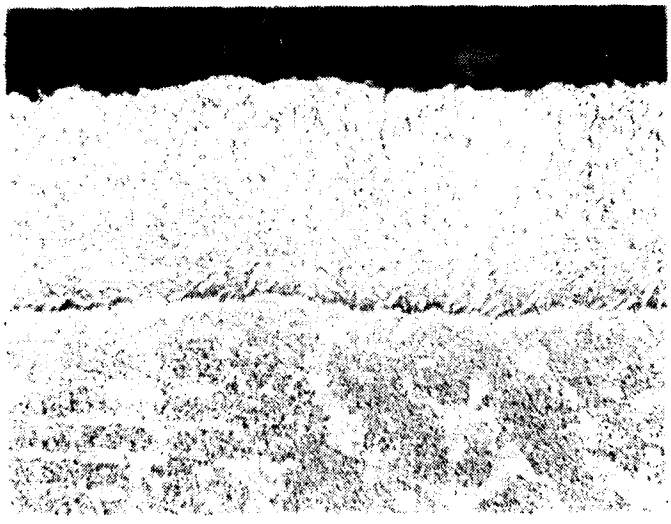

B. Specimen No. S13

Cooler Zone

Magnification: 250X

Etchant: 2% Chromic Acid

Figure 34. Microstructures of PVD CoCrAlY Coated Rene' 125 Specimens After 174 Hours of 871°C Hot Corrosion Burner Rig Test

A. Specimen No. S14

Hot Zone

Magnification: 250X

Etchant: 2% Chromic Acid

B. Specimen No. S14

Cooler Zone

Magnification: 250X

Etchant: 2% Chromic Acid

Figure 35. Microstructures of BC32 (PVD NiCrAlY) Coated Rene' 125 Specimens After 239 Hours of Hot Corrosion Rig Testing

A. Specimen No. S25

Hot Zone

Magnification: 250X

Etchant: 2% Chromic Acid

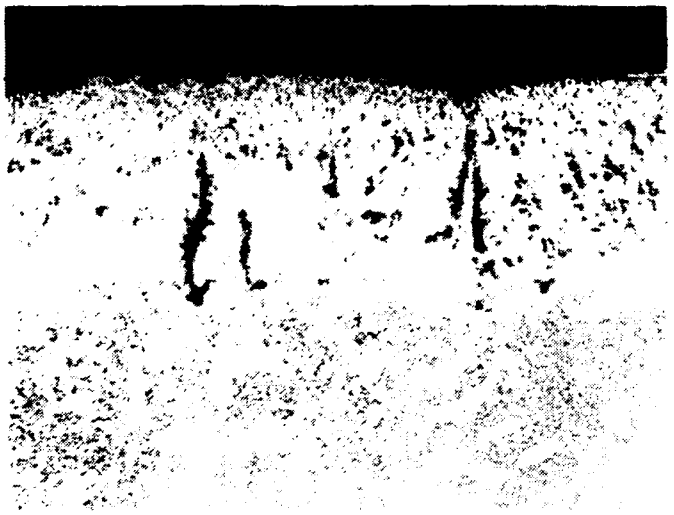

B. Specimen No. S25

Cooler Zone

Magnification: 250X

Etchant: 2% Chromic Acid

Figure 36. Microstructures of BC32 Coated Rene' 125 Specimens After 239 Hours of Hot Corrosion Rig Testing

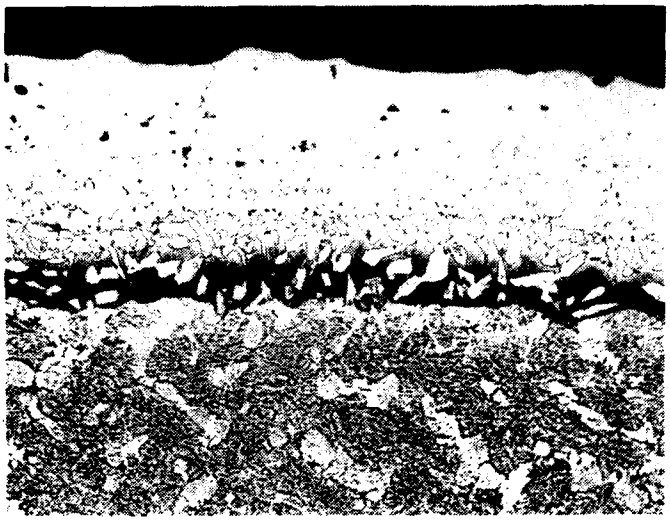

A. Specimen No. S19

Hot Zone

Magnification: 250X

Etchant: 2% Chromic Acid

B. Specimen No. S19

Cooler Zone

Magnification: 250X

Etchant: 2% Chromic Acid

Figure 37. Microstructures of CCRS Lot 8864 Coated Rene' 125 Specimens After 239 Hours of Hot Corrosion Rig Testing

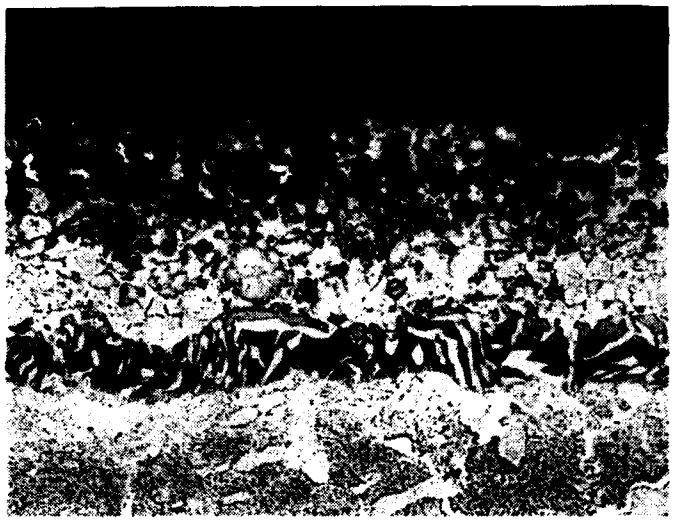

Specimen No. S8

Hot Zone

Magnification: 250X

Etchant: 2% Chromic Acid

Maximum Coating Penetration

Figure 38. Microstructure of CCRS Lot 8864 Coated Rene' 125 Specimen After 239 Hours of Hot Corrosion Rig Testing

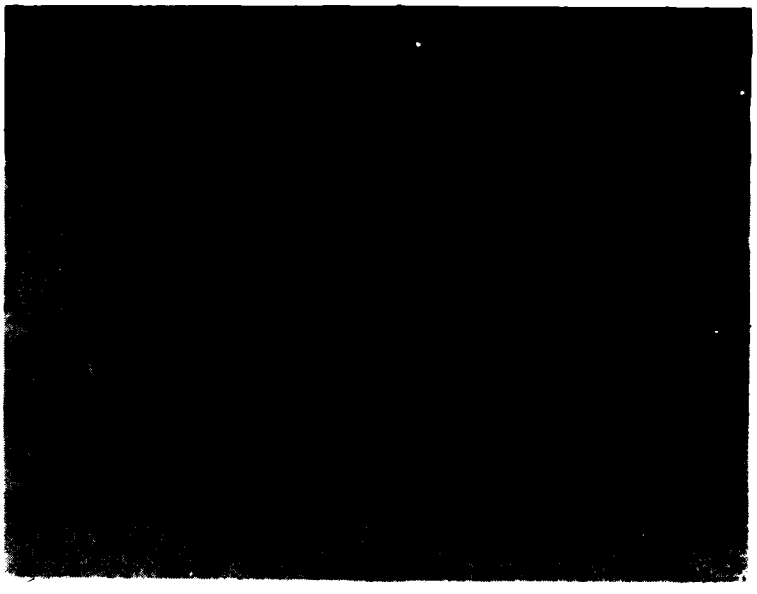

Figure 39. CCRS CoNiCrAlY Coated Rene' 125 Specimen Tested in Hot Corrosion for 478 Hours at 1700°F, 5ppm (GE); Magnification: 500X

3.4.2 X-40

Ten coated X-40 specimens were tested at STI, and visual appearance after 174 hours is shown in Figure 40. Salt deposits can be seen in the cooler region away from the hot spots of the gas path. Specimen No. Y1, which was CODEP B coated, was the only one showing gross spallation. This is probably a consequence of thermal stress cracking similar to that associated with CODEP B coated Rene' 125.

Microstructurally, the areas where the coating was not spalled showed good coverage and protection with two-thirds of the coating intact, Figure 41. Note that the layer at the corrosion/coating interface was converted from beta to a lighter etched phase, probably gamma solid solution.

PVD NiCrAlY coated X-40 performed extremely poorly in hot corrosion testing. After 174 hours, the coatings were essentially 100 percent penetrated with corrosion attack initiating at the interface and even in the substrate alloy. This is shown in Figure 42 where 75 percent of the coating was eroded away by the gas stream, and a continuous band of interfacial oxidation can be observed. Total penetration of the coating in certain spots had resulted in intergranular attack of the X-40 parent material. In the cooler regions, leaders characteristic of PVD applications were noted together with severe cracks, both of which provide direct pathways for corrodents to attack the interface.

Figure 43 shows another PVD NiCrAlY specimen with 100 percent breakdown of the coating and lateral interfacial corrison which would undermine whatever coating was left. Figure 43B shows voids and/or oxides distributed throughout 80 percent of the coating, even in the cooler areas.

CCRS CoNiCrAlY coated X-40 exhibited good hot corrosion resistance. Typical microstructures are provided in Figure 44 which shows increased porosity (the CCRS process typically results in a less dense coating) but complete protectivity.

GE reported that CCRS CoNiCrAlY, PVD CoCrAlY and CODEP B coating systems provided protection after 478 hours of testing (Fig. 45). However, the CODEP B system was 50 percent consumed as a result of Na_2SO_4 induced frontal sulfidation. GE's results agree with STI's findings that, in spite of the less dense microstructures, the CCRS CoNiCrAlY on X-40 demonstrated excellent sulfidation resistance.

3.4.3 MA754

Coated MA754 was evaluated at GE with CCRS CoNiCrAlY and PVD NiCrAlY for hot corrosion surface protection. Results showed that the CCRS coating was superior to the PVD NiCrAlY system. The tip of PVD NiCrAlY coated specimens was totally spalled, while the CCRS system showed minimal surface distress. Figure 46 shows the partially depleted (most gamma solid solution) NiCrAlY coating with chromium sulfides formed after 236 hours. On the other hand,

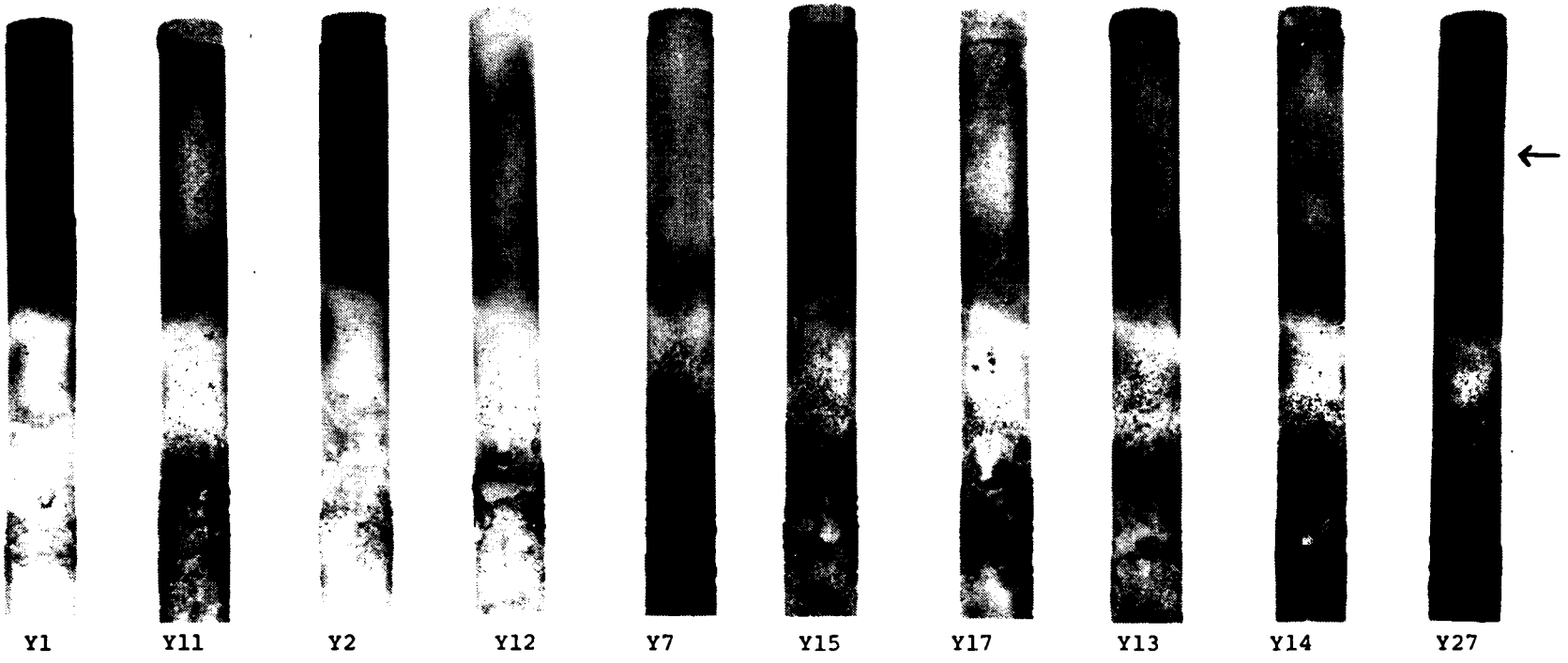

Figure 40. Macro Appearance of Coated X-40 Specimens After 174 Hours of Hot Corrosion Burner Rig Testing at 871°C (Arrow Indicates Test Area)

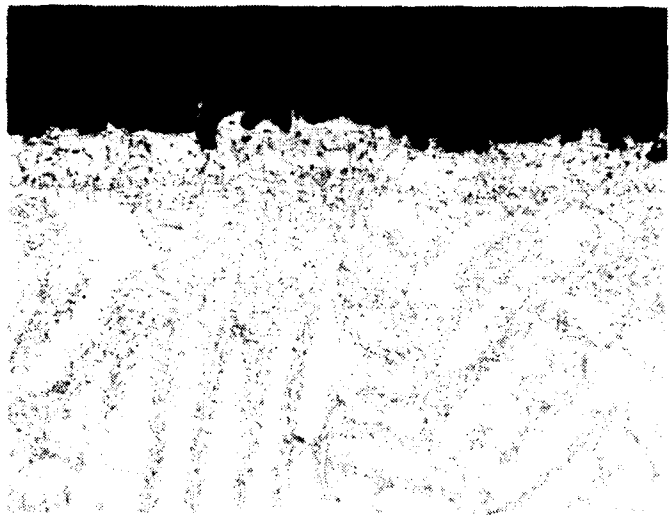

A. Specimen No. Y1

Hot Zone

Magnification: 250X

Etchant: 2% Chromic Acid

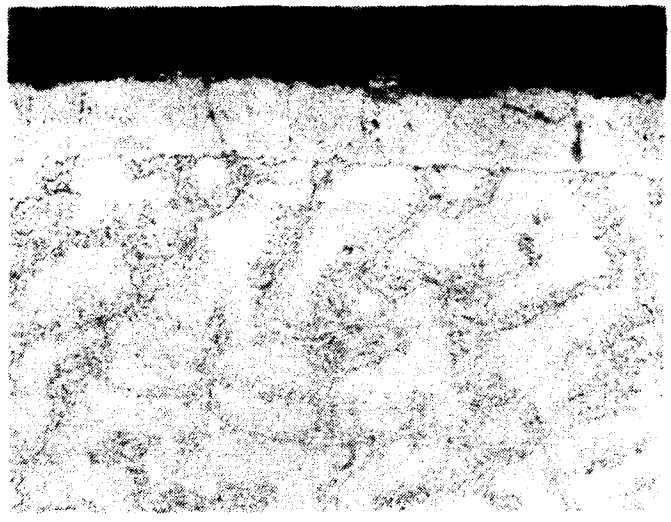

B. Specimen No. Y1

Cooler Zone

Magnification: 250X

Etchant: 2% Chromic Acid

Figure 41. Microstructures of CODEP B Coated X-40 Specimens After 174 Hours of 871°C Hot Corrosion Burner Rig Testing

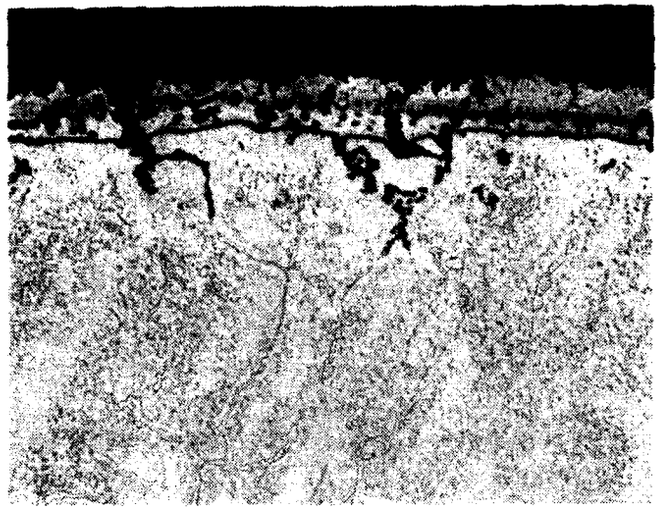

A. Specimen No. Y12

Hot Zone

Magnification: 250X

Etchant: 2% Chromic Acid

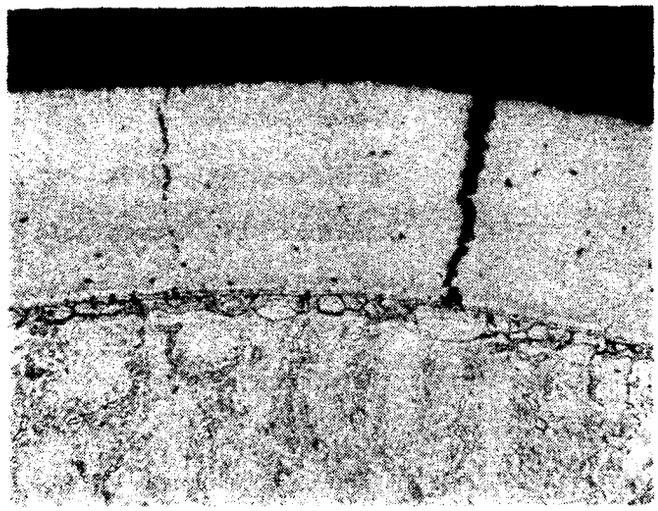

B. Specimen No. Y12

Cooler Zone

Magnification: 250X

Etchant: 2% Chromic Acid

Figure 42. Microstructures of PVD NiCrAlY Coated X-40 Specimen After 174 Hours of 871°C Hot Corrosion Burner Rig Testing

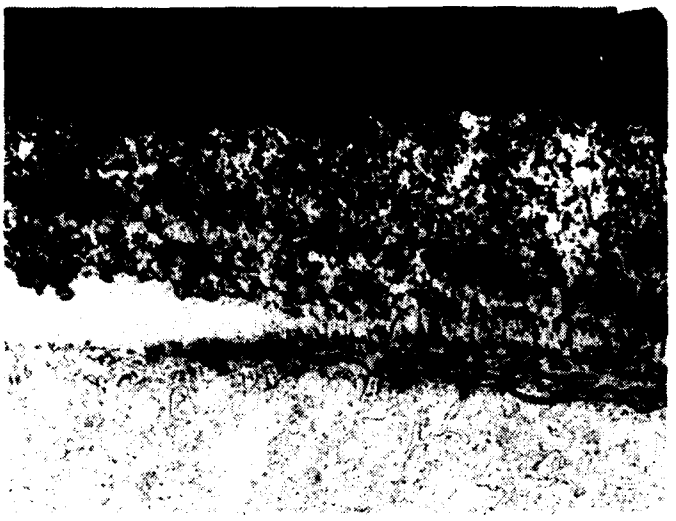

A. Specimen No. Y2

Hot Zone

Magnification: 250X

Etchant: 2% Chromic Acid

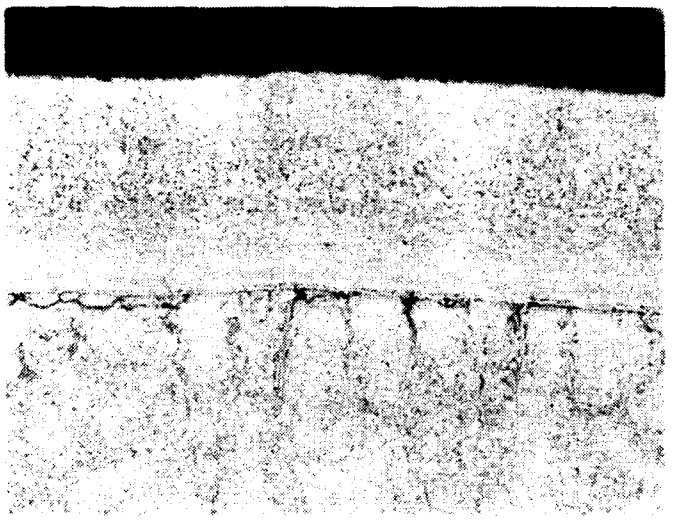

B. Specimen No. Y2

Cooler Zone

Magnification: 250X

Etchant: 2% Chromic Acid

Figure 43. Microstructures of PVD NiCrAlY Coated X-40 Specimens After 174 Hours of 871°C Hot Corrosion Burner Rig Testing

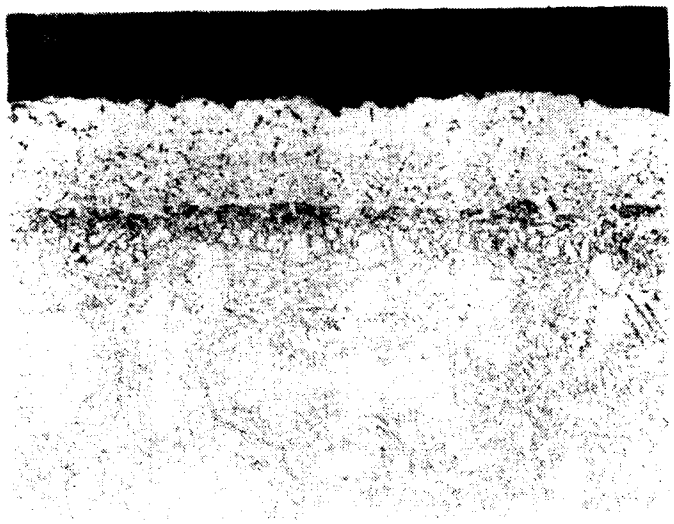

A. Specimen Y27

Hot Zone

Magnification: 250X

Etchant: 2% Chromic Acid

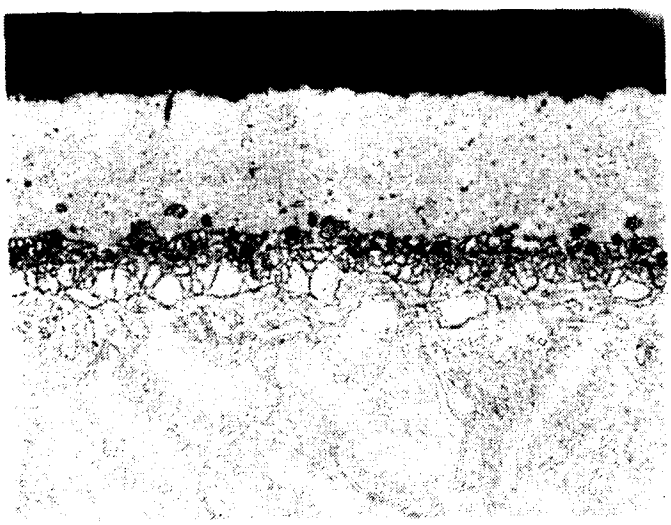

B. Specimen Y27

Cooler Zone

Magnification: 250X

Eqchant: 2% Chromic Acid

Figure 44. Microstructures of CCRS CoNiCrAlY (Lot 9653) Coated X-40 Specimens After 174 Hours of Hot Corrosion Burner Rig Testing

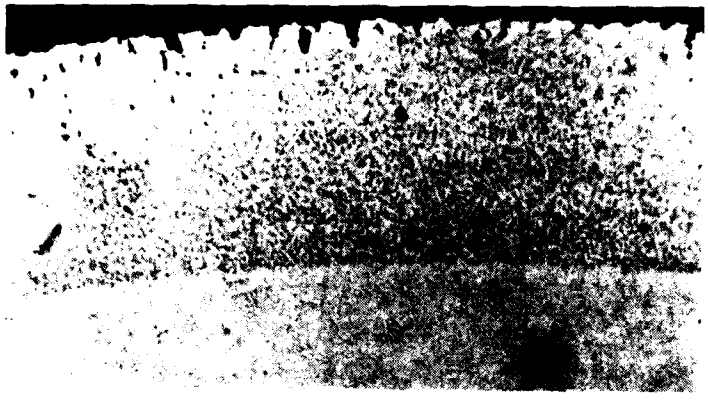

A. PVD CoCrAlY

Magnification: 250X

B. CCRS CoNiCrAlY

Magnification: 250X

C. CODEP B

Magnification: 250X

Figure 45. Photomicrographs of Coated X-40 Specimens After 478 Hours at 1700°F, 5 ppm Hot Corrosion; Note Even Though One CCRS Coating is Not Fully Dense, it Has Excellent Corrosion Resistance.

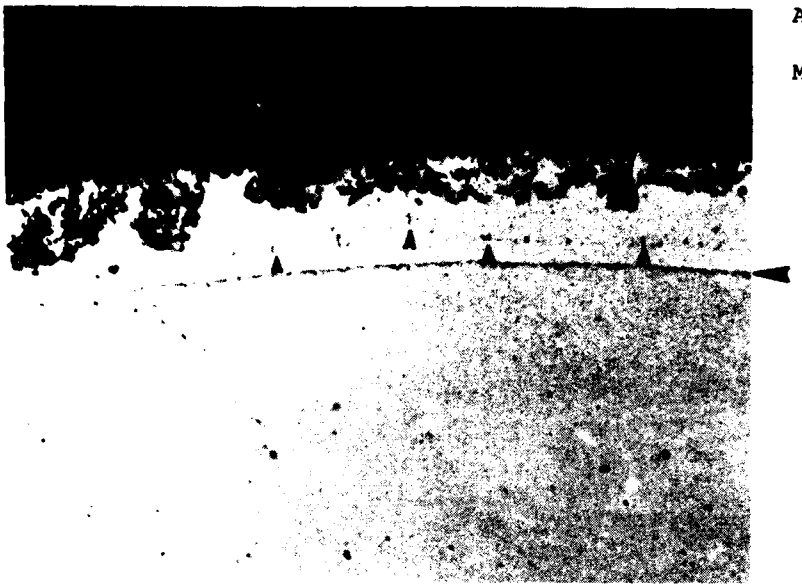

A. PVD NiCrAlY

Magnification: 250X

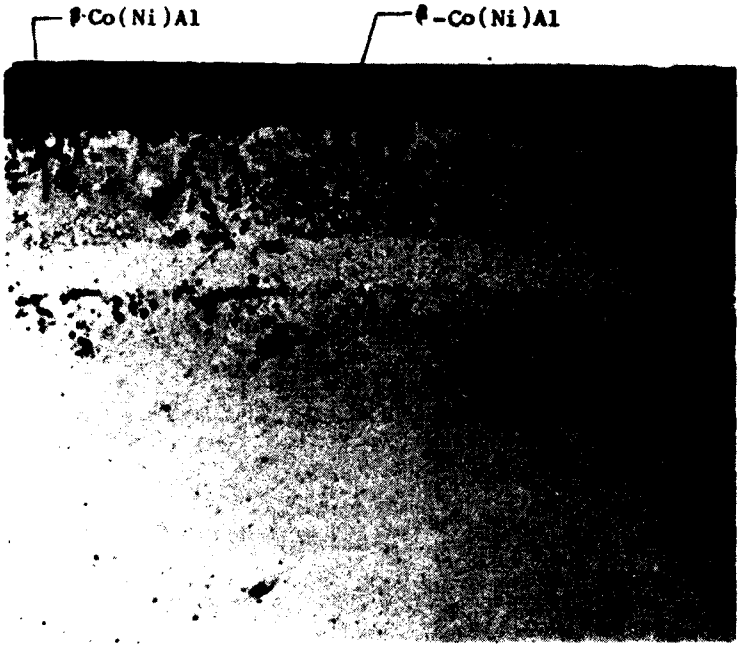

B. CCRS CoNiCrAlY

Magnification: 250X

Figure 46. Photomicrographs of Coated MA754 Specimen, Tested for 236 Hours at 1700°F, 5 ppm; Arrows Indicate Chromium Sulfides Formed with a PVD Coating

CCRS CoNiCrAlY had retained most of its beta in the matrix, and no trace of chromium sulfide was evident. A second set of pictures in Figure 47 was taken after over 400 hours of testing. Complete coating spallation was found on NiCrAlY specimens as a result of interfacial oxidation. Interestingly, similar oxides were also found, but to a much lesser degree, in the CCRS coating, but this condition remained unchanged over the test time and therefore did not enhance sulfidation.

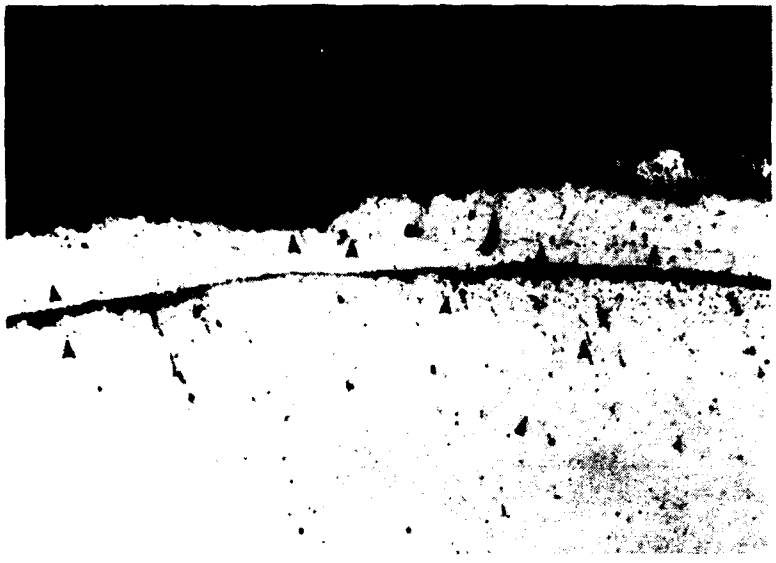

A. PVD NiCrAlY

Magnification: 250X

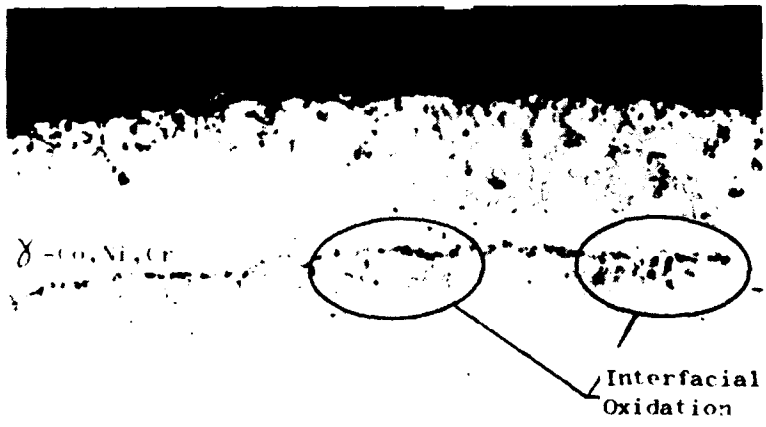

B. CCRS CoNiCrAlY

Magnification: 250X

Figure 47. Photomicrographs of Coated MA754 Specimens Tested for 409 and 478 Hours Respectively at 1700°F, 5 ppm; Note Internal Sulfide Formation (Arrows) in the PVD NiCrAlY and Gamma-Co, Ni, Cr Solid Solution in the CCRS CoNiCrAlY

3.4.4 Summary

In order to summarize the findings of both STI and GE, each coating/substrate combination tested was assigned an arbitrary rating number, with No. 1 being the highest rated coating. This is shown in Table 15. Although results from the two facilities do not always correspond exactly, some definite conclusions can be drawn.

1. Both CODEP B and CCRS CoNiCrAlY coatings provide better sulfidation protection for Rene' 125 than either PVD CoCrAlY or NiCrAlY.

2. X-40 is best protected by cobalt-containing coatings such as PVD CoCrAlY or CCRS CoNiCrAlY. Single aluminide types such as CODEP B were not adequate.

3. GE estimated that CCRS CoNiCrAlY affords better sulfidation resistance to MA754 than PVD NiCrAlY.

Table 15

Summary of GE and STI Hot Corrosion Results

Alloy	Coating	STI	GE
Rene' 125	CODEP B	1	2
	PVD CoCrAlY (BC-21)	2	-
	PVD NiCrAlY (BC-32)	3	3
	CCRS CoNiCrAlY	2	1
X-40	CODEP B	2	3
	PVD CoCrAlY (BC-21)	-	1
	PVD NiCrAlY (BC-32)	3	-
	CCRS CoNiCrAlY	1	2
MA754	PVD NiCrAlY (BC-32)	-	2
	CCRS CoNiCrAlY	-	1

3.5 DYNAMIC OXIDATION TESTS

Oxidation burner rig tests of coated alloys were conducted at GE. Three alloys were tested at 1149°C (2100°F); Rene' 125, MA754 and X-40. The CCRS CoNiCrAlY coating was applied to all alloys while PVD NiCrAlY was used on nickel-base alloys, Rene' 125 and MA754 and CODEP B and PVD CoCrAlY were applied to turbine nozzle cobalt-base alloy X-40.

Weight change data for coated Rene' 125 specimens are given in Figure 48. From the curves in the plot, both PVD NiCrAlY and CCRS CoNiCrAlY coatings experienced sharp negative gradients, i.e., weight losses, while CODEP B had a slight maximum and gained in weight during the 400-hour test. These weight change data may be somewhat misleading, as microstructural examination (Fig. 49) revealed that the CODEP B coating was 70 percent consumed locally. PVD NiCrAlY and CCRS CoNiCrAlY appeared to be unpenetrated except that aluminum depletion to replenish surface oxides had resulted in conversion to gamma solid solution instead of the beta phase, which was originally predominant in the coatings. Therefore, these coatings would be expected to show signs of failure soon.

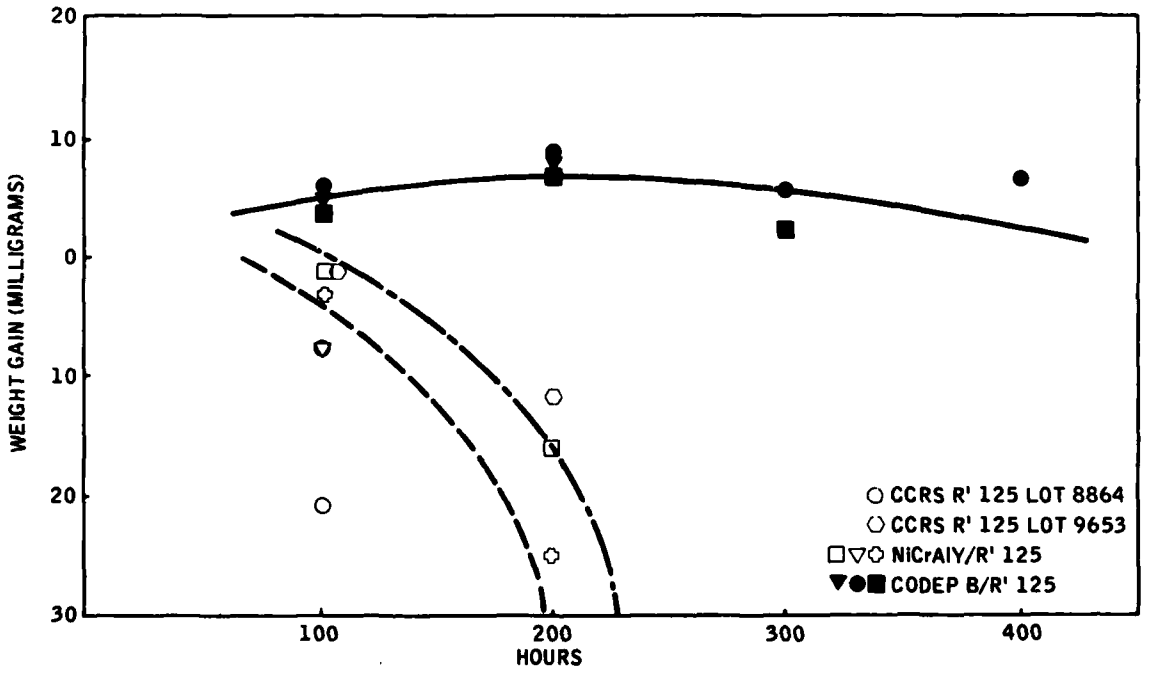

Figure 48. Weight Gain Curve for Coated Rene' 125 Tested in 1149°C (2100°F) Dynamic Oxidation (GE Data)

A. PVD NiCrAlY/Rene' 125

Magnification: 500X

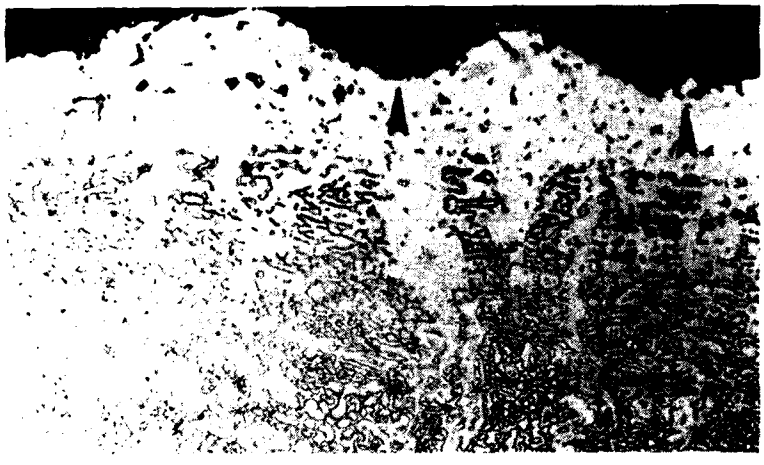

B. CODEP B/Rene' 125

Magnification: 500X

70% (Arrows) has been Attacked

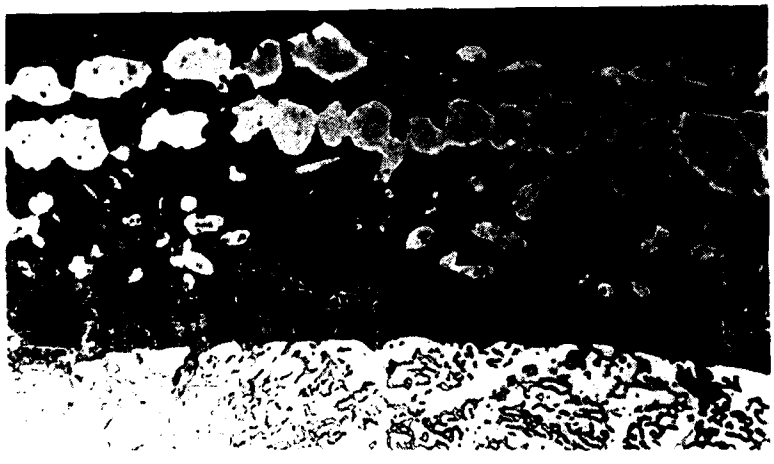

C. CCRS CoNiCrAlY/Rene' 125

Magnification: 500X

Figure 49. Photomicrographs of Coated Rene' 125 Environmental Test Specimens Tested in 1149°C Dynamic Oxidation for 525 Hours

Only two coatings were evaluated for MA754 alloy, CCRS CoNiCrAlY and PVD NiCrAlY. From the results in Figure 50 and the surface appearance of the test specimen, it can be seen that the CCRS coating was less protective than the PVD coating. The former failed in less than 300 hours, while the latter failed after 500 hours. The CCRS coatng was essentially fully penetrated, and oxidation attack of the substrate was noted. The proposed mechanism leading to coating failure was the rapid rate of aluminum diffusion from the coatings into the zero aluminum MA754 substrate. Since the CCRS composition contained 15 to 17 percent alminum while the PVD coating had only 7 to 8 percent, the higher concentration gradient induces greater diffusion leading to individual interfacial voids which compromised the integrity of the coating.

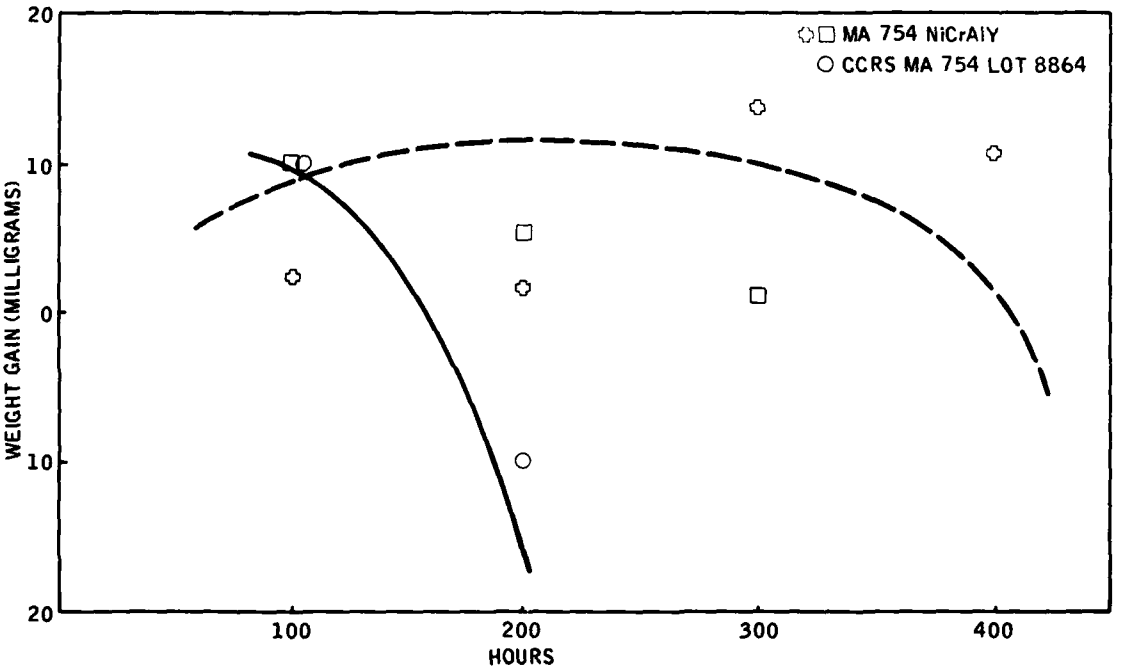

Figure 50. Weight Gain Curve for Coated MA754 Tested in 1149°C (2100°F) Dynamic Oxidation (GE Data)

Figure 51 shows that CCRS CoNiCrAlY coated X-40 was not as resistant as CODEP B and PVD CoCrAlY. The higher rate of oxidation for the CCRS coating can be traced to the large number of coating voids which provide easy access paths for oxygen to move through the coating to the interface.

An important observation noted as a result of the above discussion is that the porous CCRS CoNiCrAlY coating (X-40 and MA754) performed poorly in 1149°C dynamic oxidation. However, dense CCRS coated Rene' 125 was much more oxidation resistant and was comparable to PVD NiCrAlY.

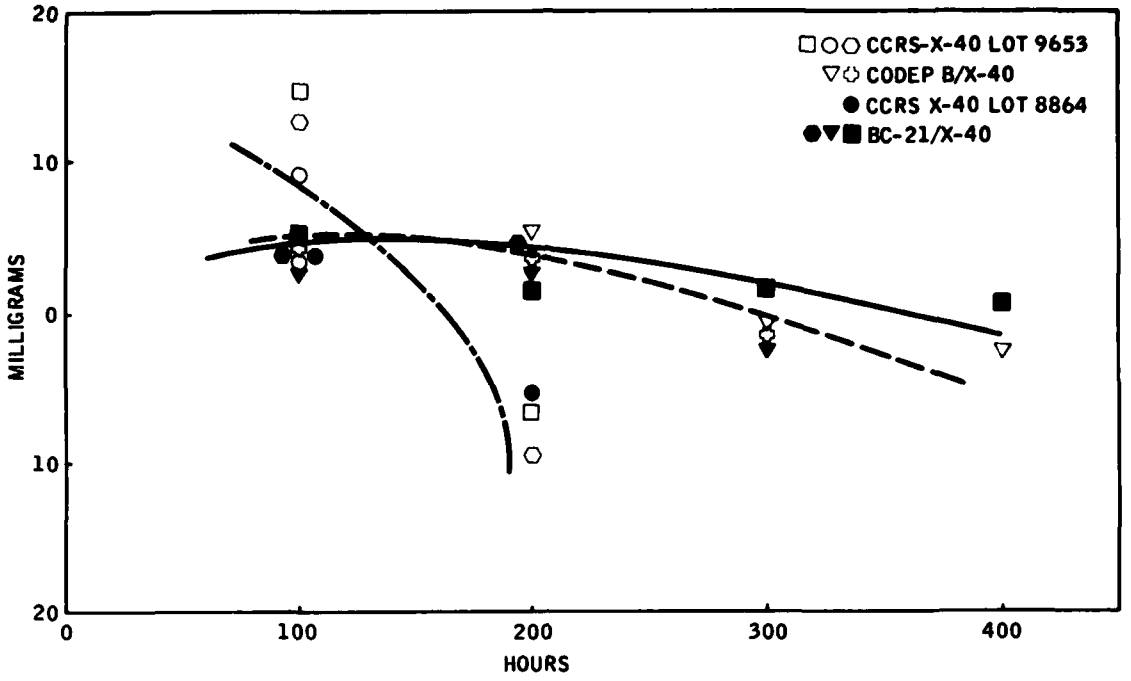

Figure 51. Weight Gain Curve for Coated X-40 Tested in 1149°C (2100°F) Dynamic Oxidtion (GE Data)

3.6 THERMAL FATIGUE TESTS

Simulated engine thermal shock (SETS) tests were conducted at GE on CCRS CoNiCrAlY, CODEP B and PVD CoCrAlY coated X-40 as well as CCRS CoNiCrAlY coated MA754. An arbitrary crack severity index (CSI) had been established by GE for this particular SETS rig, and a summarized description is included in Table 16.

A total of eight coated specimens were exposed to 250 thermal cycles from 583°C (1000°F) to 1149°C (2100°F) during 40-minute intervals. Test results obtained are shown in Table 17. At the end of the first 50 cycles, inspection showed pitting had occurred on the PVD CoCrAlY coated X-40 specimen. The next 50 cycles did not produce any additional failures. After 150 hours, three other specimens were found to be cracked at the CSI 2 level (the PVD coated specimens did not suffer further deterioration). Upon completing 250 cycles, inspection revealed that three CCRS coated specimens out of the original eight had remained fully intact and unaffected by the severe thermal shock cycles. Of the four CCRS CoNiCrAlY coated X-40 specimens, three had failed in a similar manner. In addition, the PVD coated X-40 specimen had rapidly deteriorated to 4 CSI.

Table 16

Crack Severity Index Used For GE SETS Tests

Crack Severity Index (CSI)	Description of Crack Severity
0	No cracking or surface deterioration
1	Pits at leading edge - not discernible as cracks
2	One to three cracks which do not traverse the leading edge arc
3	Four or more cracks which do not traverse the leading edge arc
4	One to three cracks which traverse the leading edge arc
5	Four or more cracks which traverse the leading edge arc
6	One to three cracks which extend past the leading edge arc
7	Four or more cracks which extend past the leading edge arc
8	One to three cracks which extend past the leading edge arc by at least 3/32 inch
9	Four or more cracks which extend past the leading edge arc by at least 3/32 inch

Therefore, it would seem that the CCRS CoNiCrAlY coated MA754 (nickel-base alloy) exhibited the best thermal fatigue shock resistance and withstood 250 cycles without any observable degradation whatsoever. This was also true of a single CCRS CoNiCrAlY coated X-40 specimen. Optical examination of all coating cracks showed base metal oxidation for the CODEP B specimen, indicating early crack initiation. Both PVD and CCRS coatings were not initially oxidized and crack lengths were shorter than in CODEP B.

Based on the above observations, it can be concluded that the CODEP B coating on X-40 had the poorest thermal fatigue life. The PVD CoCrAlY coating showed signs of coating distress early in the test, although only one crack was noted. The CCRS CoNiCrAlY coating on X-40 had excellent resistance up to 250 cycles. Once cracking was initiated, numerous cracks were observed, probably aggravated by coalescing coating voids. Therefore, since crack initiation and number of cracks are critical parameters, both CCRS CoNiCrAlY and PVD CoCrAlY coatings (on X-40 alloy) can be ranked equivalently in this respect. Finally, CCRS CoNiCrAlY coated MA754 exhibited excellent fatigue life, exceeding all other coated specimens.

Table 17

Thermal Fatigue Behavior (CSI) of Coated 15-Degree Wedge Superalloys
(See Table 15 for Explanation of CSI)

Coating/Substrate	S/N	CSI at Each Inspection Level			
		50	100	150	250
CCRS CoNiCrAlY/MA754 Lot 8864	--	0	0	0	0
CCRS CoNiCrAlY/MA754 Lot 9653	--	0	0	0	0
CCRS CoNiCrAlY/X-40 Lot 8864	C-45	0	0	0	0
CCRS CoNiCrAlY/X-40 Lot 8864	C-46	0	0	0	7
CCRS CoNiCrAlY/X-40 Lot 9653	C-4	0	0	2+	6+
CCRS CoNiCrAlY/X-40 Lot 9653	C-6	0	0	2	6+
CODEP B/X-40 High Activity	--	0	0	2	7
PVD CoCrAlY/X-40 BC-21	--	1	1	1	4

3.7 STRESS-RUPTURE TESTS

Elevated-temperature stress-rupture testing of two-cycle CCRS CoNiCrAlY coated Rene' 125 and X-40 alloys was performed at GE, Evendale. Thin-wall specimens 1.25 mm thick (sheet stock) were coated at STI using two powder lots and returned to GE for testing. The results are included in GE's report, Appendix B, but two groups are reproduced here for discussion. Figures 52 and 53 are 982°C (1800°F) stress-time plots for coated Rene' 125 and X-40 specimens, respectively.

The 982°C stress-rupture life of CCRS coated Rene'125 (both lots) fall below the -3σ curve for uncoated bar stock, as can be seen in Figure 52. The CODEP B coated specimens also suffered the same loss. However, it is important to point out that the mean curve was based on test results of "large bar" specimens. It has been previously found, both here (Ref. 8) and elsewhere (Ref. 9), that the elevated-temperature stress-rupture life of thin-walled (1.57 mm or 0.040 in.) cast nickel-base specimens fell below those of large solid bars. The principal reason cited in that investigation was the grain

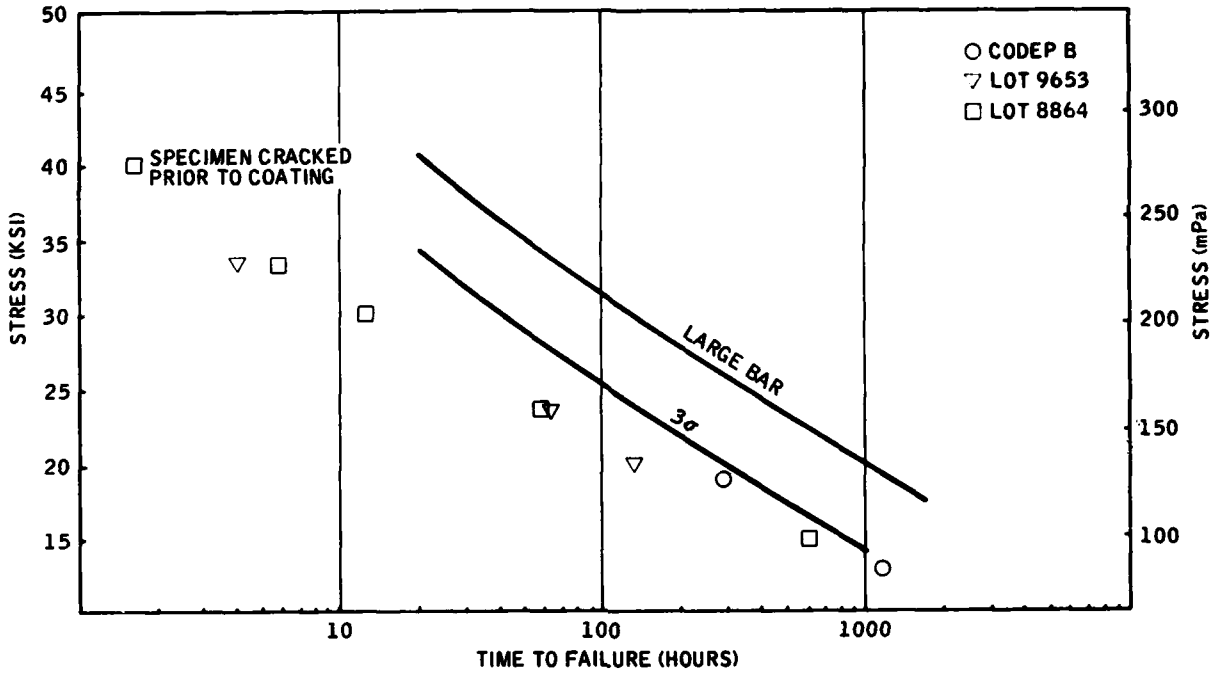

Figure 52. 982°C (1800°F) Stress-Rupture Life of CCRS Coated CoNiCrAlY Thin-Wall Rene' 125 Specimens (GE Data)

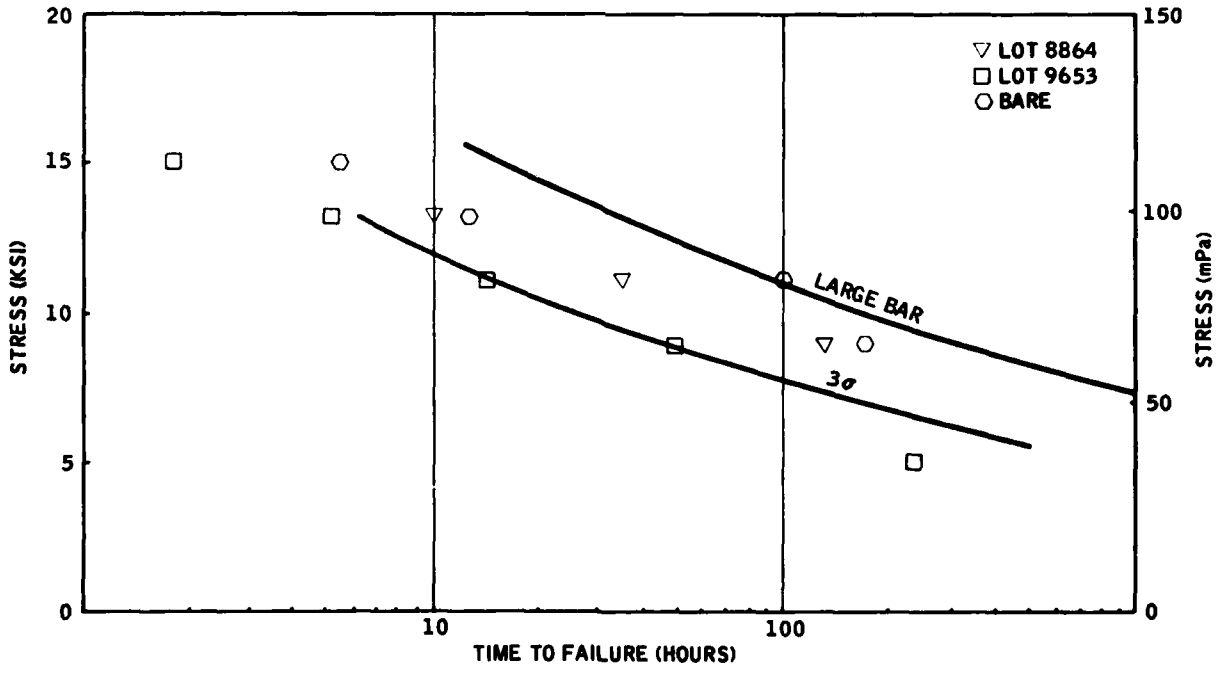

Figure 53. 982°C (1800°F) Stress-Rupture Life of CCRS Coated CoNiCrAlY Thin-Wall X-40 Specimens

size, the grain size being very dependent on specimen size and casting parameters. Therefore, the results reported here are not truly representative of the deteriorative effects of the CCRS process on stressrupture behavior as this "thin wall" effect was not factored out of this test. Post-test metallography showed that entrapped alumina particles (from the pack) at the coating surface caused severe cracks to initiate and propagate intergranularly into the substrate alloy (Fig. 54). These embedded alumina grains are associated generally with medium or low pack aluminization where movement of nickel outward from the substrate exceeds inward flux of aluminum, thus causing the aluminide layer to form around the small inert Al_2O_3 particles. This phenomenon is generally not observed in high-activity aluminum packs.

Figure 54.

Scanning Electron Microscope Shot of Surface of Dense Coated Rene' 125 Stress-Rupture Specimen After Test Showing Entrapped Surface Alumina and Surface Cracking (Arrows)

Magnification: 625X

In the case of CCRS coated X-40 alloy, most of the data points (Fig. 43) fell within the 3σ curve. Again, this curve was established using large bars instead of thin-wall specimens. Lot 8864 appeared to exhibit better rupture life than Lot 9653. In fact, Lot 8864 coated specimens compared very favorably to uncoated baseline values. Microstructurally, the CCRS CoNiCrAlY coating (cobalt-base alloy) had a more porous structure, as seen in Figure 55. Some internal oxides were observed after exposure to 982°C near the voids and also alpha-chromium areas.

In summary, it should be emphasized that the baseline stress-rupture values to which the CCRS CoNiCrAlY coated specimens were compared were derived from a different and much more favorable geometric configuration; namely, large round bars. Therefore, the strength degradation observed for coated Rene' 125 was not demonstrated to be caused solely by coating processing. Furthermore, the unaffected load-bearing cross-sectional area of the thin-wall specimens would be significantly affected by coating application while the

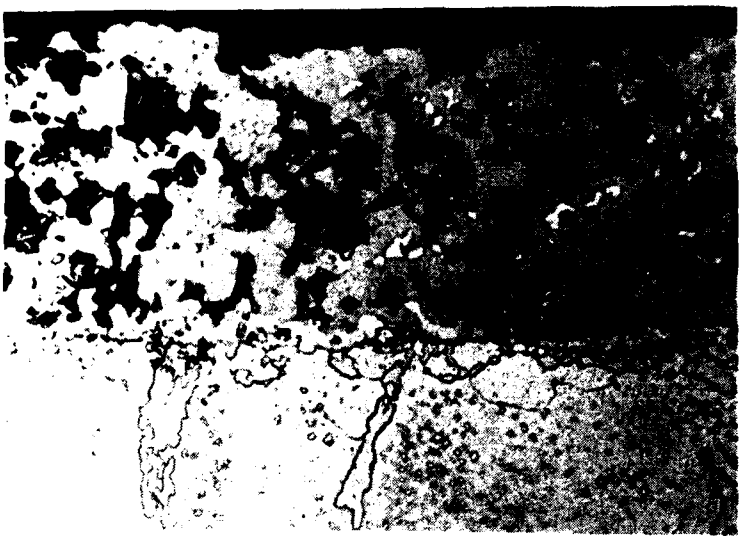

Figure 55. Typical CCRS CoNiCrAlY Coated X-40 Stress-Rupture Specimen Tested at 1800°F at 75.8 MPa (11 ksi) Showing Coating Voids and Preferential Oxidation Near the Coating Alpha-Chromium Particles and Voids (Arrows)

same coating applied to a larger test specimen would minimally affect the available load-bearing area. In other words, any coating of significant thickness (50-130 μm) such as PVD, CCRS, or aluminide when applied to thin-wall specimens would notably affect the rupture strength of the base material since the coating area is a significant fraction of the total area. Aside from the above geometric considerations, it can be concluded that CCRS CoNiCrAlY coated X-40 retained adequate rupture strength at 982°C. Coated Rene' 125, however, exhibited reduced rupture life with severe surface cracking. CODEP B coated Rene' 125 also suffered strength degradation in a comparable manner to CCRS coated Rene' 125.

4

SCALEUP ANALYSIS

Although the CCRS process for coating multiple vane segments is not ready for scaleup at this time, a detailed process sequence (Table 6) for applying the CCRS CoNiCrAlY coating to the TF34 vane segment was critically examined to estimate the capital equipment, labor and materials required for the volume production of this coating. This process was also broken down into two subdivisions, one for new parts and one for rebuildable ones. The size of the facility to be used for application of this coating was taken as one which could process 75,000 nozzles per year. The materials required for coating the nozzle are noted in Table 18 and the equipment required, in addition to that which is standard in diffusion aluminizing blades and vanes, is noted in Table 19. The result of this analysis is contained in Table 20.

These estimates indicate that the CCRS process for application of CoNiCrAlY coatings to two vane segements is quite economical in terms of the capital labor, material and energy requirements. For example, the major difference between this process and conventional pack aluminizing is in the modifier application step, which STI projects will add 533×10^{-4} hours per part to the coating processing time for these parts and also require the application of five grams of modifier powder.

Table 18

Material and Energy Required for CCRS CoNiCrAlY Application
(In Addition to that Required for Pack Aluminized Coatings)

Process Step	Per Nozzle
Material	
Modifier Application	
Stearic Acid	0.2 gm
10-20 μm Co-20Ni-25Cr-0.5Y Argon Atomized Powder	5.0 gm
Energy	
DC Current (100 volt compliance)	200 mg (1 min) 1/6 joule

Table 19

Capital Equipment Required for CCRS Coating Application
(In Addition to that Used to Apply Pack Aluminide Coatings)

Electrophoretic Tank	1.5' x 1' x 1' (l x w x h)
Constant DC Current Power Supply	300 A with compliance of 100 V DC
Fluidized Bed	1.5' x 1' bed area 1 " expanded bed depth 10 μm diffuser
Fluidizing Air Supply	30 m^3/hour 103 KPa gauge
Air Circulating Oven	156 kW, 200°C

Table 20

Labor Requirements for CCRS CoNiCrAlY Coating Application
(Based on Annual Coating of 75,000 Two-Vane Nozzle Segments)

Process Step	Labor/Part (hours)
Cleaning (New Parts)	
Vapor Degreasing	1.9×10^{-4}
Alkaline Cleaning	1.9×10^{-4}
	3.8×10^{-4}
Cleaning (Overhauled Parts)	
Abrasive Blast	160.0×10^{-4}
Vapor Degreasing	1.9×10^{-4}
Acid Etch (two times)	15.0×10^{-4}
Water Rinse (four times)	2.5×10^{-4}
Alkaline Etch (two times)	15.0×10^{-4}
Vapor Honing	160.0×10^{-4}
Ultrasonic Cleaning (water)	0.5×10^{-4}
Stripping (smut removal)	1.9×10^{-4}
Forced Air Drying	7.4×10^{-4}
	364.0×10^{-4}
Modifier CoNiCrY Application	
Attach Masking and Loading	166.0×10^{-4}
Electrophoretic Deposition (five times)	21.0×10^{-4}
Water Rinse (five times)	21.0×10^{-4}
Fluid Bed Immersion (five times)	2.1×10^{-4}
Forced Air Drying (five times)	240.0×10^{-4}
Mask Removal	83.0×10^{-4}
	533.0×10^{-4}
Inspection (two times)	160.0×10^{-4}
Reaction Sintering (CoNiCrAlY Formation)	
Attach Masking and Retort Loading (two times)	320.0×10^{-4}
Retort Sealing (two times)	14.0×10^{-4}
Retort Purging (two times)	14.0×10^{-4}
Retort Firing (two times)	150.0×10^{-4}
Part Cleaning (air blast)	83.0×10^{-4}
Part Cleaning (air blast-pressure wash)	160.0×10^{-4}
	741.0×10^{-4}
Total Labor Required - New Part	1438.0×10^{-4}
Total Labor Required - Overhauled Part	1798.0×10^{-4}

5

CONCLUSIONS AND RECOMMENDATIONS

Based on the findings obtained in this program, the following conclusions are drawn.

5.1 CONCLUSIONS

1. The single-cycle CCRS CoNiCrAlY coating is the only known coating process that can produce fine grain structure throughout the coating. This two-phase microstructure (beta plus gamma solid solution) results in a highly ductile coating system that is superior to PVD and pack aluminide coatings in strain accommodation.

2. The dual-cycle CCRS CoNiCrAlY coating is less ductile than its single-cycle counterpart due to the retention of a uniform continuous layer of beta (Ni, Co)-Al near the coating surface. The beta phase provides excellent hot corrosion resistance relative to other coatings tested.

3. While several non-line-of-sight methods of MCrY powder deposition were investigated, including fluidized bed and electrophoresis, none were 100 percent successful in depositing a uniform and fully dense coating on double-vane segments. However, the electrophoretic/fluidized bed process shows good potential and when fully developed should be capable of depositng a uniformly dense bisque.

4. Additional refinements the of E/FB process will be required to coat multiple vane segments such that, upon subsequent aluminizing, full densification can be achieved on all gas path surfaces.

5. In general, the CCRS CoNiCrAlY coating on nickel-base alloy, such as Rene' 125 and MA754 is fully dense while the same coating on cobalt-base X-40 exhibits varying levels of porosity.

6. The compositions of the CCRS CoNiCrAlY coatings formed on nickel-base alloys (Rene' 125 and MA754) and cobalt-base alloys are, respectively:

   Co(bal) - 33 to 42 Ni - 6 to 10 Cr - 12 to 19 Al - Y

   Co(bal) - 18 Ni - 10 to 20 CR - 14 to 16 Al - Y

   The nominal composition of the CoNiCrY bisque is 55Co-20Ni-15Cr-<1Y. Therefore, it can be concluded that in the case of nickel alloys, the

diffusion of nickel outward from the substrate is a significant phenomenon in coating densification, with a corresponding movement of Cr in the opposite direction (inward). Consequently, the resulting coating formed is nickel rich with low chromium content. In the case of cobalt-base alloys with only 10 percent nickel present in the substrate, the aluminum does not rapidly diffuse from the coating to the substrate, primarily because of the greater stability of NiAl.

7. Hot corrosion, thermal fatigue, cyclic fatigue, oxidation and mechanical property test results obtained by both STI and GE indicate that CCRS CoNiCrAlY coated Rene' 125 was equivalent to or superior to PVD CoCrAlY and NiCrAlY coatings. The only exception was the degradation of stress-rupture properties of CCRS coated Rene' 125 alloy.

8. In the case of X-40 alloy, the CCRS CoNiCrAlY coating was found to have poorer cyclic fatigue and oxidation lives than PVD and CODEP B coatings. It can be postulated that the high void level in the coating helped promote coating failure.

9. Generally, no evidence of batch lot differences was noticed in thermo-mechanical property testing. However, GE noted that in thermal fatigue (SETS) and environmental resistance (oxidation and hot corrosion) testing, Lot 9653 showed less surface distress than Lot 8864. Process control is apparently still variable.

10. The CCRS CoNiCrAlY coating has the potential of being the lowest cost overlay process currently under consideration, including PVD, sputtering and low-pressure argon plasma spraying.

5.2 RECOMMENDATIONS

1. Additional efforts will be needed to extend the protection of CCRS CoNiCrAlY coating to clustered airfoils. The E/FB method of modifier deposition will need to be systematically varied and refined in order to ensure uniform coverage of complex parts.

2. The formation of 100 percent dense coatings on cobalt-base alloys can be approached in several ways. First, the composition of the MCrY powder can be adjusted to allow increased volume expansion upon aluminization. This implies that instead of a CoNiCrAlY coating, a NiCoCrAlY composition might be more suitable for cobalt-base alloys. Another possible approach is to plate or deposit a thin film of nickel over the cobalt alloy prior to application of the CCRS coating.

3. Concurrent with coating composition variation, the activity of the aluminizing pack can be adjusted as a secondary means of composition control, particularly to increasing the total amount of aluminum deposited on a CoNiCrY coated cobalt-base alloy or that deposited on a nickel-base alloy.

AD-A085 197 SOLAR TURBINES INTERNATIONAL SAN DIEGO CA F/G 21/5
DEVELOPMENT AND EVALUATION OF PROCESSES FOR DEPOSITION OF NI/CO--ETC(U)
SEP 79 L HSU, W G STEVENS, A R STETSON F33615-76-C-5379
UNCLASSIFIED SR79-R-4571-18 AFML-TR-79-4097 NL

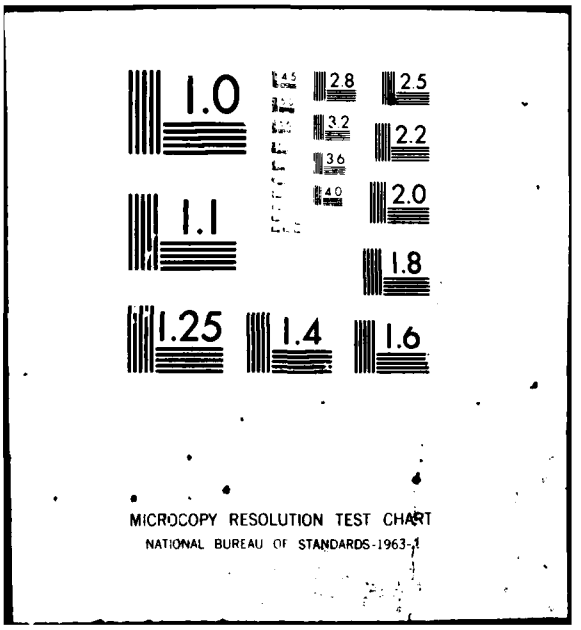
1.0
1.1
1.25
1.4
1.6
1.8
2.0
2.2
2.5
2.8
3.2
3.6
4.0
MICROCOPY RESOLUTION TEST CHART
NATIONAL BUREAU OF STANDARDS-1963-A

4. Further study is required to alleviate the deterioration of elevated-temperature rupture life of coated Rene' 125. This may be achieved by appropriate heat treat cycles applied as post-coating processing.

5. This current investigation showed that the CCRS CoNiCrAlY coating can form a highly resistant surface for protection of MA754. Further investigations should be performed to substantiate the promising results obtained thus far.

6. Al_2O_3 particle inclusions were observed in the coating throughout the program and these inclusions were found to act as stress risers which can promote rapid failure. However, this problem is commonly associated with low-activity aluminization and additional efforts are needed to exclude the fine Al_2O_3 particles from being entrapped near the surface of the coating.

6

REFERENCES

1. Stevens, W.G. and Stetson, A.R., "Controlled Composition Reaction Sintering Process for Production of MCrAlY Coatings", AFML/AFSC Technical Report AFML-TR-76-91 (Aug. 1976).

2. Aldred, P., "Rene' 125, Development and Application", Society of Automotive Engineers, 752049.

3. Gutfinger, C. and Abuaf, N., "Application of Fluidized Beds to Coating Processes", Fluidization Technology, Vol. II. ed by D.L. Kearins, Hemisphere Publ. Corp., Washington.

4. Landbrook, A.M., "Fluidized Bed Coating", Encyclopedia of Polymer Science and Technology, Vol. 3, Ed. H.F. Mark, N. Gaylord, N.M. Bitales, Interscience, John Wiley, New York (1965).

5. Goward, G.W., "Materials and Coatings for Gas Turbine Hot Section Components", Gas Turbine Materials Conference Proceedings, Washington, DC (Oct. 1972).

6. Moore, V.S., Brentnall, W.D. and Stetson, A.R., "Evaluation of Coatings for Cobalt- and Nickel-Base Superalloys", NASA-Lewis Contract NAS3-9401.

7. "Nickel-Base Alloys", The International Nickel Company, Inc., revised edition (1974).

8. M. Reed, STI, Internal Report (1976).

9. Ryan, K.H., "Comparative Evaluation of Coated Alloys for Turbine Components of Advanced Aircraft Gas Turbine Engines", Vol. 1, Summary and Analysis of Testing and Evaluation and Vol. 2, Test Results; General Motors Report under Air Force Contract F33615-69-C-1615 (Jan. 1972).

APPENDIX A

CCRS CoNiCrAlY COATING WEIGHT CHANGES

APPENDIX A

CCRS CoNiCrAlY Coating Weight Changes

Specimen Number	Lot Number	Bisque Weight (mg/cm^2)	Coating Weight (mg/cm^2)
Test: STI Tensile Specimens			
Alloy: Rene' 125			
R20	9653	32	*
R49	8864	25	*
R50	8864	47	*
R53	8864	46	*
R55	9653	46	*
R60	8864	50	*
R56	8864	51	*
R61	8864	45	*
R74	9653	46	*
R76	9653	48	*
R94	9653	-	*
R96	9653	48	*
Alloy: X-40			
X21	8864	47	*
X22	9653	46	*
X23	8864	46	*
X24	9653	48	*
X25	8864	50	*
X26	9653	50	*
X27	8864	31	*
X28	9653	33	*
X37	8864	46	*
X38	9653	46	*
X39	8864	50	*
X40	9653	45	*
Test: DBTT			
Alloy: Rene' 125			
R46	8864	33	*
R47	8864	36	*
R48	8864	29	*
R58	9653	45	*
R62	8864	45	*
R63	9653	47	*
R64	9653	48	*
R75	9653	50	*
R77	9653	45	*

* Not determined due to aluminization of threads

Specimen Number	Lot Number	Bisque Weight (mg/cm^2)	Coating Weight (mg/cm^2)
Test: DBTT			
Alloy: Rene' 125			
R88	8864	27	*
R89	8864	34	*
R90	8864	33	*
R93	9653	49	*
R95	9653	45	*
Test: Cycle Fatigue			
Alloy: Rene' 125			
R7	8864	45	*
R8	8864	47	*
R9	9653	46	*
R10	9653	49	*
R11	8864	49	*
R12	8864	48	*
R13	9653	49	*
R14	9653	46	*
R17	9653	32	*
R18	9653	27	*
R21	8864	26	*
R25	8864	32	*
Alloy: X-40			
X5	8864	45	*
X7	9653	47	*
X9	8864	28	*
X10	8864	28	*
X11	9653	24	*
X12	9653	30	*
Alloy: MA754			
A2	8864	46	*
A3	8864	46	*
A4	8864	50	*
A5	9653	46	*
A6	9653	46	*
A7	9653	48	*
Test: Hot Corrosion			
Alloy: Rene' 125			
S4	8864	49	60
S8	8864	45	56
S9	9653	46	59
S19	8864	46	59

* Not determined due to aluminization of threads

Specimen Number	Lot Number	Bisque Weight (mg/cm^2)	Coating Weight (mg/cm^2)
Test: Hot Corrosion			
Alloy: Rene' 125			
S20	9653	45	58
S31	9653	50	64
Alloy: X-40			
Y7	8864	50	57
Y13	9653	51	58
Y14	9653	49	56
Y15	8864	46	52
Y17	8864	50	57
Y27	9653	48	54
Test: GE Stress Rupture Specimens			
Alloy: Rene' 125			
C17	9653	50	69
C18	9653	45	64
C19	9653	64	78
C20	9653	45	65
C21	9653	45	65
C22	9653	46	65
C23	9653	47	66
C24	9653	45	60
C25	9653	46	59
C26	9653	48	68
C27	9653	46	65
C28	9653	51	71
C29	8864	49	68
C30	8864	45	65
C31	8864	50	69
C32	8864	47	67
Alloy: X-40			
C7	9653	51	58
C8	9653	51	58
C9	9653	46	53
C10	9653	50	57
C11	9653	50	57
C12	9653	48	55
C13	9653	46	53
C14	9653	46	53
C15	9653	49	57
C16	9653	45	52
C38	8864	50	58
C39	8864	49	57
C40	8864	50	58

Specimen Number	Lot Number	Bisque Weight (mg/cm^2)	Coating Weight (mg/cm^2)
Alloy: X-40			
C41	8864	51	58
C42	8864	52	59
C43	8864	50	57
Test: Thermal Fatigue			
Alloy: Rene' 125			
C33	9653	51	59
C34	9653	47	56
C35	9653	44	53
C36	8864	50	60
C37	8864	50	60
Alloy: X-40			
C4	9653	49	59
C5	9653	50	60
C6	9653	45	56
C44	9653	45	55
C45	8864	49	60
C46	8864	50	61
Alloy: MA754			
C1	8864	50	61
C2	9653	48	59
C3	9653	48	60
Test: Burner Rig			
Alloy: Rene' 125			
(7 specs)	9653	∿46	*
(2 specs)	8864	∿46	*
Alloy: X-40			
(7 specs)	9653	∿46	*
(2 specs)	8864	∿49	*
Alloy: MA754			
(7 specs)	9653	∿45	*
(2 specs)	8864	∿46	*

* Specimens were not individually identified

APPENDIX B

GENERAL ELECTRIC REPORT

EVALUATION OF SOLAR CCRS ENVIRONMENTALLY PROTECTIVE COATINGS FOR TURBINE HARDWARE

R79AEG195

EVALUATION OF SOLAR CCRS ENVIRONMENTALLY PROTECTIVE COATINGS FOR TURBINE HARDWARE

Phase II G.E. Subcontract Final Report

Performed Under Purchase Order 3654-32007-P35(CR)

For

Solar Turbines International
An Operating Group of International Harvester

Contract F33615-76-C-5379

by

W. D. Grossklaus

General Electric Company
Aircraft Engine Group
Materials and Process Technology Laboratories
Cincinnati, Ohio 45215

SUMMARY

1. CCRS CoNiCrAlY coatings on X-40 and Rene' 125 cause thin wall rupture degradation greater than -3 standard deviation units, when compared to the bare alloy. The probability of specimen failure is increased by the presence of coating defects, such as voids and entrapped pack alumina particulates.

2. Both the DBTT and SETS behavior of CCRS coatings indicate they are superior to CODEP B but do not perform as well as PVD coatings.

3. The structure of CCRS coatings deposited on X-40 is generally two-phase beta and dispersed alpha-chromium and not fully dense, while that deposited on Rene' 125 is a single beta with small amounts of gamma present and is fully dense.

4. The CCRS CoNiCrAlY coatings exhibit mixed environmental resistance when investigated on X-40, Rene' 125 and MA754. In 2100°F dynamic oxidation they are poorer than either CODEP B, PVD CoCrAlY (BC21), or PVD NiCrAlY (BC32). However, at 1700°F, 5 ppm salt hot corrosion, the CCRS coatings are superior to CODEP B, equivalent to PVD CoCrAlY and show some improvement in environmental resistance over PVD NiCrAlY. This is a result of their high cobalt levels.

5. Aircraft hardware coating capabilities for the CCRS process was demonstrated on X-40, TF34 HPT paired vanes and Rene' 125 F101 HPT blades. The vane coatings were semi-dense (i.e., porous and exhibited wide variations in the coating thickness). However, on blades, a dense adherent coating with thickness control was obtained. Also, the post-coating film cooling capacities of the vane were substantially reduced as a result of the process.

6. The CCRS process appears to improve performance over conventionally coated CODEP B Rene' 125 blades, but it does not perform as well as PVD. However, as a cobalt-base, paired vane coating, it is unacceptable - i.e., not equivalent to CODEP B and will require further process modifications.

This report summarizes the work done by General Electric from 25 March 1977 to 15 December 1978 on subcontract P.O. 3654-32007-P35(CR), "Evaluation of Solar CCRS Environmentally Protective Coatings for Turbine Hardware". The CCRS coatings evaluated were NiCrAlY and CoNiCrAlY deposited on both Rene' 125 and X-40 mechanical and environmental test specimens. Three X-40, TF34 paired 1ststage HPT vanes and two Rene' 125, F101 1st-stage HPT blades were also coated using the CCRS process and evaluated. However, early in the program it was decided to discontinue the CCRS NiCrAlY investigation due to Solar's inability to provide dense, uniformly coated specimens with consistent composition and microstructure. Coatings produced were porous with aluminum levels that varied from 8 to 16 weight percent and a non-uniform, two-phase microstructure. The goal of the program was to provide a dense, single-phase, beta-Ni(Co)Al additive coating. The CCRS NiCrAlY overlay coating status is contained in Solar Report RDR 1874-8.

Results of the CCRS coating investigation on the mechanical properties and environmental resistance of coated specimens and airfoil procesing is presented. The data is arranged as follows:

- Specimen preparation and test procedures
- Coating microstructure
- Mechanical properties and environmental resistance
- CCRS coating process adaptation.

1.0 SPECIMEN PREPARATION AND TEST PROCEDURES

1.1 Material

All X-40 and Rene' 125 specimens tested in this report were conventionally cast by Howmet Corporation to G.E. metal specifications C50TF21B (X-40) and C50TF60 (Rene' 125). Specimens were cast to rough drawing dimensions and machined to size. The drawing numbers used are summarized as follows:

G.E. Drawing Number	Specimen Type
4013163-112W-P8	Modified (0.050" thick) flat sheet - Stress rupture
4013163-112W-P8	Modified (0.050" thick) flat sheet - DBTT
4013135-718	Single wedge SETS specimen
-	Environmental test specimen 1.500" long by 0.125" diameter with rounded tip

The turbine blades and vanes (Figs. B-1 and B-2) used for the coating study were obtained from engineering stores and conformed to the preceeding specifications. The specimen drawings are shown in Figures B-3, B-4 and B-5.

Figure B-1.

Photograph of an F101, 1st-stage, HPT Blade

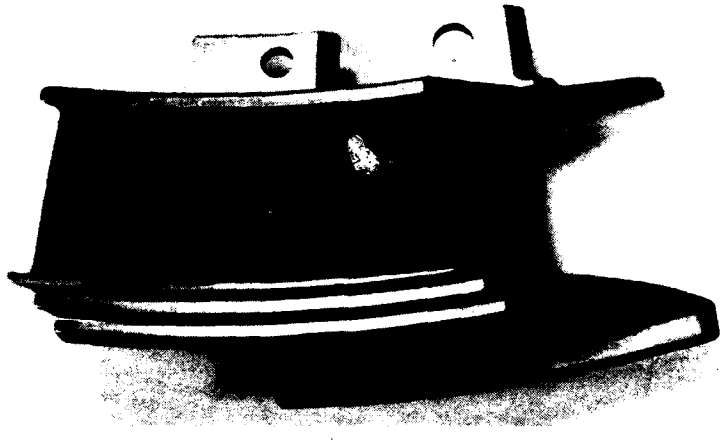

Figure B-2.

Photograph of a TF34, 1st-Stage, HPT Paired Vane

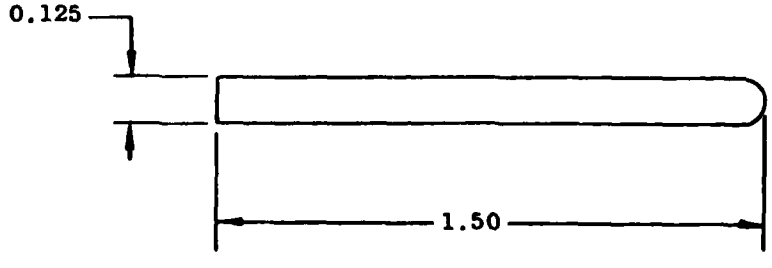

Figure B-3. Pin Specimen Used for Oxidation and Hot Corrosion Testing

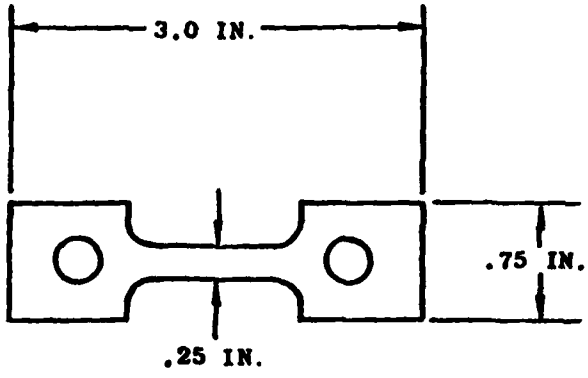

Figure B-4. Specimen Configuration for Thin Wall Effects Stress-Rupture Testing; 15-60 Mils Thick; Gauge Section Not to Scale

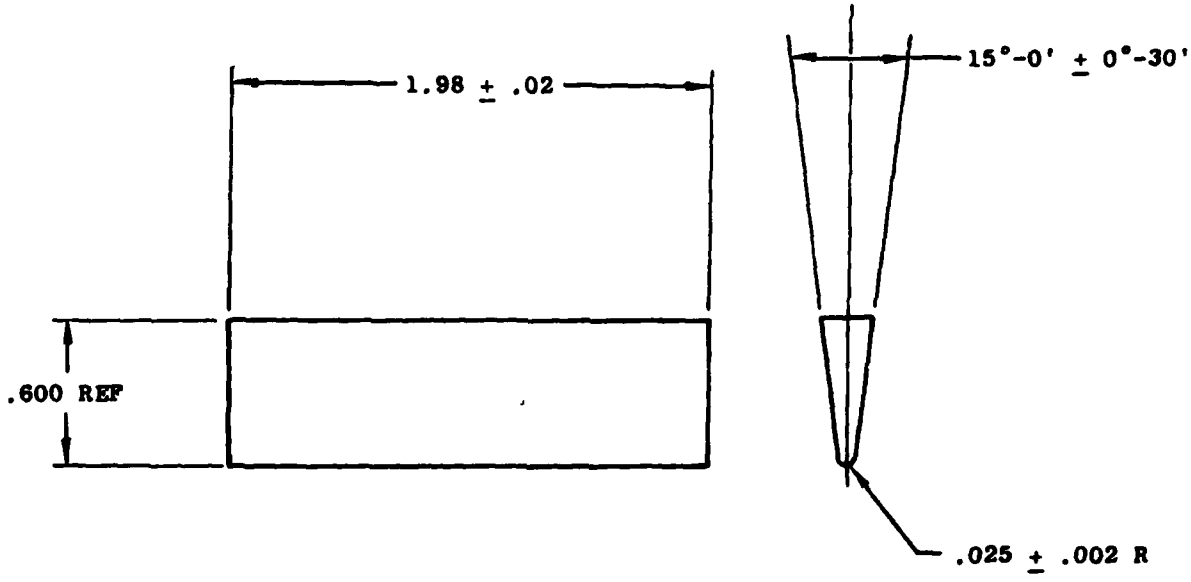

Figure B-5. Thermal Fatigue Specimen Configuration for SETS Test

1.2 Specimen Processing

All bare specimens tested received the following standard heat treatments:

Rene' 125	2150°F for 2 hours 1975°F for 4 hours 1500°F for 16 hours
X-40	Alloy used in as-cast condition

All coated mechanical test specimens received the standard alloy solution heat treatments and the following coating parameters:

CODEP B (Rene' 125 only)	CODEP B pack (i.e., low-activity aluminum pack utilizing a volatile Halide activator, 4 hours at 1975°F in hydrogen)
	Coating thickness nominally 0.002"
	Post-coating ductilizing - 4 hours at 1975°F in vacuum
	Alloy age (Rene' 125) - 16 hours at 1500°F in vacuum
CODEP B (X-40 only)	CODEP B pack (i.e., high-activity aluminum pack utilizing a volatile Halide activator, 4 hours at 1925°F in hydrogen)
	Coating thickness nominally 0.002"
	Post-coating ductilizing - 4 hours at 1925°F in vacuum
PVD NiCrAlY (Rene' 125 only)	Ni-21Cr-8Al-0.4Y nominal BC32 feed bar (vapor deposited from bar stock at 1850°F for 1.3 hours)
	Coating nominally 0.003-0.005"
	Post-coating steel shot peened
	Post-coating ductilization - 4 hours at 1975°F in vacuum
	Alloy age (Rene' 125) - 16 hours at 1500°F in vacuum
PVD CoCrAlY (X-40 only)	Co-22Cr-11Al-0.4Y nominal BC21 feed bar (vapor deposited from bar stock at 1850°F for 0.8 hour)
	Coating nominally 0.003-0.005"
	Post-coating ductilization for 4 hours at 1975°F

CCRS - There were two coating systems tested:

1. Dual cycle (line-of-sight process) for all mechanical and environmental test specimens and blades.

    - CoNiCrY powder using a cellulose binder sprayed onto specimens to form bisque.

- Medium activity controlled composition pack aluminide for 8 hours at >1900°F in hydrogen
- Rejuvenate medium activity controlled composition pack aluminide used previously for 8 hours at >1900°F in hydrogen - total 16 hours
- Post-coating ductilizing 4 hours at 1975°F in vacuum
- Alloy age (Rene' 125 only) - 16 hours at 1500°F in vacuum

2. Single-cycle (out-of-line-of-sight process) for all paired vanes
   - CoNiCrY powder deposited using a fluidized process and organic pre-sprayed binder to deposit a bisque
   - Medium activity controlled composition pack aluminide for 8 hours at >1900°F in hydrogen
   - Rejuvenate medium activity controlled composition pack aluminide used previously for 8 hours at >1900°F in hydrogen - total 16 hours
   - Post-coating ductilizing 4 hours at 1975°F in vacuum

1.3 Test Procedures

The following conditions and test procedures were used to evaluate the mechanical properties and environmental tests used in this report. They are as follows:

1.3.1 Mechanical Properties Testing

Stress Rupture

1800°F, Axial loading, 1 to 1000 hours

Ductile Brittle Transition Temperature (DBTT)

Coated sheet specimens were step loaded to produce 0.2% (in./in.) strain increments (strain rate 0.005 in./in.) until the coating cracked in the temperature range of 900-1500°F. A plot of cracking strain versus testing temperature is then generated to yield the DBTT.

Simulated Engine Thermal Shock (SETS)

Tests were conducted on the SETS rig designed and built in MPTL. This machine rapidly heats a specimen leading edge by radiation and conduction, holds for a specified time and rapidly cools the leading edge. For a given specimen geometry, the independent variables are the maximum temperature, and the heating and cooling rates.

The dependent variable is the number of cycles to crack. An arbitrary crack severity index (CSI) has been established for the SETS equipment and is summarized as follows:

Crack Severity Index (CSI	Description of Crack Severity
0	No cracking or surface deterioration
1	Pits at leading edge - not discernible as cracks
2	One to three cracks which do not traverse the leading edge arc
3	Four or more cracks which do not traverse the leading edge arc
4	One to three cracks which traverse the leading edge arc
5	Four or more cracks which traverse the leading edge arc
6	One to three cracks which extend past the leading edge arc
7	Four or more cracks which extend past the leading edge arc
8	One to three cracks which extend past the leading edge arc by at least 3/32 inch

See Reference 1 for a detailed description of the testing procedure. The typical thermal cycle used to evaluate the SETS specimens, both wedges and airfoils, is shown in Figure B-6.

1.3.2 Environmental Testing

Dynamic Oxidation

Coated specimens, rotated at 0.05 Mach, were tested at 2100°F using a natural gas fired flame and cycled 16 times per hour. They were tested for up to 600 hours.

Hot Corrosion

Coated specimens, rotated at 0.05 Mach, were tested at 1700°F, 5 ppm salt using JP-5 fuel and cycled one time per hour. They were tested for up to 500 hours.

2.0 COATING MICROSTRUCTURE

Representative samples of the various CCRS coatings deposited on X-40 and Rene' 125 were investigated for:

- Structure
- Phases present
- Chemistry

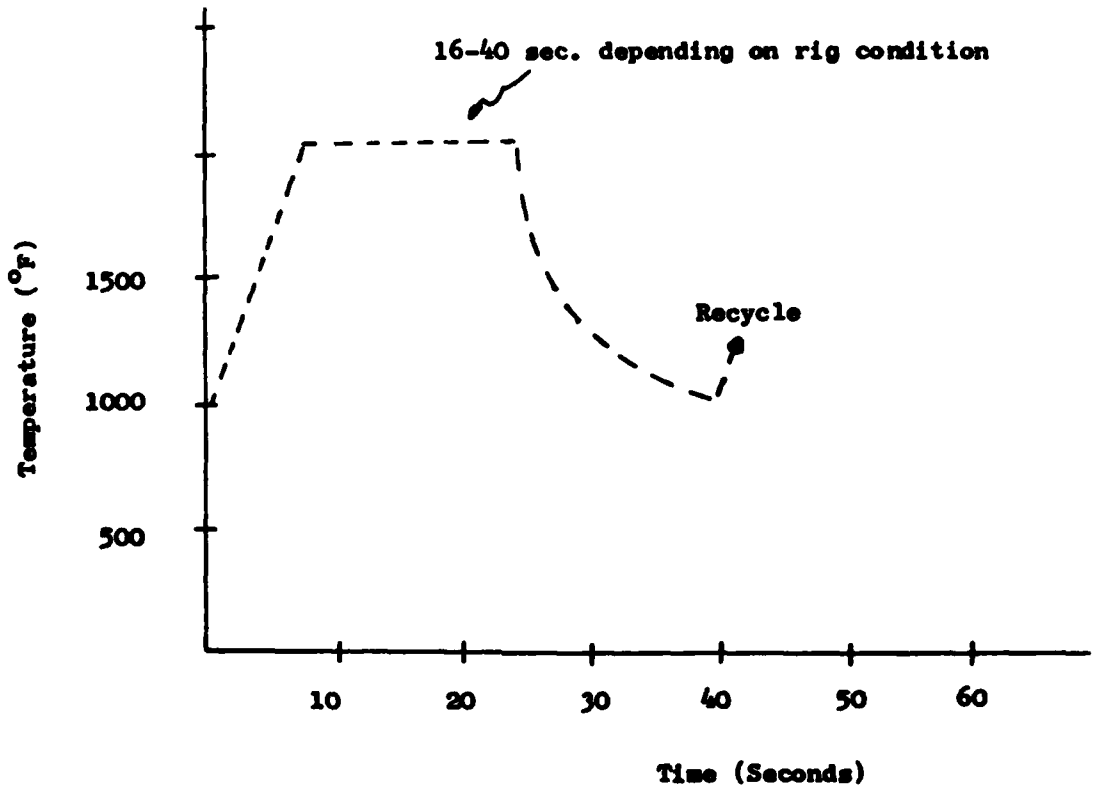

Figure B-6. Typical Thermal Cycle Encountered on the Leading Edges of SETS Wedge Specimens

Standard metallographic techniques were used including SEM/EDAX and microprobe analysis. In all cases only the CCRS CoNiCrAlY coatings were investigated.

2.1 CCRS/X-40

Metallographic investigation of the as-received CCRS CoNiCrAlY deposited on X-40 revealed it was less than completely dense with approximately 3 to 4 percent porosity evident. The coating is an add-on type (0.002" diffusion zone), approximately 0.003" thick and has a coating structure similar in appearance to CODEP B on X-40 (Fig. B-7). Two phases were evident within the coating, a predominantly beta-Co(Ni)Al matrix phase with large amounts of alpha-chromium precipitated throughout. Also, at the coating/parent metal interface, a continuous chromium-rich phase, probably $Cr_{23}C_6$, was evident along with the presence of internal, acicular shaped oxides. Coating phase identification was verified by SEM/EDAX analysis shown in Figure B-8. This coating structure was predominantly the same on both the as-received mechanical test specimens and oxidaton pins.

Microprobe analysis of the coated CCRS/X-40 specimens gave a nominal composition of Co-16Ni-10-20Cr-15Al-Y (unable to check for Y but believed to be between 0.2 and 1.2 weight percent). A typical microprobe diffusion profile is shown in Figure B-9.

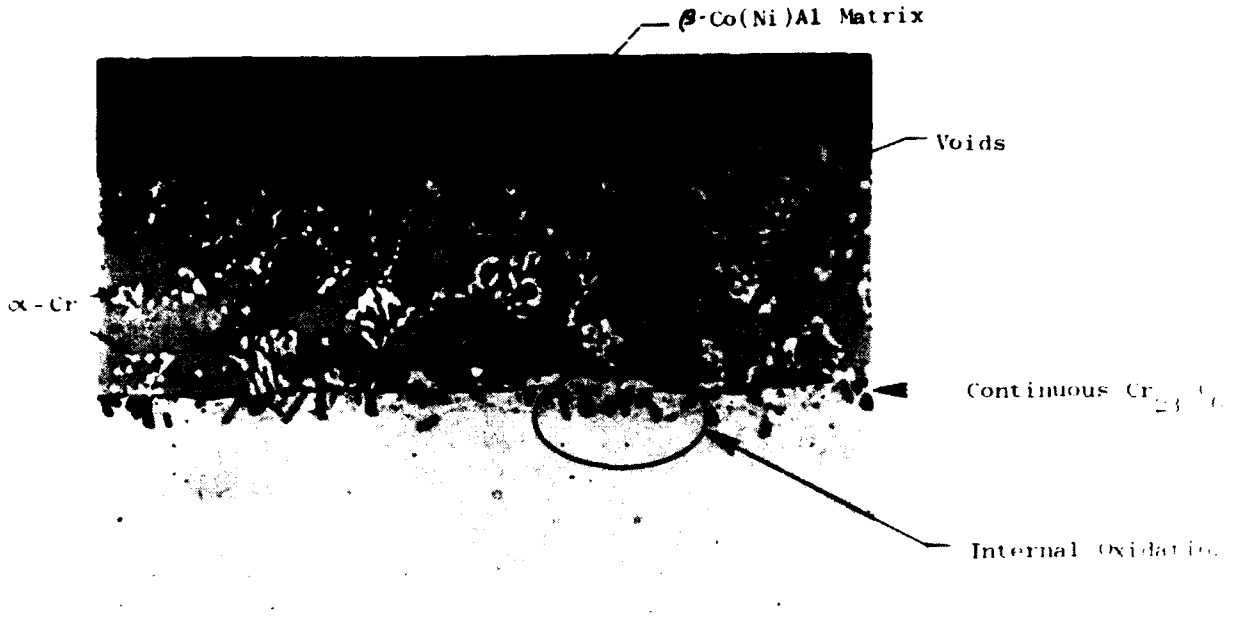

Figure B-7. Photomicrograph of a CCRS CoNiCrAlY Coated X-40 Specimen; Magnification: 500X

2.2 CCRS/Rene' 125

Metallographic investigation of the as-received CCRS CoNiCrAlY deposited on Rene' 125 showed a fully dense, add-on type coating. The additive layer was predominantly single-phase beta-Ni(Co, Cr)Al with some gamma-NiCo(Cr) solid solution evident at prior beta grain boundaries for the mechanical test specimens and two-phse beta-Ni(Co, Cr)Al/gamma-NiCo(CR) solid solution for the oxidation pins. Large (0.001-0.002") entrapped alumina particles were also evident at the surface of all CCRS coated Rene' 125 specimens, Figure B-10. It is assumed these particles were entrapped during the pack cementation cycle of the CCRS coating process.

A two-phase beta/gamma diffusion zone, 0.001 to 0.0015 inch thick, was evident on both types of specimens. This large a diffusion zone is not normally encountered in PVD MCrAlY type coatings (0.00025-0.0005" normal for PVD) and resulted from excess diffusion of aluminum into the parent metal during the long, i.e., 16 hours at >1900°F, diffusion pack cementation cycle. Small amounts of sigma phase were also evident within the parent metal adjacent to the diffusion zone. However, this is not expected to affect base metal properties. Phase identification was verified by SEM/EDAX shown in Figure B-11.

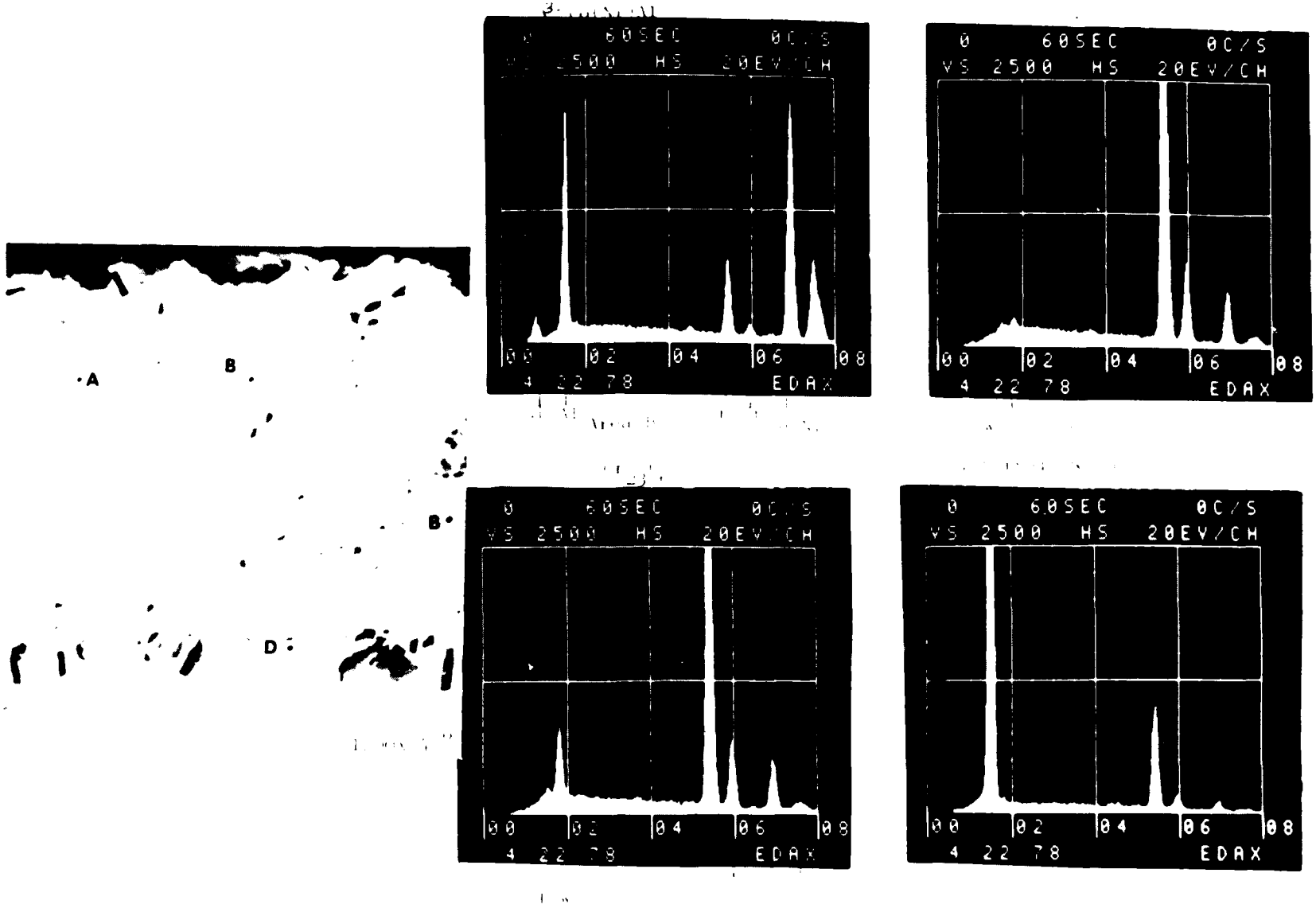

Figure B-8. SEM/EDX Analysis of a Fully Processed CCRS CoNiCrAlY Coated X-40 TF34 Paired Vane

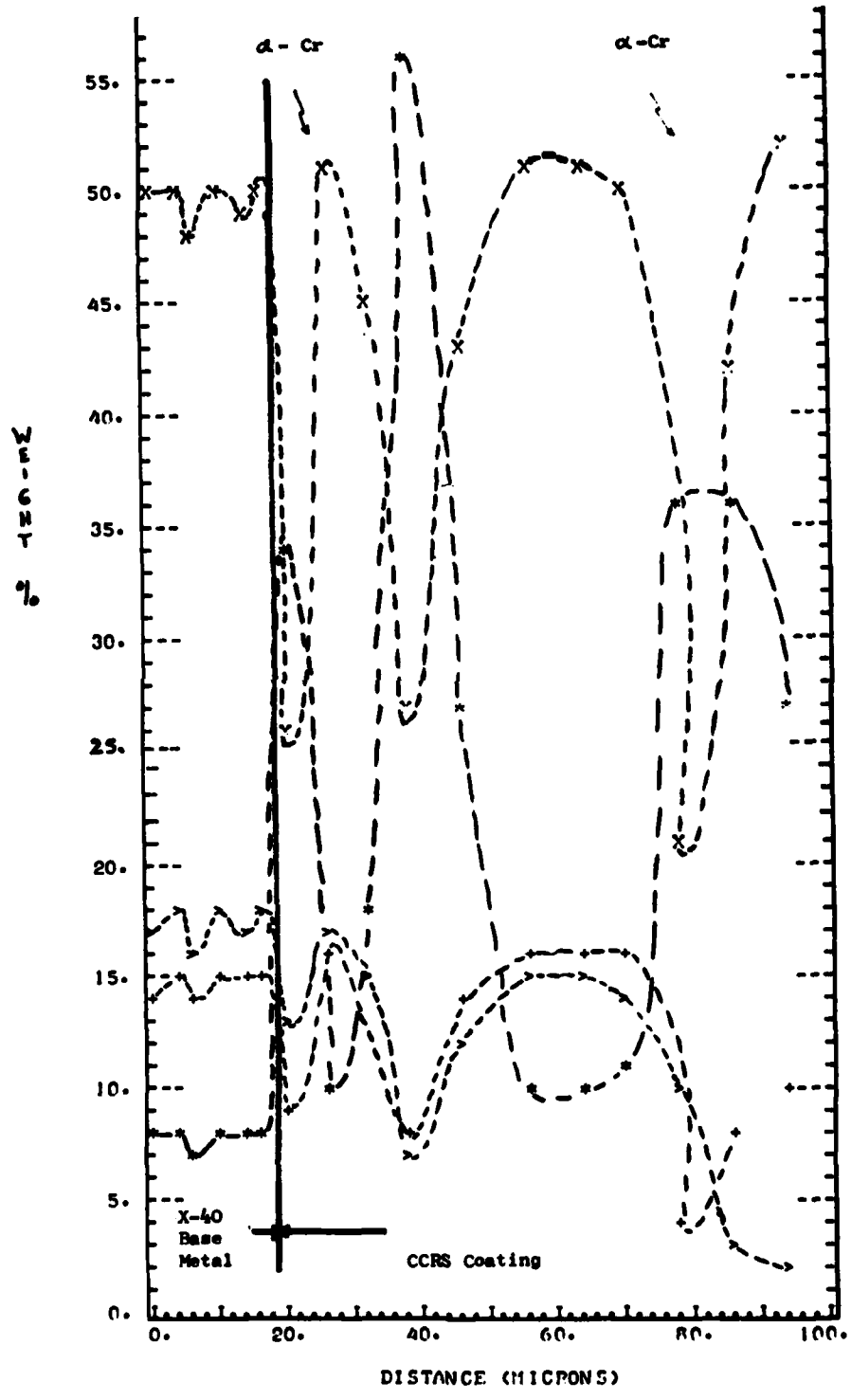

Figure B-9. Typical Microprobe Diffusion Profile

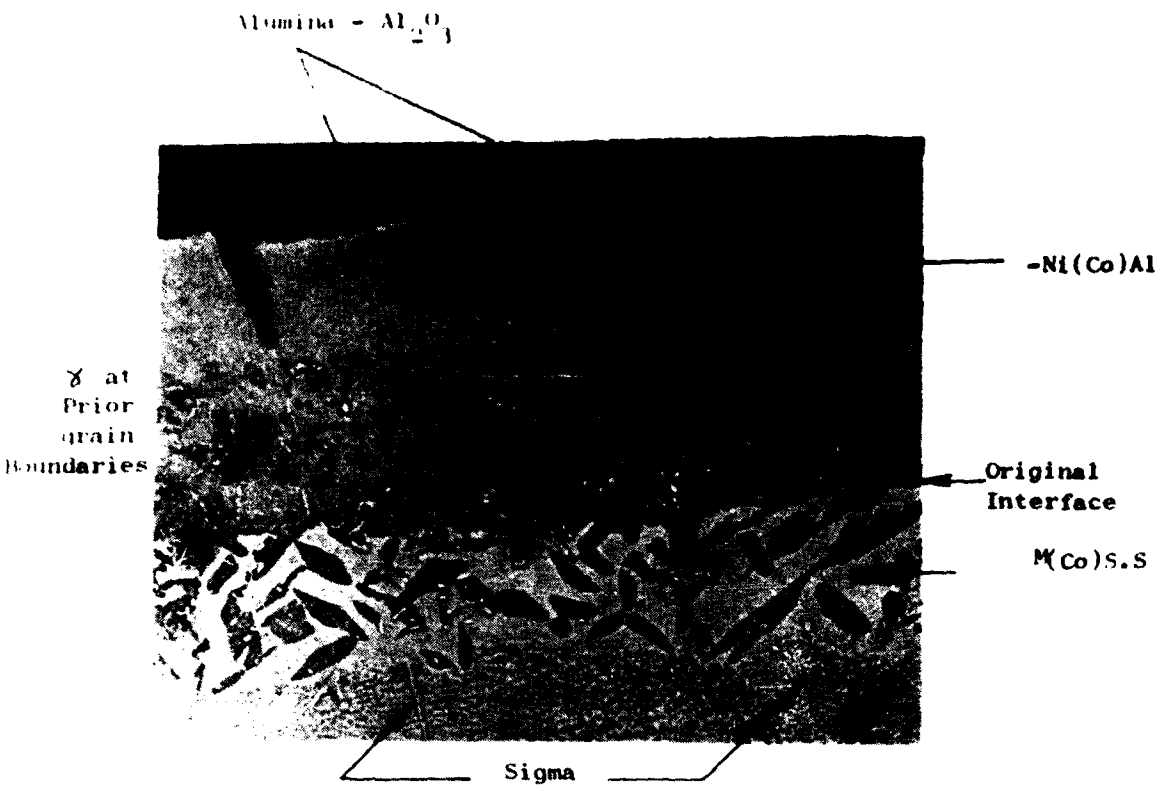

A. As-Received Mechanical Test Specimens

B. Environmental Test Pins. Arrows Denote Large Areas of Gamma, Ni(Co) Solid Solution

Figure B-10. Photomicrographs of CCRS CoNiCrAlY Coated Rene' 125 Specimen Showing Difference in Structure Between Coatings; Mag: 500X

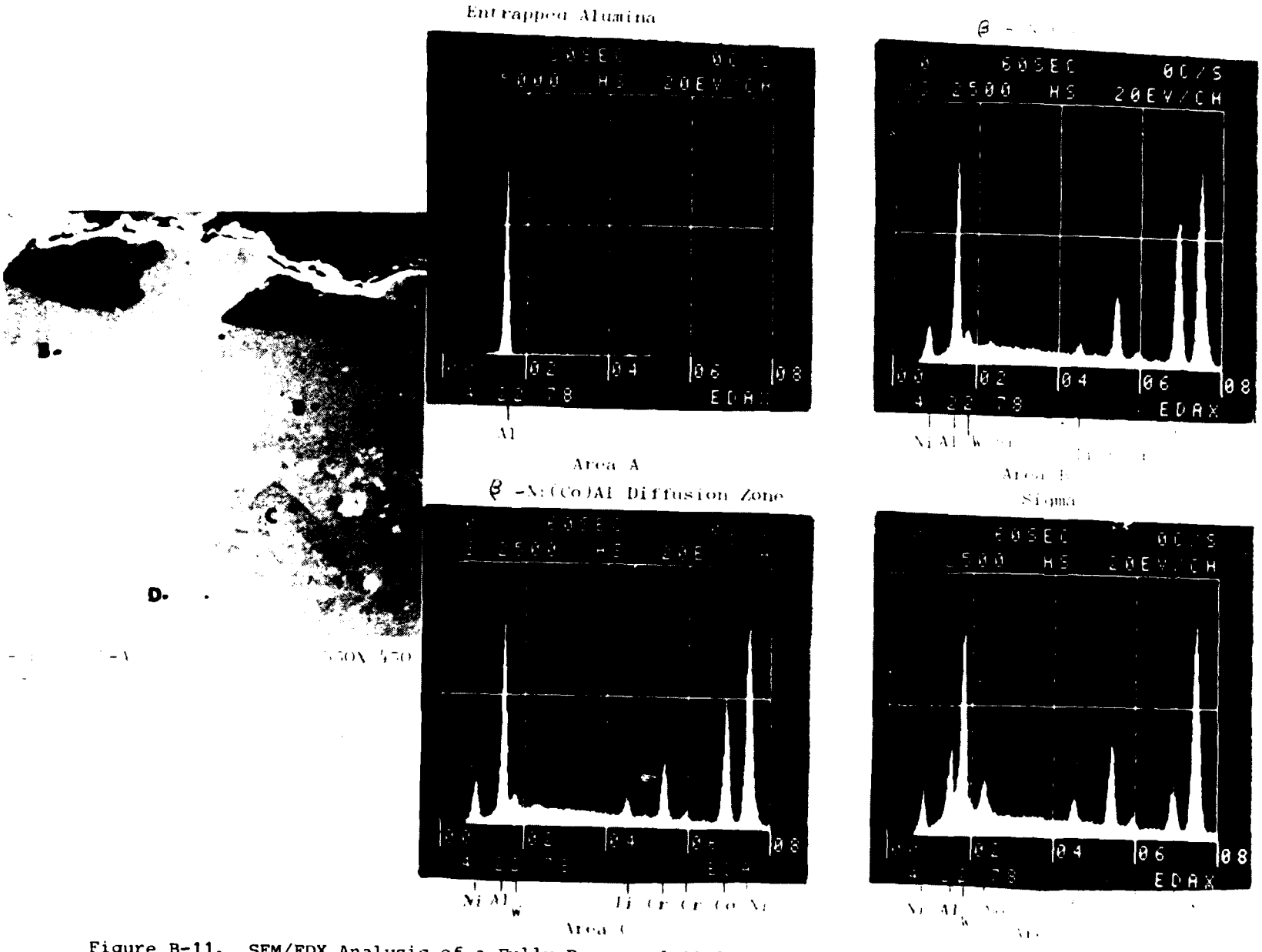

Figure B-11. SEM/EDX Analysis of a Fully Processed CCRS CoNiCrAlY Coated Rene' 125 F101 HPT Blade

Microprobe analysis of the CCRS coatings found in the mechanical properties specimens was nominally 42Ni, 33Co, 7Cr, 14 Al and Y (unable to check Y, but believed to be between 0.2-1.0 weight percent, since no yttride precipitate phases were observed. The maximum yttrium solubility is about 1 to 1.3 weight percent.) A typical microprobe diffusion profile is shown in Figure B-12.

3.0 MECHANICAL PROPERTIES AND ENVIRONMENTAL RESISTANCE

3.1 Mechanical Properties

Mechanical property tests were performed on CCRS CoNiCrAlY coated X-40 and Rene' 125. The following tests were used:

- Ductile-brittle transition temperature (DBTT)
- Thin wall stress rupture
- Thermal mechanical fatigue (SETS)

3.1.1 Ductile-Brittle Transition Temperature (DBTT)

The DBTT of CCRS CoNiCrAlY, Lot 9653, coatings on X-40 and Rene' 125 were determined by plotting the strain required to produce a dectable crack (standard Zyglo fluorescent penetrant techniques were used to determine the onset of cracking) isothermally in the temperature range of 900-1500°F. A plot of the curve obtained is shown in Figure B-13.

The DBTT's of the CCRS coated Rene' 125 and X-40 specimens were equivalent. The strain versus temperature curve indicates a DBTT between 1250-1350°F.

3.1.2 Stress Rupture

Stress-rupture tests were conducted on both bare and CCRS CoNiCrAlY coated X-40 and CCRS CoNiCrAlY coated Rene' 125, 0.050" thin wall sheet specimens. Thin wall specimens were investigated in an attempt to simulate the effects of the coating on an actual airfoil. The tests were conducted at 1800°F and involved two coating lots, 9653 and 8864. The results of all tests are presented in Tables B-1 and B-2 and graphically in Figure B-14.

The test results for the coated CCRS Rene' 125 specimens fall below the -3 sigma (standard deviation units) curve for bare Rene' 125. This observed loss (25-30%) is slightly greater than that recorded for CODEP B on Rene' 125 (see Fig. B-14). SEM analysis of the failed specimens indicates that severe surface cracking occurred which was caused by the presence of large entrapped alumina particles on the specimen surface, Figure B-15. Analysis indicates the specimens failed as a result of surface initiated coating cracsk. These cracks then propagated into the parent metal causing intergranular cracking (Fig. B-16). Cracking may also have been facilitated through formation of a very large, coarse, beta/gamma diffusion zone. This zone is expected to be weaker than the fine gamma/gamma prime network of the parent alloy. Analysis of the CCRS coated X-40 specimens indicate the results fall either on or between the -3 sigma curve for bare, large bar and thin wall X-40,

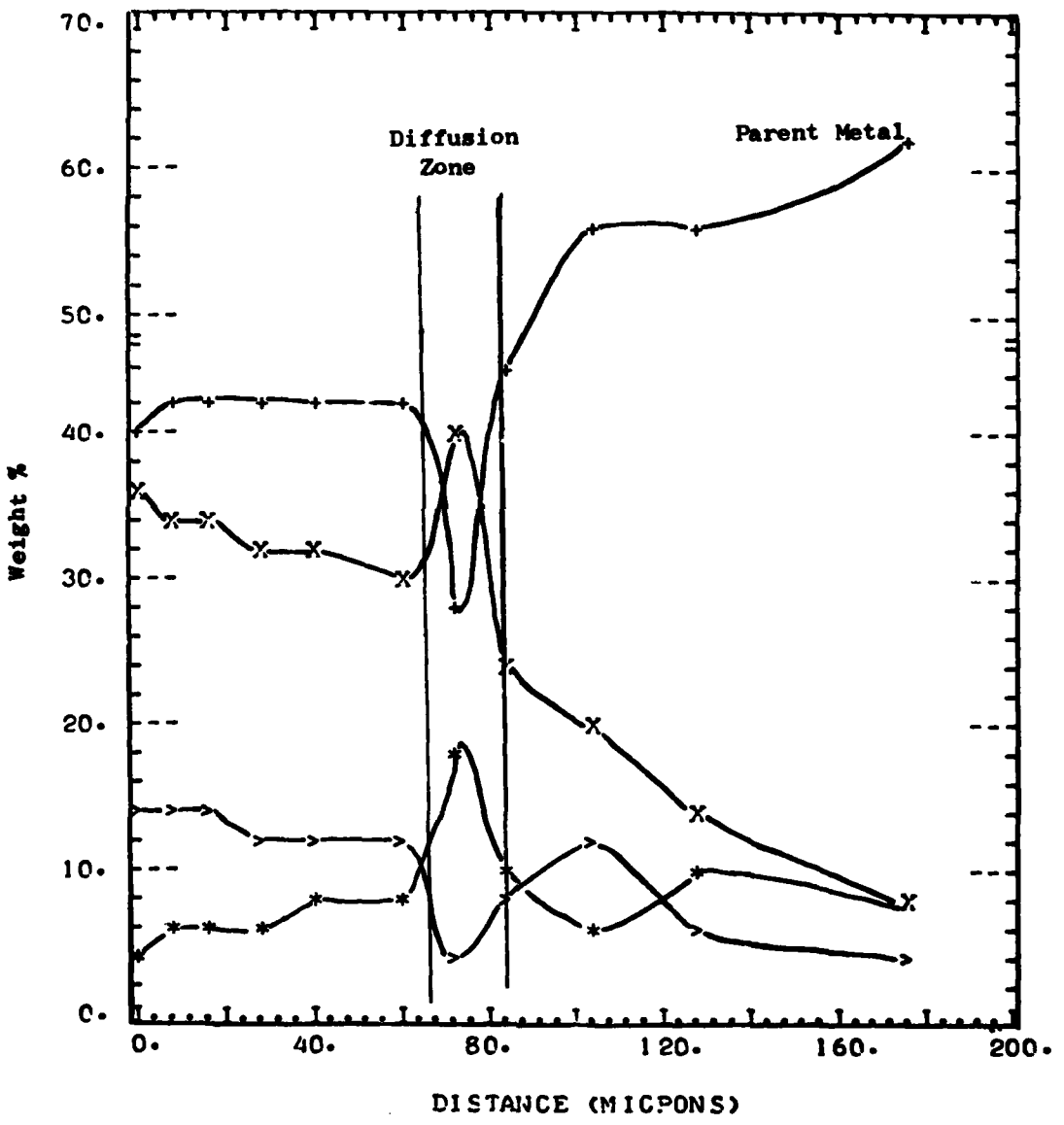

Figure B-12. Typical Microprobe Scan of the CCRS CoNiCrAlY Coating Deposited on Rene' 125 Mechanical Test Specimens

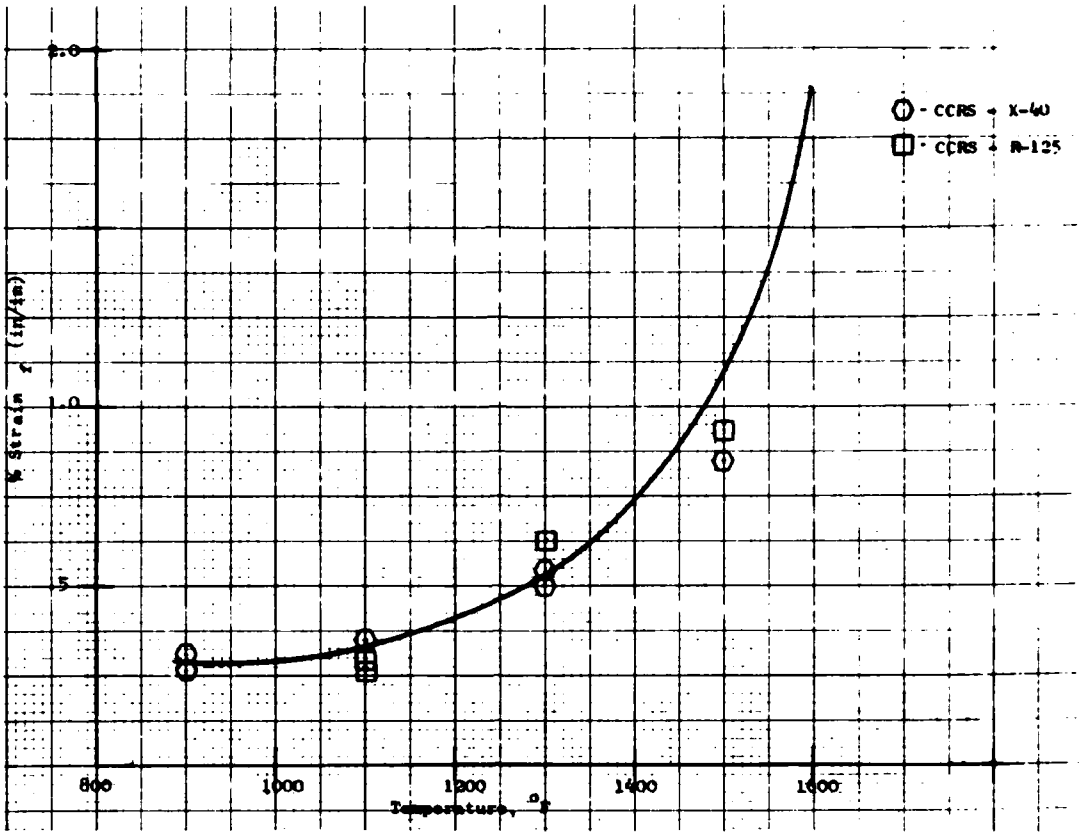

Figure B-13. Strain to Cracking Versus Temperature Curve for CRS CoNiCrAlY Coated X-40 and Rene' 125

Table B-1

1800°F Stress Rupture Results for Bare and CCRS CoNiCrAlY Coated X-40
0.050 Inch Thin Wall Sheet Specimens

Specimen Number	Stress* (ksi)	Life (hrs)	Elong. (%)
(Lot 9653)			
C-7	15.0	1.8	19.5
C-9	13.0	5.2	23.3
C-8	5.0	213.5	4.7
C-10	9.0	48.6	13.3
C-15	11.0	14.0	18.0
(Lot 8864)			
C-38	13.0	10.6	32.3
C-41	11.0	35.5	25.7
C-43	9.0	128.2	27.9

* All Stress Calculated using uncoated specimen dimensions

Table B-2

1800°F Stress Rupture Results for Bare and CCRS CoNiCrAlY Coated Rene' 125
0.050 Inch Thin Wall Sheet Specimens

Specimen N	Stress* (ksi)	Life (Hrs)	Elong. %
CCRS Coated			
(Lot 9653)			
C-22	15	625.7	9.5
C-18	24	60.7	8.9
C-20	20.0	149.4	8.0
C-23	34.0	6.0	5.3
C-26	30.0	12.4	4.9
C-27	40.0	1.5	3.8
(Lot 8864)			
C-31	34.0	4.0	4.0
C-30	24.0	64.9	7.0

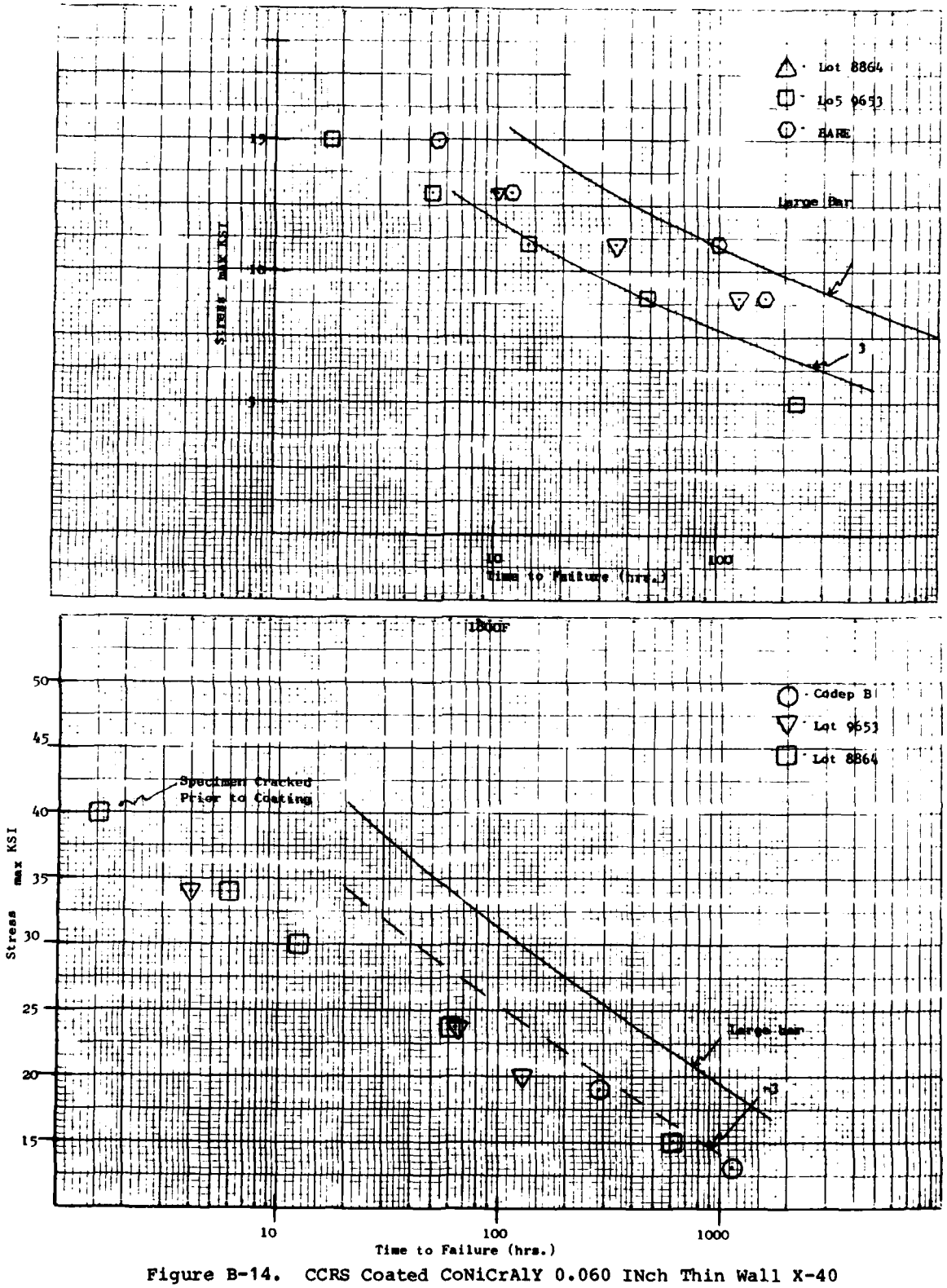

Figure B-14. CCRS Coated CoNiCrAlY 0.060 INch Thin Wall X-40

Magnification: 625X

Figure B-15. SEM Shot of Surface of a Dense CCRS CoNiCrAlY Coated Rene' 125 Stress-Rupture Specimen After Test Showing Large Amounts of Entrapped Surface Alumina and Severe Surface Cracking (Arrows)

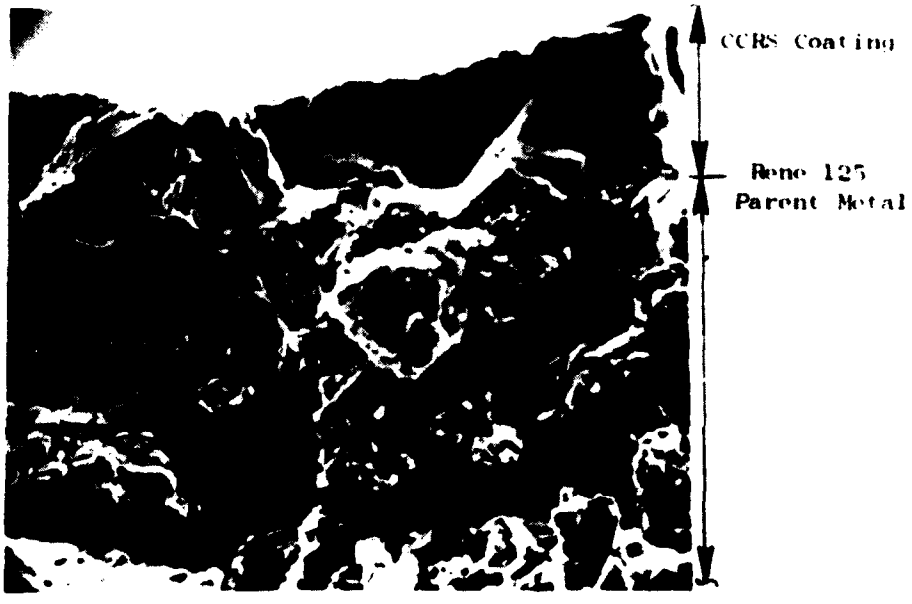

Magnification: 700X

Figure B-16. SEM Shot of a Stress-Rupture Tested Dense CCRS CoNiCrAlY Rene' 125 Specimen Showing Intergranular Cracking as the Result of a Surface Initiated Crack (Arrows)

depending on the coating lot, Table B-2. Coating defects or inclusions, such as those observed for the Rene' 125 specimens, were not observed. Also, the severe surface cracking observed on Rene' 125 was not present.

Metallographic evaluation of the CCRS coating after test showed severe distress of the coating resulting from preferential oxidation at the alpha-Cr/beta-CoAl matrix interface (Fig. B-17). However, since the test temperature was above the coating DBTT (i.e., 1250-1350°F), very little cracking within the coating was observed, i.e., in this temperature range the coating is ductile, allowing significant plastic deformation and stress relief. Processing voids, inherent to the coating, are also evident.

Crack propagation appears to have been initiated at either the coating surface, oxidation its and/or at voids. These sites then act as stress risers, resulting in crack formation and eventual specimen failure.

Generally, thin sections show lower rupture lives than thick sections. Strength degradation results from the combined effects of geometric acceleration of the fracture, increases statistical probability of unfavorably oriented grains and grain boundaries, the influence of the environment, and coating crack initiation. Both CCRS and coated CoNiCrAlY X-40 and Rene' 125 produced lower than anticipated lives when compared to the bare alloy properties.

3.1.3 Thermal Fatigue (SETS)

In order to assess the thermal fatigue resistance of CCRS CoNiCrAlY coated superalloys, several coating/substrate combinations used for gas turbine applications were investigated. The various systems are summarized in the following:

Various Coating/Substrate System SETS Tested

Coating	Substrate
CCRS CoNiCrAlY (Lot 8864)	X-40
CCRS CoNiCrAlY (Lot 9653)	X-40
High activity CODEP B	X-40
PVD CoCrAlY (BC21)	X-40
CCRS CoNiCrAlY (Lot 8864)	MA754
CCRS CoNiCrAlY (Lot 9653)	MA754

CCRS CoNiCrAlY coated Rene' 125 SETS specimens were not investigated.

The CSI reading for each system investigated are presented in Table B-3. In the cases investigated, the PVD CoCrAlY was found superior to CCRS CoNiCrAlY on X-40 while both were superior to CODEP B on X-40. Visually, however, CCRS coating Lot 9653 appears to have less distress and environmental attack than did Lot 8864. This suggests further process controls may be necessary. Both coating lots showed no evidence of cracking on MA754.

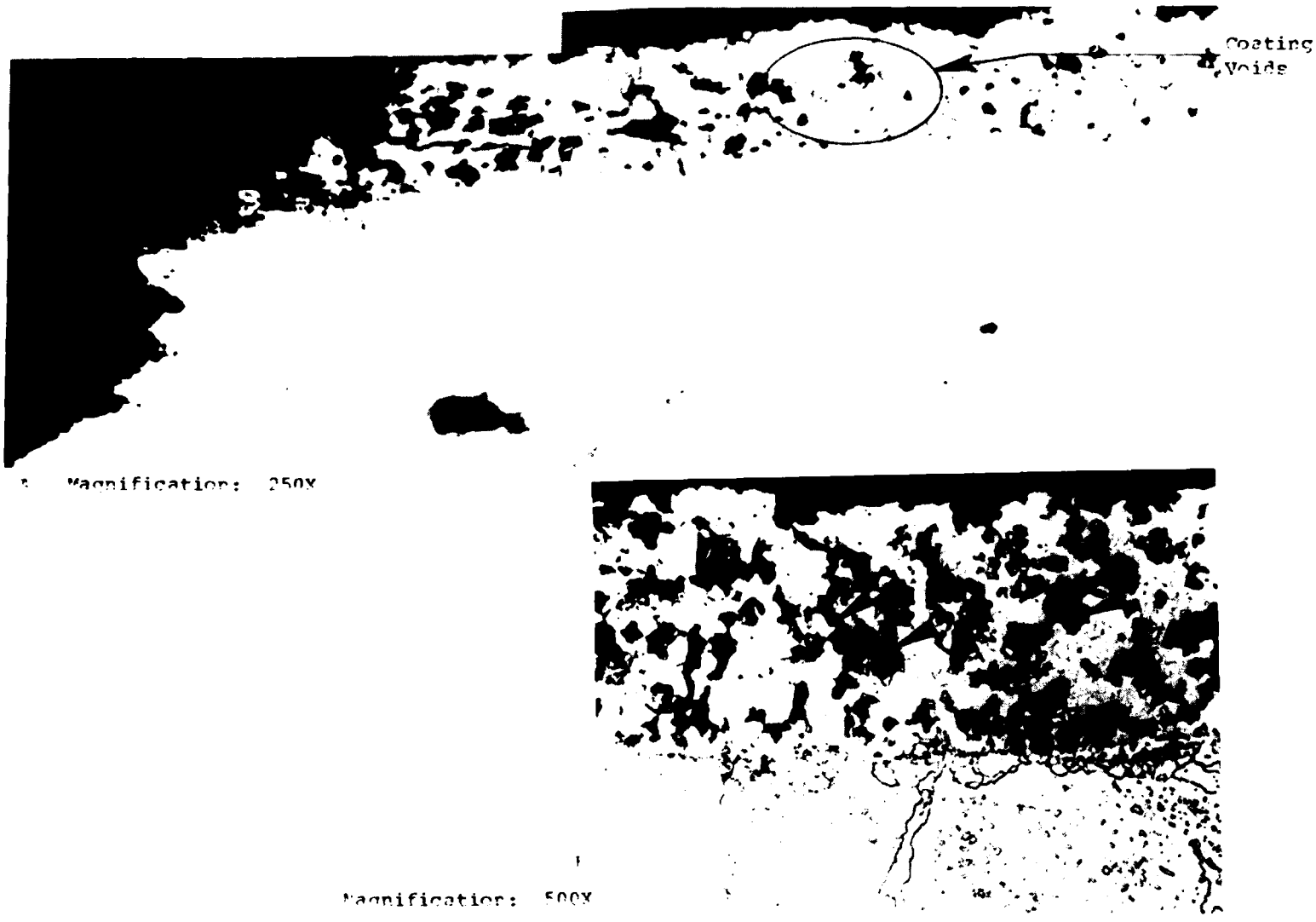

Figure B-17. Typical CCRS CoNiCrAlY/X-40 Stress Rupture SpecimenTested at 1800°F at 11 Ksi Showing (A) Coating Voids and (B) Preferential Oxidation Near Coating Alpha-Chromium Particles and Voids

Table B-3

Thermal Fatigue Behavior (CSI) of Bare and Coated Nickel-Base Superalloys

Coating/Substrate	S/N	CSI AT EACH INSPECTION INTERVAL			
		50	100	150	250
CCRSCoNiCrAlY/MA-754 Lot 8864	-	0	0	0	0
CCRS CoNiCrAlY/MA-754 Lot 9653	-	0	0	0	0
CCRS CoNiCrAlY/X-40 Lot 8864	C-45	0	0	0	0
CCRS CoNiCrAlY/X-40 Lot 8864	C-46	0	0	0	7
CCRS CoNiCrAlY/X-40 Lot 9653	C-4	0	0	2+	6+
CCRS CoNiCrAlY/X-40 Lot 9653	C-6	0	0	2	6+
Codep B/X-40 High Activity	-	0	0	2	7
PVD CoCrAlY/X-40 BC-21	-	1	1	1	4

Macroscopic and metallographic evaluation of the coated X-40 specimens was done. Macroscopically, the CODEP B specimens appeared to crack very early during testing but only a few cracks were observed. Conversely, the CCRS coated specimens showed slightly arrested crack formations compared to CODEP B, but when cracking occurred, many more cracks were visible. The PVD CoCrAlY showed only one crack across the entire specimen, Figure B-18.

Metallographic evaluation of the CCRS CoNiCrAlY coated X-40 specimens after test indicated that both Lots 8864 and 9653 had large percentages of voids present. These act as stress risers under an applied load, resulting in multiple crack initiation (see Fig. B-19). Also, an analysis of the cracks on all specimens revealed less oxidation of the parent metal substrate than for the CODEP B coatings, indicating earlier crack initiation for CODEP B. The crack lengths were also less.

It is interesting to note not only the effect of coating type on fatigue but also the effect of base alloy. The MA754, an oxide dispersion strengthened (ODS) alloy, showed no coating distress after 250 cycles. This alloy is much stronger than X-40 at high temperatures and has superior creep strength. This would affect the amount of plastic strain seen by the coating.

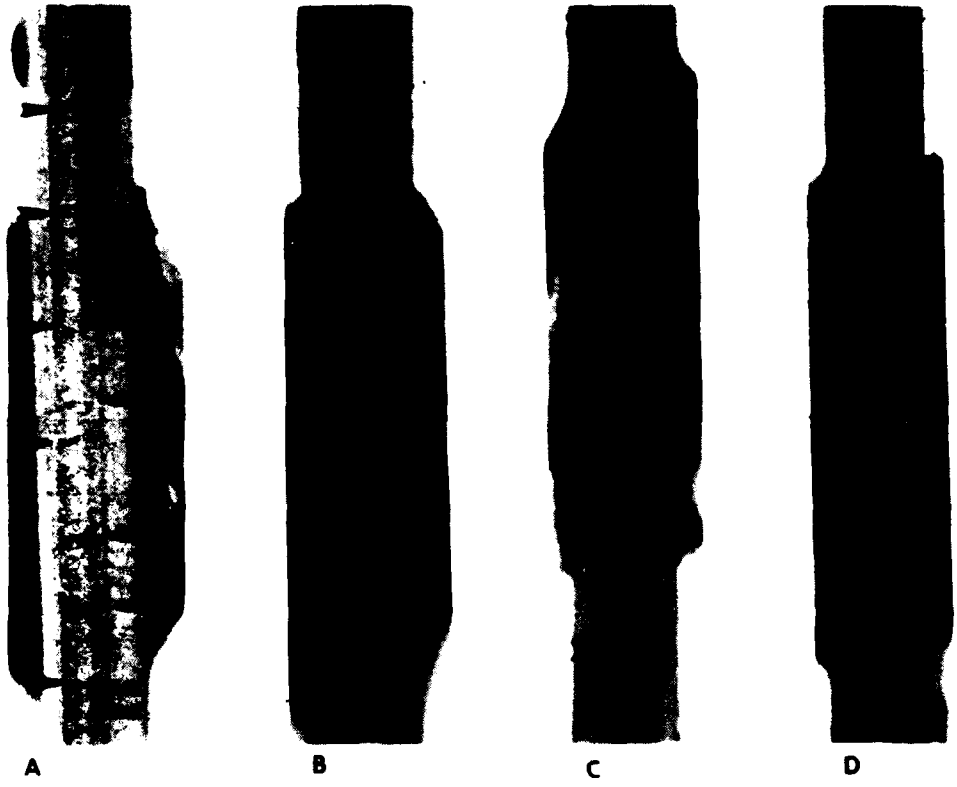

Figure B-18. Macrophotographs of Leading Edges of Tested SETS Wedges; (A) CCRS CoNiCrAlY/X-40 Lot 8864; (B) CCRS CoNiCrAlY/X-40 Lot 9653; (C) CODEP B/X-40 and (D) PVD CoCrAlY/X-40

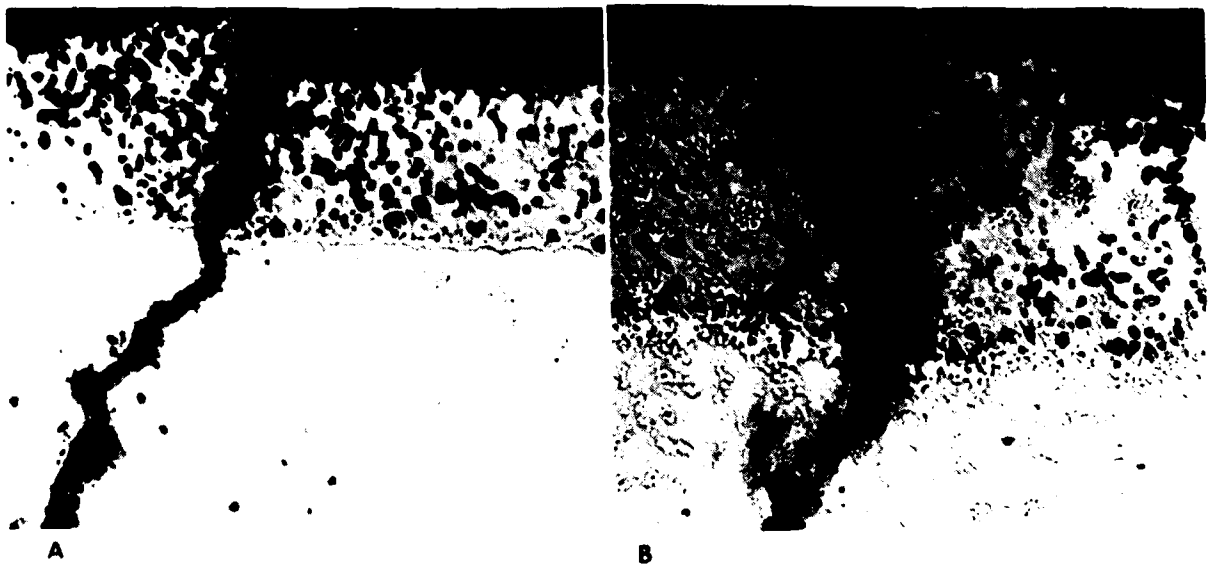

Figure B-19. CCRS CoNiCrAlY Coated X-40 Coated X-40 SETS Wedge Specimens After Test; (A) Lot 864 and (B) Lot 9653; Showing Porous Nature of One Coating (Magnification: 500X)

3.2 Environmental Resistance

In order to obtain the oxidation and corrosion resistance of CCRS CoNiCrAlY coating, several different coating/substrate combinations were investigated which have gas turbine applications. They are as follows:

Coating	Substrate
CCRS CoNiCrAlY	Rene' 125
CODEP B	Rene' 125
PVD NiCrAlY (BC32)	Rene' 125
CCRS CoNiCrAlY	MA754
PVD NiCrAlY (BC32)	MA754
CCRS CoNiCrAlY	X-40
CODEP B	X-40
PVD CoCrAlY (BC21)	X-40

All specimens were given appropriate post-coating heat treatments and then tested both in dynamic oxidation at 2100°F and in hot corrosion at 1700°F, 5 ppm salt for up to 525 hours. Simple weight gain curves for all systems tested in dynamic oxidation are shown in Figures B-20 through B-22. Two coating lots were investigated, 8864 and 9653. In all cases, coating Lot 8864 did not perform as well as Lot 9653 regardless of substrate.

3.2.1 Dynamic Oxidation

X-40

Results of the dynamic oxidation test indicate that on X-40 both the CODEP B and BC21 coatings were superior to CCRS CoNiCrAlY with failure of the CCRS coating occurring within 200 hours. Macrophotographs of the test specimens after 525 hours, respectively, are presented in Figure B-23. These clearly show that extensive spallation and coating separation has occurred for the CCRS coating.

Metallographic evaluation after 325 and 525 hours was done and is shown in Figures B-24 and B-25. It shows that the CCRS coating apparently failed through preferential attack around the high chromium (alpha-Cr) and through rapid attack of the coating-metal interface. Interfacial attack was facilitated through rapid transport of oxygen to the interface via voids within the coating. Even after 325 hours (Fig. B-24) substantial amounts of the coating have been consumed, with no Al_2O_3 forming beta-Co(Ni)Al phases visible and internal oxidation of the parent X-40 material evident. Conversely, the PVD CoCrAly coating was still protective after 525 hours, showed no evidence of substrate oxidation, and contained large amounts of beta-Co(Ni)Al (Fig. B-25). The CODEP B coatings, however, showed some evidence of substrate internal oxidation after 525 hours, although it was more protective than CCRS and did not show a spotty type of localized coating failure.

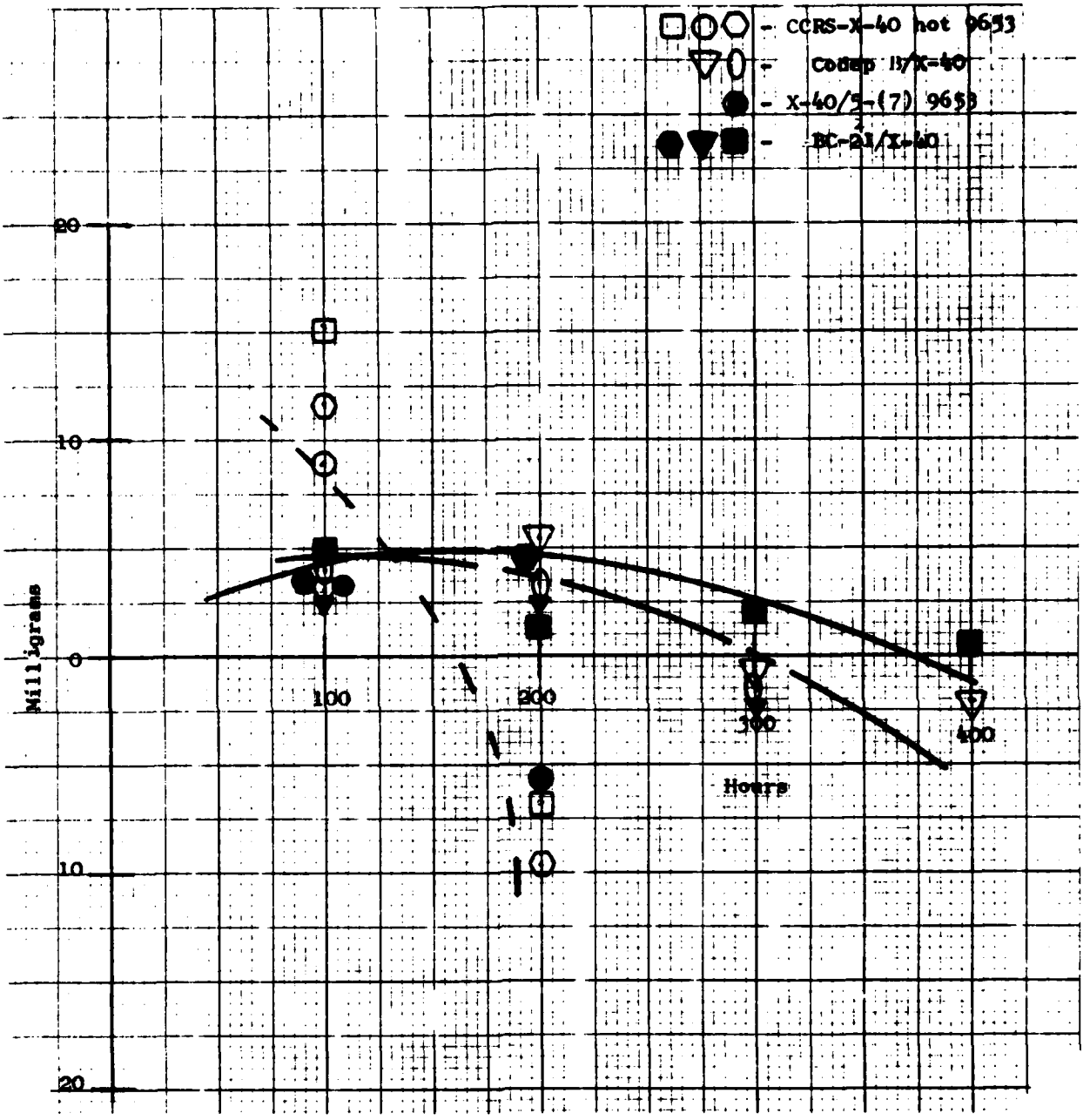

Figure B-20. Weight Gain Curve for CCRS CoNiCrAlY Coated X-40 Tested 15 2100°F Dynamic Oxidation

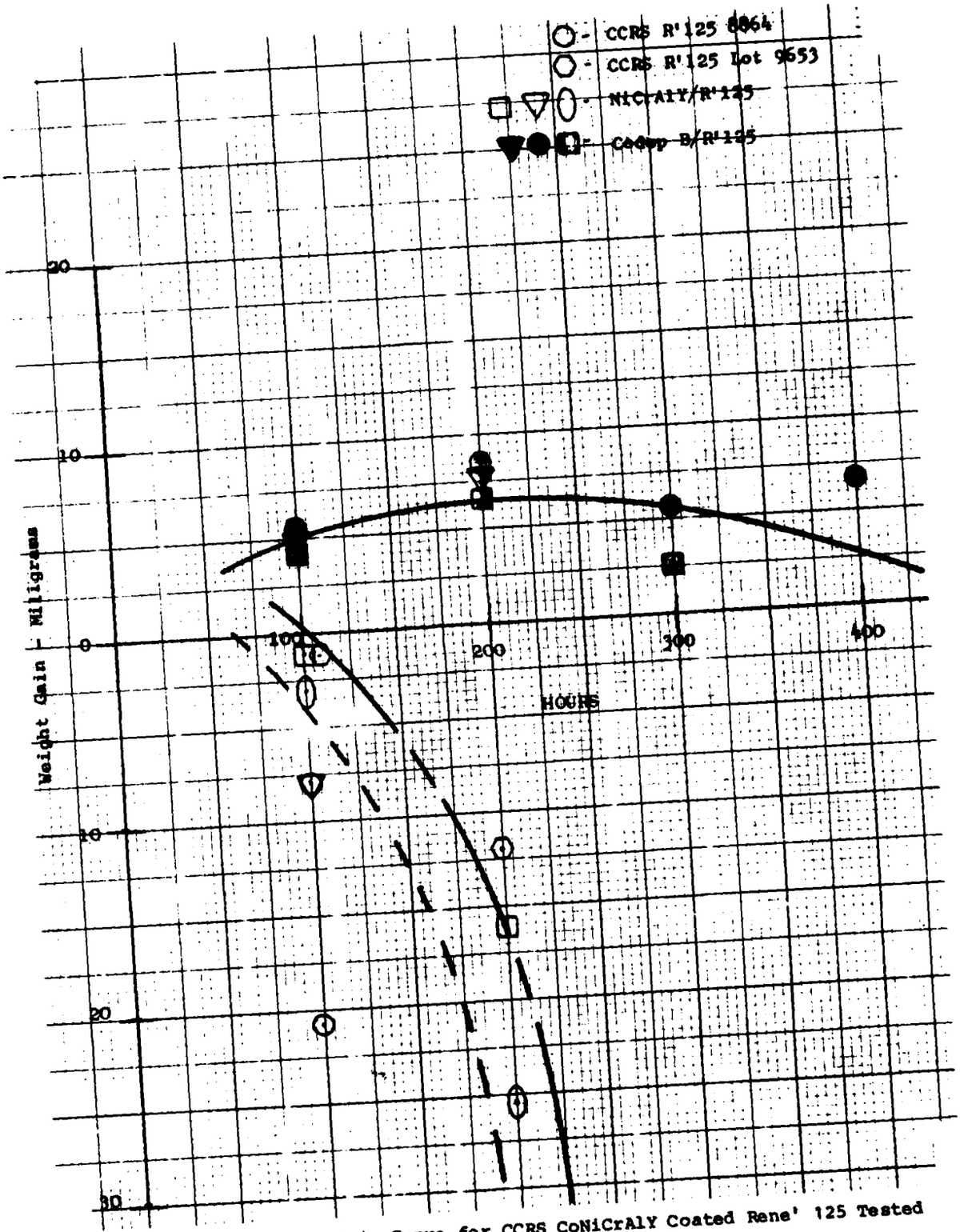

Figure B-21. Weight Gain Curve for CCRS CoNiCrAlY Coated Rene' 125 Tested in 2100°F Dynamic Oxidation

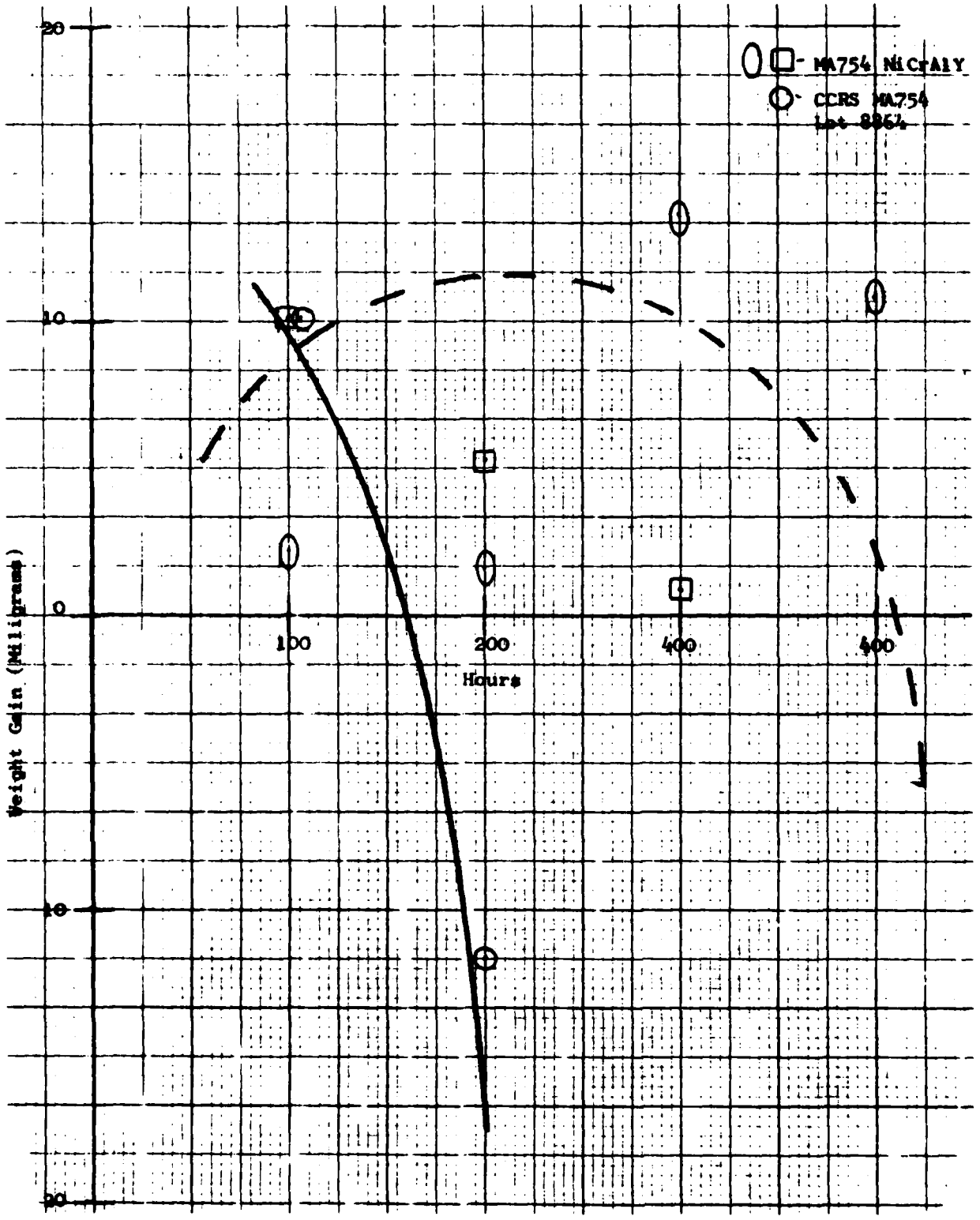

Figure B-22. Weight Gain Curve for CCRS CoNiCrAlY Coated MA754 Tested in 2100°F Dynamic Oxidation

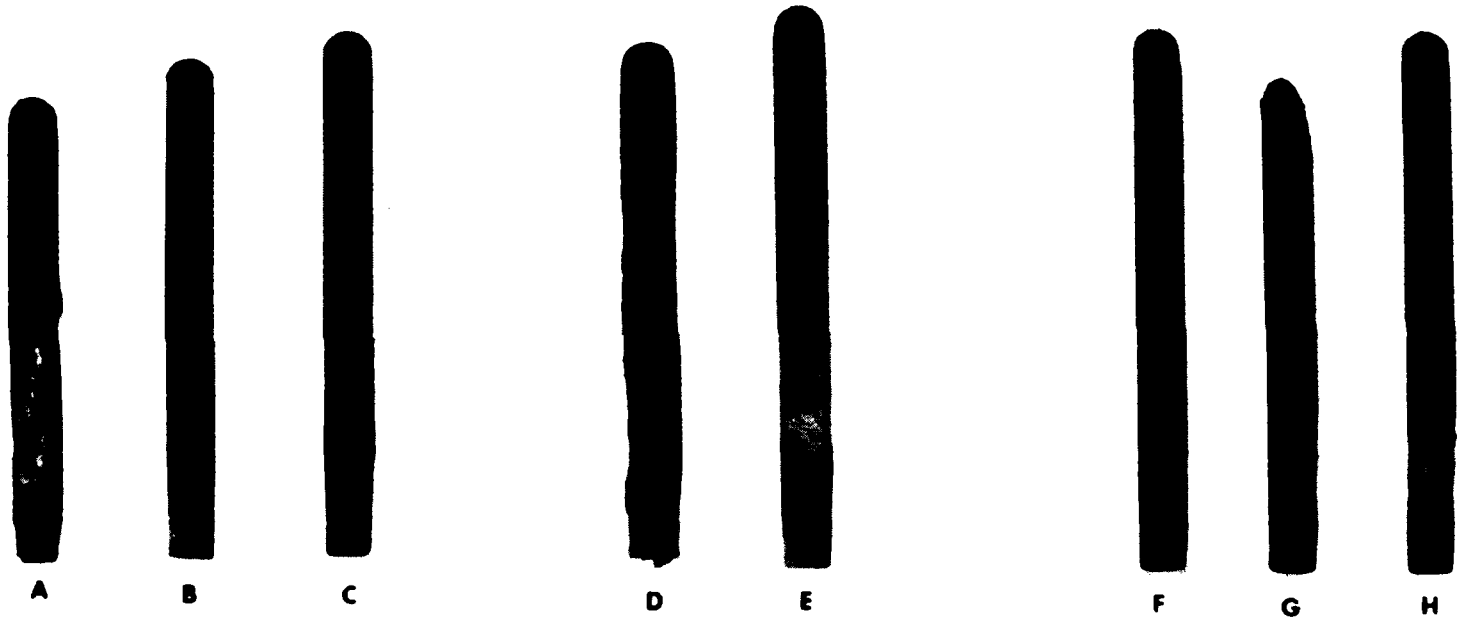

Figure B-23. Macrophotographs of Coated X-40, Rene' 125 and MA754 Environmental Test Specimens Tested in 2100°F Dynamic Oxidation for 525 Hours
(A) CCRS CoNiCrAlY/X-40; (B) CODEP B/X-40; (C) PVD CoCrAlY/X-40;
(D) CCRS CoNiCrAlY/MA754; (E) PVD NiCrAlY/MA754; (F) CODEP B/Rene' 125;
(G) CCRS CoNiCrAlY/Rene' 125; (H) PVD NiCrAlY/Rene' 125

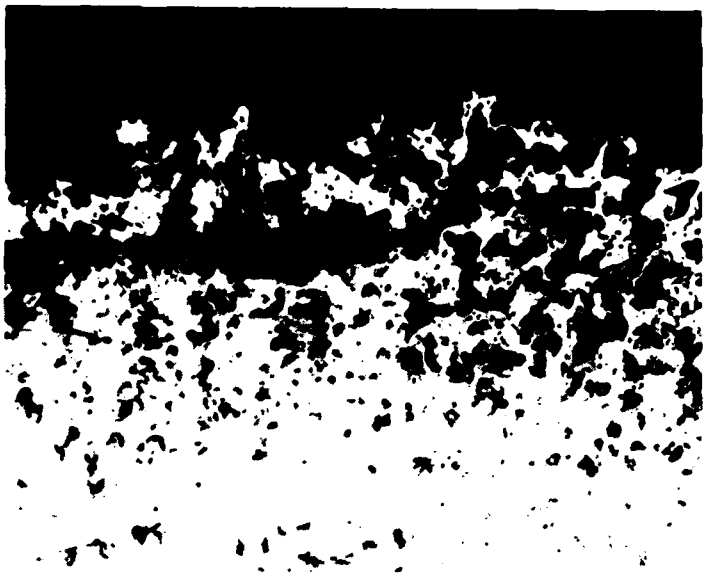

A. CCRS CoNiCrAlY/X-40

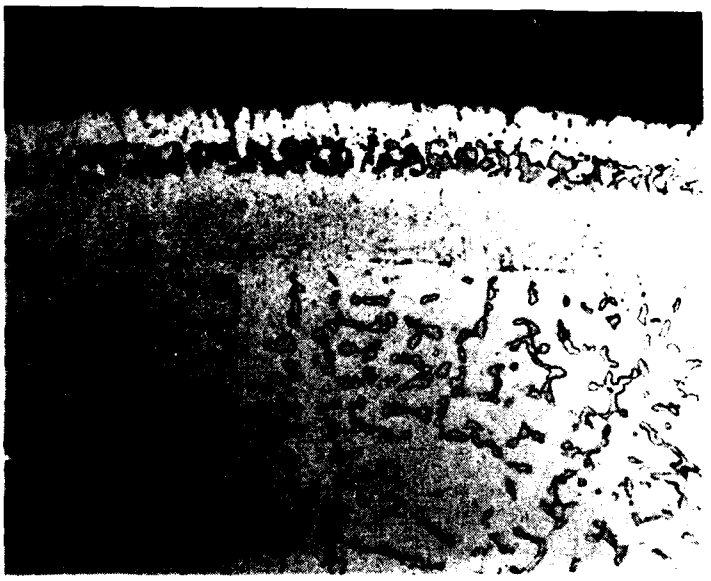

B. PVD CoCrAlY/X-40. Note Porous Nature of CCRS Coating and Preferential Attack of the High Chromium Phases

Figure B-24. Photomicrographs of Coated Specimens Tested in 2100°F Dynamic Oxidation for 325 Hours; Magnification: 500X

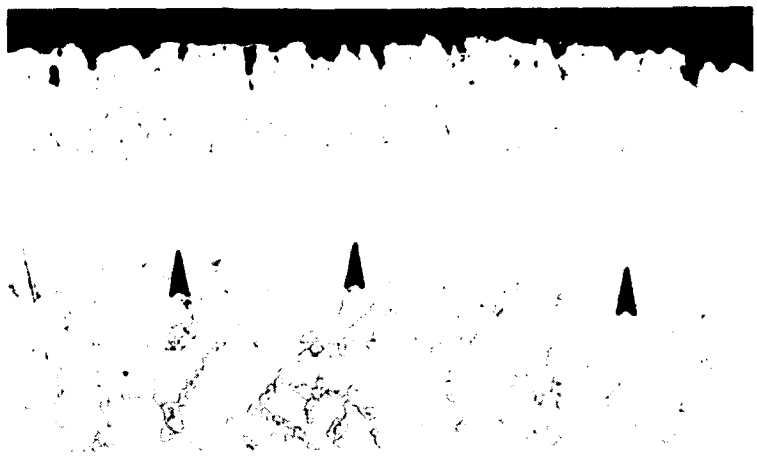

A. PVD CoCrAlY/X-40

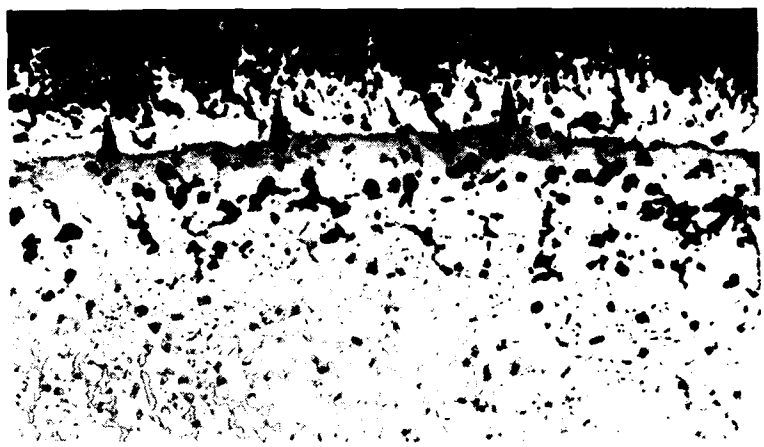

B. CODEP B/X-40

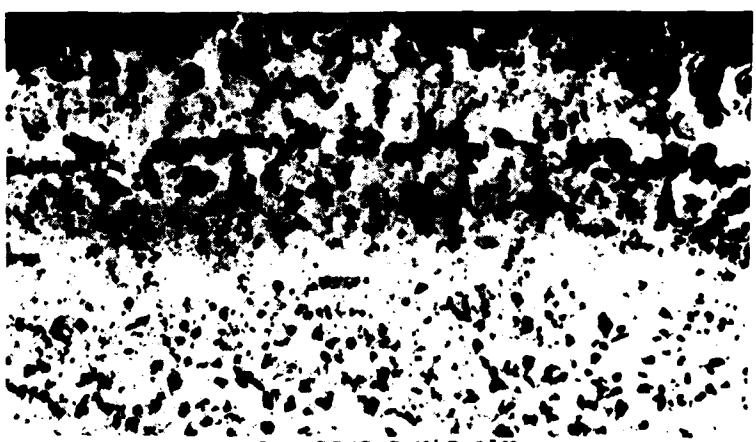

C. CCRS CoNiCrAlY

Figure B-25. Photomicrographs of Coated Specimens Tested in 2100°F Dynamic Oxidation for 525 Hours. Arrows, Original Interface. Magnification: 500X

Rene' 125

Dynamic oxidation tests of the Rene' 125 coatings indicated that all three candidate coatings were protective, with rough equivalence between the CCRS CoNiCrAlY and PVD NiCrAlY. The CODEP B coating was not as resistant. Macrophotographs of representative specimens are shown in Figure B-23.

Metallographic evaluation of the specimens after 525 hours, Figure B-26, shows that the CODEP B specimen is still protective, but locally about 70 percent penetrted. Both the CCRS and PVD coatings were not penetrated; they were, however, converted predominantly to gamma-nickel, columbium solid solution with small amounts of either gamma prime, Ni_3Al or beta-Ni(Co)Al present. Since the high content aluminum phases, beta-NiAl and gamma prime-Ni_3Al, are necessary in order to form a continuous alumina protective scale, these coatings would be expected to show signs of failure within the next 100-200 hours of testing.

MA754

Dynamic oxidation testing of the CCRS CoNiCrAlY and PVD NiCrAl coated MA754 specimens indicated that the PVD NiCrAlY coatings performed better than the CCRS CoNiCrAlY systems which failed after less than 300 hours. However, after 525 hours the PVD coating was also more protective. Macrophotographs of the pins after 525 hours are shown in Figure B-23. Severe distress and spallation of the CCRS CoNiCrAlY coating is evident.

Metallographic analysis of the pins indicated that the CCRS coatings failed through preferential oxidation of the low aluminum phase (the coatng was two-phase beta-Ni(Co)Al and gamma-NiCo solid solution with some voiding present, and through continuous void formation at the coating-metal interface (Fig. B-27). Since MA754 has no aluminum, these are thought to be Kirkendall type voids resulting from the rapid diffusion of aluminum into the parent metal. These voids then coalesce, causing coating spallation and subsequent attack.

When investigated, the PVD NiCrAlY coating showed signs of interfacial voiding and internal oxidation of the MA754 material. However, due to the lower aluminum content of the PVD coatings (i.e., 7 to 8% as opposed to 14% for the CCRS CoNiCrAlY) a longer transient time to the onset of spallation was observed, Figure B-28. During the 525 hours exposure, the PVD NiCrAlY coating has apparently changed from beta-NiAl plus gamma prime-Ni_3Al/gamma-NiCr solid solution to a gamma/gamma prime structure which is primarily gamma.

A. PVD NiCrAlY/Rene' 125

Magnification: 500X

B. CODEP B/Rene' 125

Magnification: 500X

70% (Arrows) has been Attacked

C.

Magnification: 500X

Figure B-26. Photomicrographs of Coated Rene' 125 Environmental Test Specimens Tested in 2100°F Dynamic Oxidation for 525 Hours

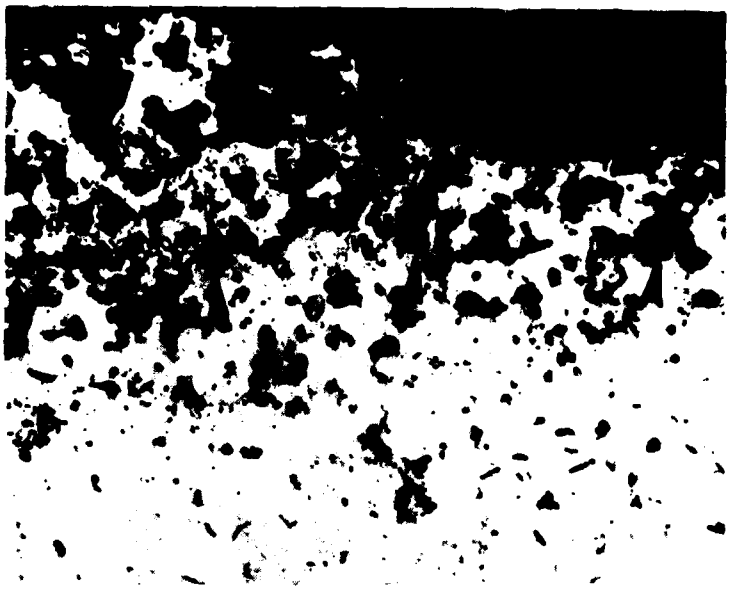

Figure B-27. CCRS CoNiCrAlY Coated MA754 Specimen After Dynamic Oxidation Testing at 2100°F for 325 Hours. Extensive Coating Distress and Interfacial Void (Arrows) has Occurred. Also, Substantial Internal Oxidation of the Parent Metal is Evident. Magnification: 500X

3.2.2 Hot Corrosion

Hot corrosion testing indicated that all coating systems investigated provided substrate protection after 478 hours at 1700°F, 5 ppm. However, both the CCRS CoNiCrAlY and PVD CoCrAlY coatings on X-40 revealed less coating surface distress. Macrophotographs of the specimens after test are shown in Figure B-29.

Metallographic evaluation of the specimens after test revealed that both the CCRS CoNiCrAlY and PVD CoCrAlY coatings on X-40 had substantially more coating remaining than CODEP B, Figure B-30. No sulfidation of the parent metal was observed. Also, even though the CCRS coating was less than fully dense, it still exhibited excellent corrosion resistance. All the specimens showed typical Na_2SO_4 induced frontal sulfidation attack. This process is much more severe for simple aluminides, such as CODEP B, which do not contain active element additions such as yttrium.

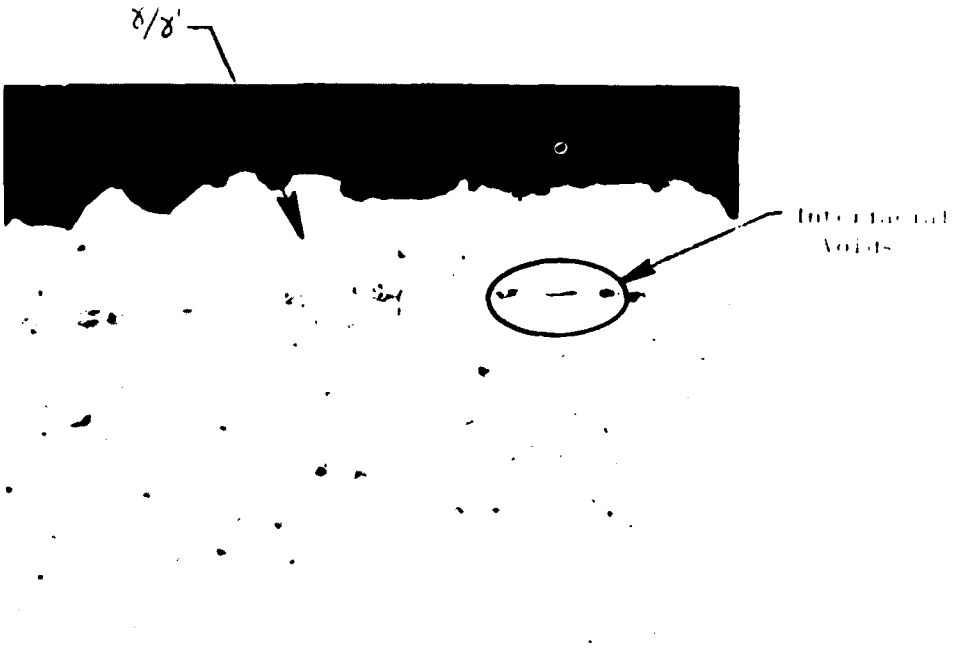

A. 328 Hours

B. 525 Hours

Figure B-28. PVD NiCrAlY Coated MA754 Tests in 2100°F Dynamic Oxidation. Note Interfacial Voiding has Begun After 325 Hours but Does Not Cause Internal Oxidation of the Parent MA754 (Arrows) Until 525 Hours.

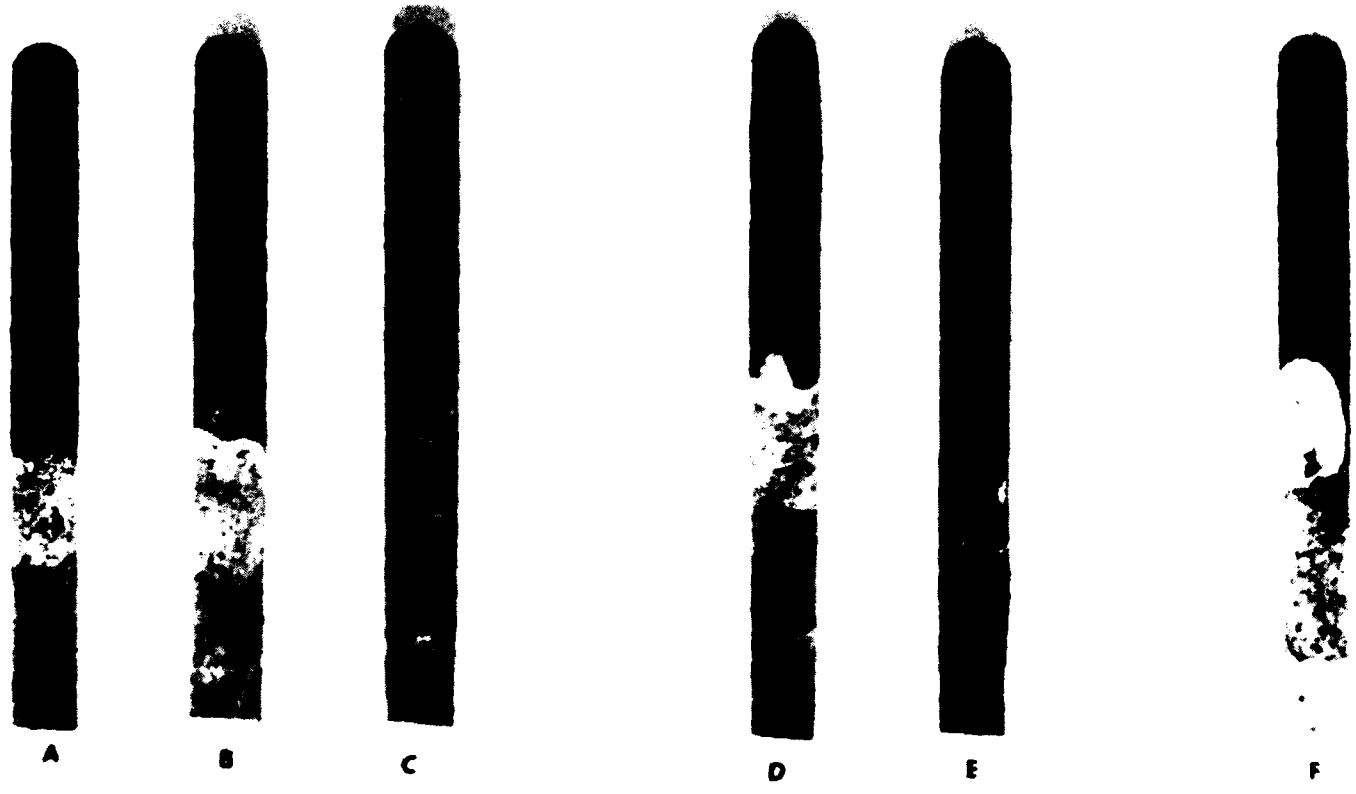

Magnification: 2.5X

Figure F-29. Macrophotographs of Coated X-40, MA-754 and Rene' 125 Specimens After Corrosion Tests at 1700°F, 5ppm for 478 Hours. (A) Codep B/X-40, (B) CCRS CoNiCrAlY/X-40, (C) PVD CoCrAlY/X-40, (D) PVD NiCrAlY/MA-754, (E) CCRS CoNiCrAlY/MA-754 and (F) CCRS CoNiCrAlY/Rene' 125

A. PVD CoCrAlY

B. CCRS CoNiCrAlY

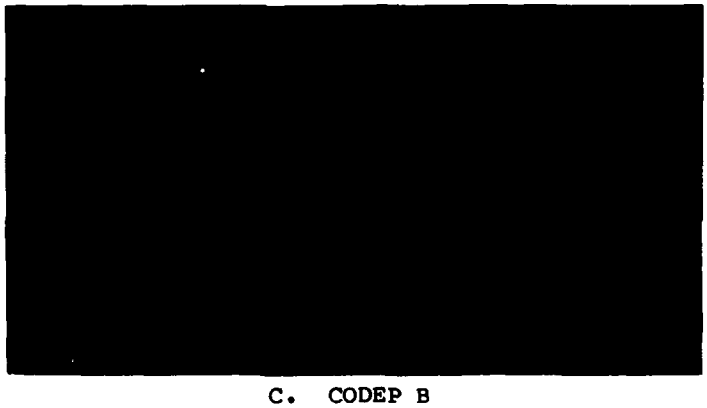

C. CODEP B

Figure B-30. *Photomicrographs of Coated X-40 Specimens After 478 Hours at 1700°F, 5 ppm Hot Corrosion. Note Even Though One CCRS Coating is Not Fully Dense, it Has Excellent Corrosion Resistance.*

Rene' 125

The CCRS CoNiCrAlY and CODEP B coatings provided adequate protection of the substrate, with no parent metal sulfidation after 478 hours at 1700°F, 5 ppm. The PVD NiCrAlY coatings failed prematurely after 190 hours due to preferential attack of the uncoated specimen base. Normal life expectancy for this coating is greater than 400 hours. A macrophotograph of the CCRS CoNiCrAlY coating is shown in Figure B-29. Of the three coatings tested, the CCRS coatings appeared to offer the best performance, probably due to a higher cobalt content, ie., 32-36 weight percent cobalt.

Metallographic evaluation of the test specimens after 478 hours indicated about 70 percent penetration of the CODEP B coating had occurred. However, only 10 to 15 percent penetration of the CCRS coating was visible. Also, while the CODEP B coating was predominantly single phase beta-NiAl, the CCRS coating consisted of a dense, two-phase structure, beta-Ni(Co)Al and gamma-NiCoCr solid solution (Fig. B-31). Frontal attack, characteristic of normal Na_2SO_4 sulfidation, was observed.

MA754

Hot corrosion testing at 1700°C, 5 ppm for 478 hours showed that the CCRS CoNiCrAlY coated MA754 system was superior to PVD NiCrAlY. Macrophotographs of the tested pins are shown in Figure B-29. The complete penetration of the PVD NiCrAlY is evident near the specimen tip while the CCRS coating shows only a limited amount of surface distress.

Metallographic analysis of the CCRS CoNiCrAlY and PVD NiCrAlY coated MA754 specimens was done. Photomicrographs of the tested pins are shown in Figures B-32 and B-33. After 236 hours of testing, the formation of chromium sulfides and depletion of the high aluminum phases (i.e., beta plus gamma prime/gamma - predominantly gamma) are evident in the PVD NiCrAlY. However, no sulfides are visible within the CCRS coatng and large amounts of retained beta-Ni(Co)Al (regions of high aluminum) indicate substantial coating life. Preferential attack, similar to that observed in oxidation, appears to have occurred in regions of low aluminum, high chrome and the specimen metal interface. However, this mode of attack does not seem to have spread after 478 hours (Fig. 33). Conversely, the PVD NiCrAlY shows almost complete coating spallation, chromium sulfide formation within the parent metal and large amounts of nickel oxide (Fig. B-33).

The interfacial scale attack and subsequent scale spallation of the PVD NiCrAlY coatngs are thought to be the result of Kirkendall type voiding. This effect apparently is diminished, i.e., transient time to void formation increased in the CCRS coatng by the addition of cobalt. Cobalt additions offer improved corrosion resistance and apparently slows down the diffusion of aluminum through the coating. A 0.4 mil zone, gamma-cobalt, nickel, chromium solid solution in the CCRS coatings adjacent to the parent metal was formed on all specimens. This may have further increased the aluminum gradient

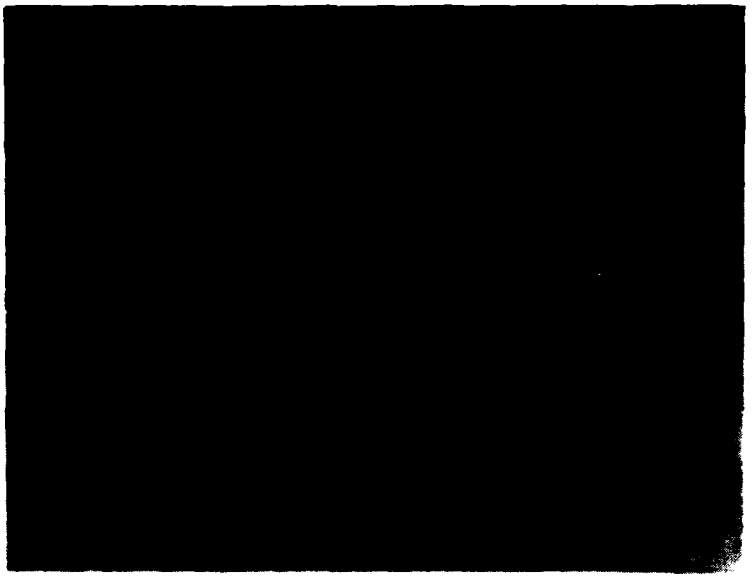

Figure B-31. CCRS CoNiCrAlY Coated Rene' 124 Specimen Tested in Hot Corrosion for 478 Hours at 1700°F, 5 ppm. Magnification: 500X

between the coating and substrate, lowering the driving force for diffusion and hence void formation. Also, some interfacial oxidation of all CCRS CoNiCrAlY coatings on MA754 was observed, even in the as-tested condition.

4.0 CCRS COATING PROCESS ADAPTATION

In order to check the feasibility of the CCRS coating process, three X-40, TF34 paired 1st-stage HPT vanes and two Rene' 125, F101 1st-stage HPT blades were coated by Solar and evaluated by General Electric. The following airfoil coating properties were investigated:

- Coating structure and chemistry
- Airfoil coating distribution
- Post-coating air flow

4.1 Airfoil Coating Structure and Chemistry

Metallographic evaluation of the CCRS CoNiCrAlY coating, deposited using the single-cycle process, showed structures similar to that obtained for the mechanical test specimens. The coating is predominantly an add-on type and consists of a beta-Co(Ni)Al matrix phase with large amounts of alpha-chromium precipitated throughout. Coating structure varied from a semi-dense structure (Fig. B-34a) on the predominant airfoil sections to a porous, loosely bonded structure (Fig. B-34b) near cooling holes, especially at the pressure side bleed trailing edge region.

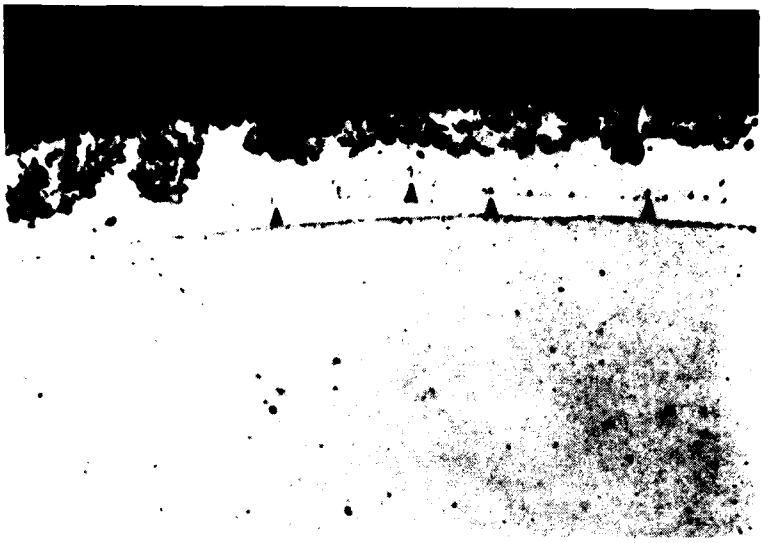

A. PVD NiCrAlY

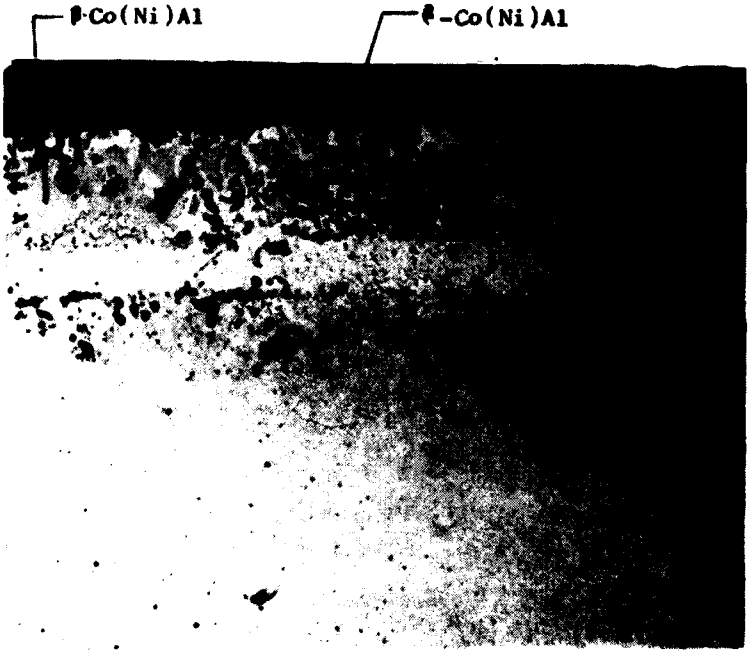

B. CCRS CoNiCrAlY

Figure B-32. Photomicrographs of Coated MA754 Specimens Tested for 236 Hours at 1700°F, 5 ppm. Arrows Indicate Chromium Sulfides Formed With the PVD Coating
Magnification: 250X

A. PVD NiCrAlY

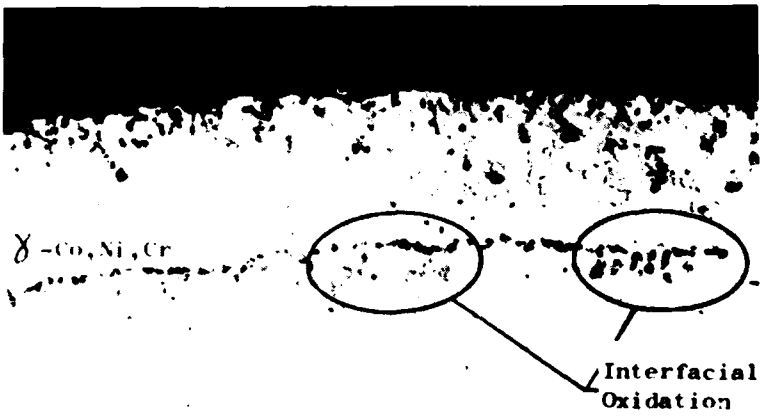

B. CCRS CoNiCrAlY

Figure B-33. Photomicrographs of Coated MA754 Specimens Tested for 409 and 478 Hours Respectively at 1700°F, 5 ppm. Note Internal Sulfide Formation (Arrows) in A and Gamma-Co,Ni,Cr Solid Solution in B. Magnification: 250X

A. Airfoil

B. Cooling Holes and Pressure Side Bleed Holes

Figure B-34. Photographs of CCRS CoNiCrAlY Coating on X-40, TF34 1st-Stage HPT Paired Vane. Note Change in Structure From Coating Deposited on A and B.
Magnification: 500X

When the CCRS CoNiCrAlY coating deposited on the Rene' 125 F101, 1st-stage HPT blades was investigated, a predominantly single-phase beta-Ni(Co)Al matrix with small amounts of gamma-Ni, cobalt, chromium solid solution was observed. The coating is an add-on type (i.e., does not consume base metal, although a large 0.0008 inch diffusion zone is apparent) and exhibits some porosity (Fig. B-35). However, unlike the vane pair, the coating was consistent across the entire airfoil and was close to full density at cooling hole surfaces.

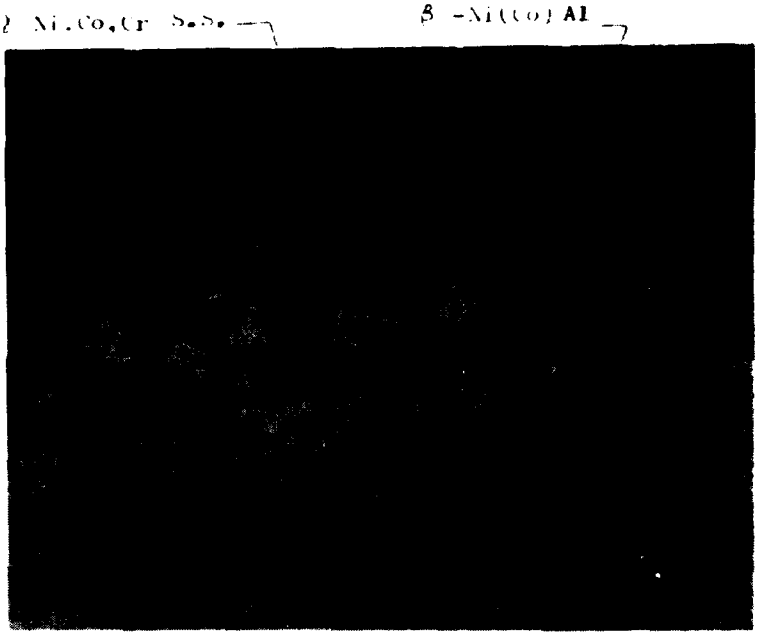

Figure B-35. Photomicrograph of a CCRS CoNiCrAlY Coating on a Rene' 125 F101 1st-Stage HPT Blade. Note (Arrows) Small Amounts of Coating Porosity. Magnification: 500X

Microprobe analysis of the CCRS coated X-40 and Rene' 125 vanes and blades gave a nominal composition of Co(bal)/18Ni/10-20Cr/14-16Al/Y (not determined) and Co(bal)/33-40Ni/6-10Cr/19-12Al/Y (not determined) respectively. Typical microprobe diffusion profiles are shown in Figures B-36 and B-37.

4.2 Airfoil Coating Distribution

The thickness distribution of the fully coated CCRS CoNiCrAlY coatings on X-40, TF34 1st-stage HPT paired vanes and Rene' 125 F101 1st-stage HPT blades was investigated. One CCRS coated vane pair and one coated blade wer cut up for analysis. Metallographic thickness profiles are shown in Tables B-4 and B-5. CCRS coated thickness measured at the airfoil midspan showed a variation of 0.0012 to 0.006 inch for vanes and 0.0031 to 0.006 inch for the blades. The thickest and thinnest areas encountered on the vanes were at the leading edges and trailing edges, while for the blade, the thickest areas were at the airfoil leading edge and convex suction surfaces. A normal distribution for a

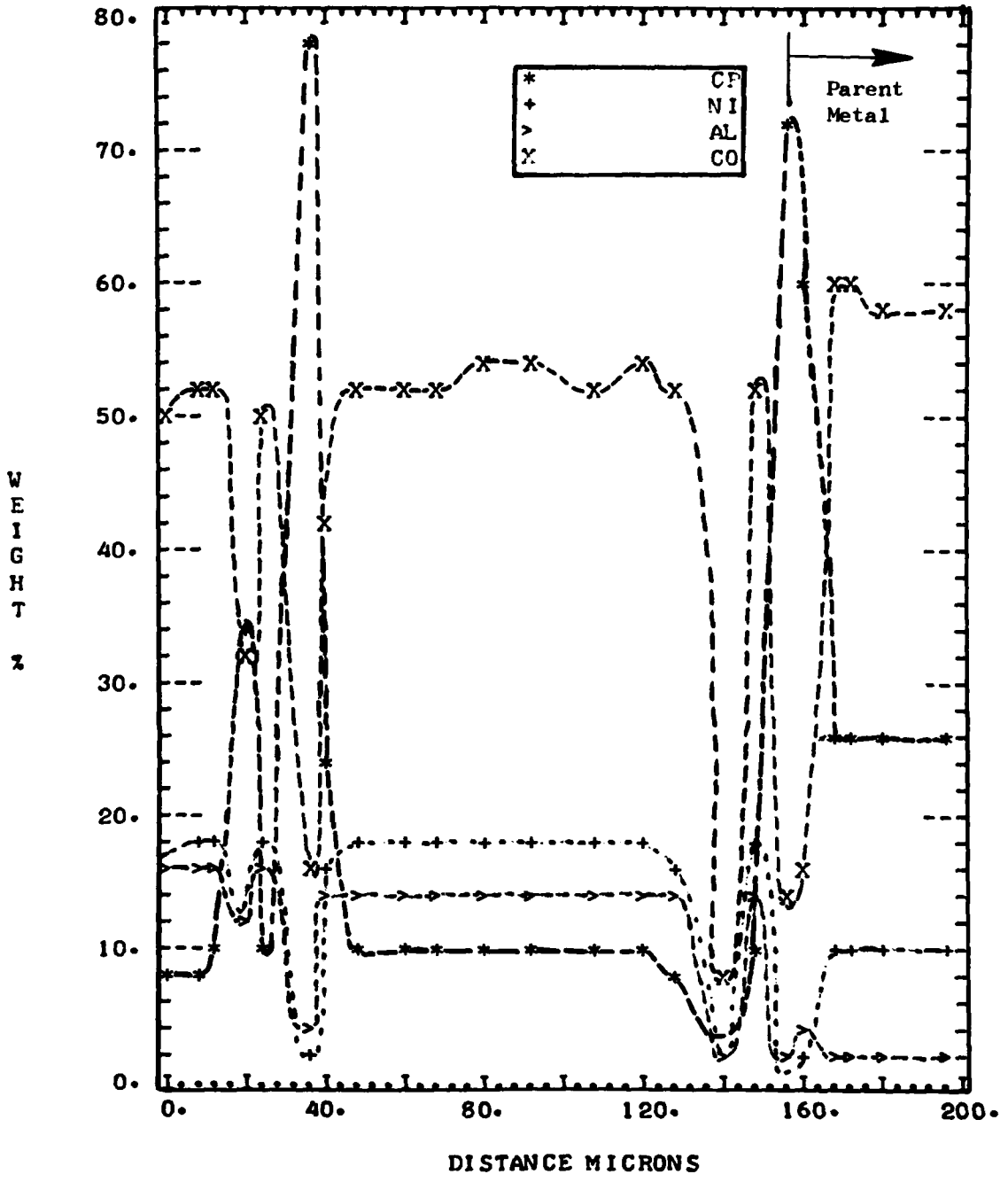

Figure B-36. Typical Microprobe Trace of CCRS CoNiCrAlY Coating Deposited on X-40, TF34, 1st-Stage HPT Paired Vane

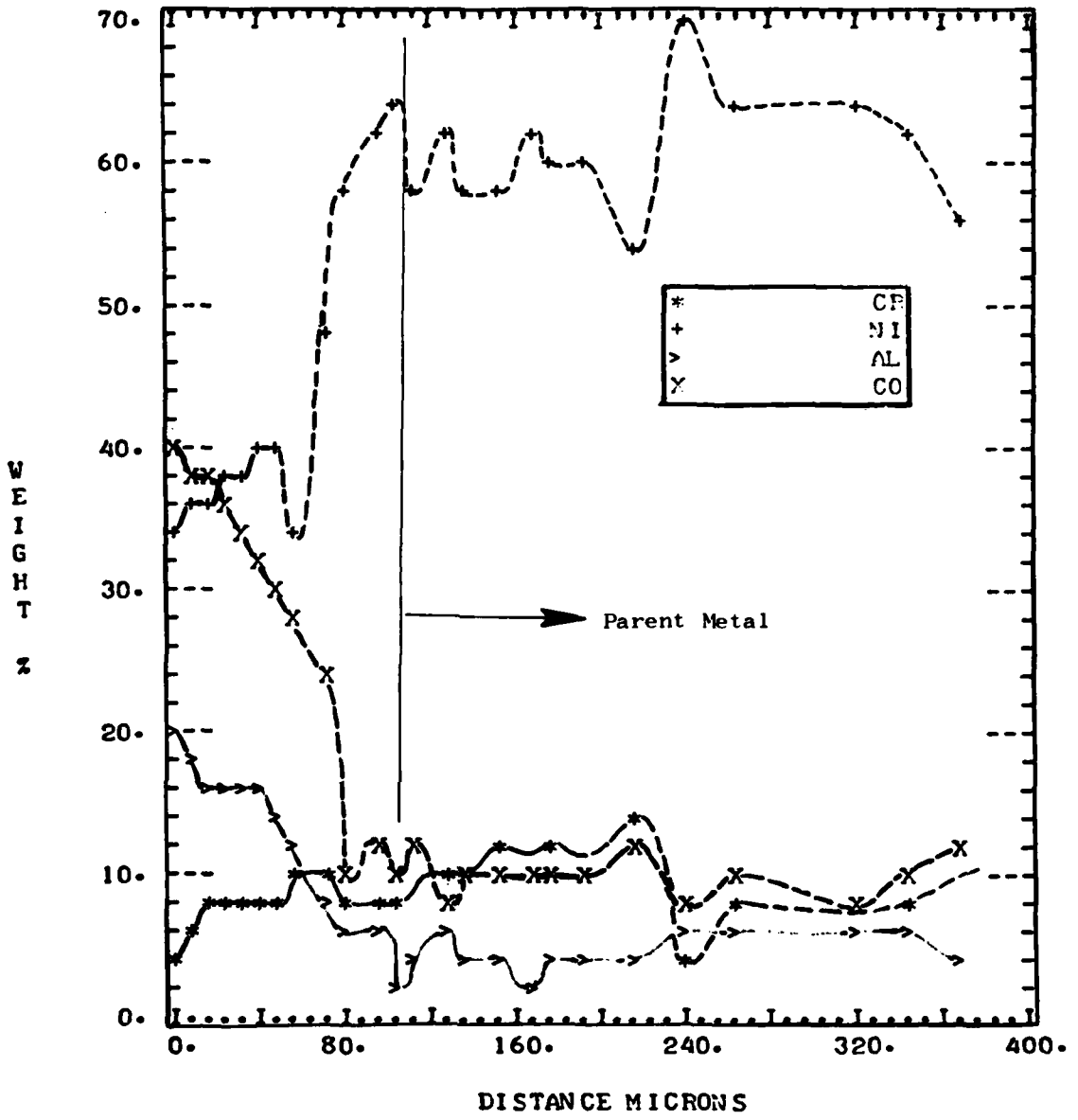

Figure B-37. Typical Microprobe Trace of CCRS CoNiCrAlY Coating Deposited on Rene' 125, F101, 1st-Stage HPT Blade

Table B-4

COATING THICKNESS DISTRIBUTION OF CCRS CoNiCrAlY COATED
R-125 F101 1st STAGE HPT BLADE
PROFILE POSITION (.001")

BLADE S/N	*% SPAN	1	2	3	4	5	6	7	8	9	10	11	12
130789	10	3.8	3.0	4.0	3.1	2.5	5.5	3.2	3.1	3.3	3.8	6.0	3.7
	40	3.6	3.2	4.1	4.2	3.5	4.6	3.5	3.2	3.5	4.1	5.3	3.2
	70	3.7	2.3	3.5	4.0	2.9	3.0	3.8	3.3	3.5	5.0	5.0	3.5

* % Span - Position on AIRFOIL as Measured From the Platform.

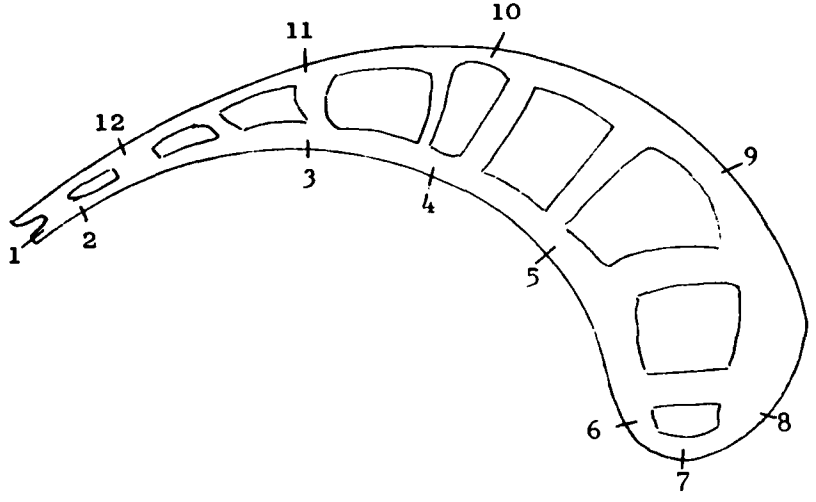

Table B-5

COATING THICKNESS DISTRIBUTION OF A CCRS CoNiCrALY COATED
X-40, TF34, 1st Stage HPT Blade

Profile Position (.001")

Blade S/N	*% Span	1	2	3	4	5	6	7	8	9	10	11	12	13	14	15
T8330	10	1.4	1.2	1.2	2.2	1.8	3.2	3.2	5.2	4.4	3.2	3.6	2.8	2.4	2.6	2.4
	50	1.2	2.8	1.4	2.4	2.0	2.8	3.6	6.0	4.0	4.0	6.4	4.8	3.2	2.2	2.4
	90	1.6	1.1	1.2	2.2	2.0	2.0	2.2	4.8	5.2	1.8	2.0	2.4	5.2	2.4	2.0
T8105	10	3.2	2.0	2.6	2.0	2.2	1.6	2.8	6.4	4.8	3.6	3.2	2.6	3.2	2.6	2.0
	50	3.2	2.8	3.0	3.2	3.4	2.2	2.0	6.4	5.6	6.4	5.0	3.2	3.2	2.4	3.2
	90	2.0	1.6	1.6	2.2	1.4	2.0	3.0	4.0	6.5	6.3	5.6	4.6	2.7	2.7	3.2

*% Span - Position and Airfoil as Measured from the Platform

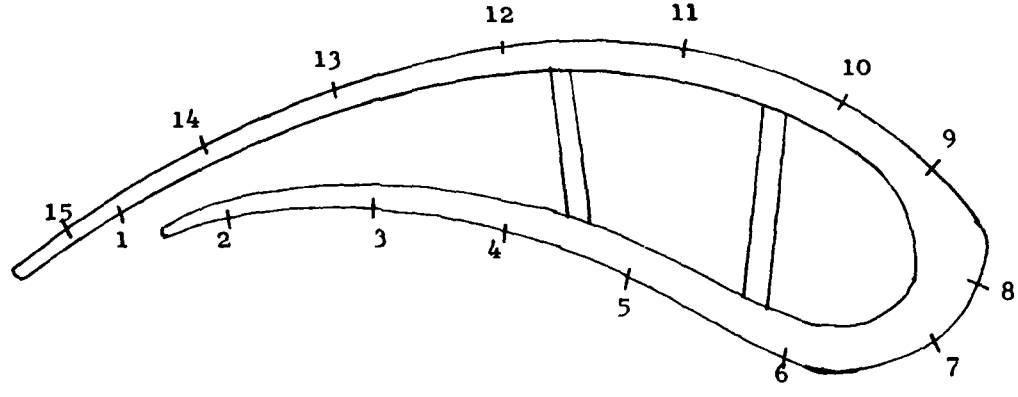

PVD coating is 0.003 to 0.005 inch. Using this as a criterion, it would appear that only the blades showed thickness variations equivalent to PVD. However, since vanes are non-rotating parts and subject to low mechanical stresses (larger thermally produced stresses are normally encountered), the wider nominal vane distribution may be acceptable.

4.3 Post-Coating Airflow

In a check of the compatibility of the CCRS CoNiCrAlY process applied to TF34 paired vanes, three fully coated 1st-stage vane pairs were (coolant) airflow tested after coating. Reductions in coolant airflow were observed in all vanes (as compared to bare) and resulted from reductions in cooling hole orifice size. The reduction in hole cross-sectional area was the result of excessive bisque buildup and aluminiding during the pack cementation cycle of the CCRS process. Results are shown in Table B-6. Changes in coolant airflow for the CCRS CoNiCrAlY coated F101 blades were not investigated.

Table B-6

CCRS CoNiCrAlY COATED X-40, TF34 1ST STATE HPT PAIRED

VANE AIR FLOW CHECK DATA

* Per Cent Reduction in Flow

Vane Pair	Blade S/N	5+4+3	5+4+3+2	TOTAL
1	T8289	.75	1.86	.68
	T1719	7.21	7.06	7.06
2	T8330	44.17	31.86	19.92
	T8105	30.06	21.35	20.48
3	S6948	35.60	26.1	14.3
	S4819	38.20	19.2	4.39

* When measuring flow, none numbered areas were masked off.

Numbers

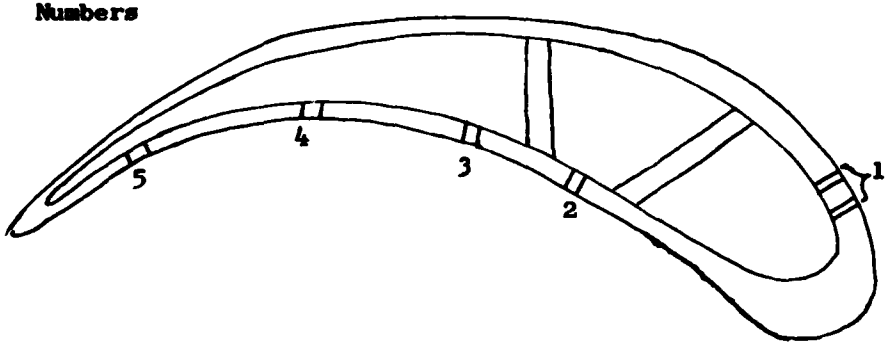

denote AIRFOIL film cooling hole Location, for instance 5 denotes film cooling hole at trailing edbe.

*U.S.Government Printing Office: 1980 — 657-084/657